# Analysis and Evaluation of Human Motions Based on Musculoskeletal Model Incorporating Redundant Muscles and Muscle Fatigue Property

Nishida, Isamu

(Degree)
博士（工学）

(Date of Degree)
2012-03-25

(Date of Publication)
2012-11-20

(Resource Type)
doctoral thesis

(Report Number)
甲5496

(URL)
https://hdl.handle.net/20.500.14094/D1005496

Doctoral Dissertation

# Analysis and Evaluation of Human Motions Based on Musculoskeletal Model Incorporating Redundant Muscles and Muscle Fatigue Property

January 2012

Department of Mechanical Engineering,

Graduate School of Engineering, Kobe University

Isamu Nishida

# Doctoral Dissertation

# Analysis and Evaluation of Human Motions Based on Musculoskeletal Model Incorporating Redundant Muscles and Muscle Fatigue Property

# 冗長筋群と筋肉疲労を考慮した筋骨格モデルによる人体動作の解析と評価

January 2012

Department of Mechanical Engineering,

Graduate School of Engineering, Kobe University

Isamu Nishida

## Abstract

Previously, computer human models that duplicate the properties and the functions of human have been developed. They are used for the evaluation of product designs and for the improvement of working environments, rehabilitation procedures and performance analysis in sports. However, they usually use a rigid segment model, which can only calculate physical values such as reach, net forces and net moments, and evaluate only the open-loop motions. Some of them use a musculoskeletal model that can estimate muscle forces. Estimation of muscle forces during motions is important to analyze more realistic situations. But they do not usually consider the roles of antagonistic muscles and biarticular muscles. Furthermore, computer human models that can evaluate muscle fatigue progress have not been developed yet.

This study proposed a method to evaluate a walking cycle, which is the closed-loop motion, using a human rigid segment model. This study also investigated a musculoskeletal model that considers the roles of antagonistic muscles and biarticular muscles. In addition, a proposed method to estimate muscle forces during complex motions was applied to several dynamic motions. Furthermore, this study investigated a mechanism of muscle fatigue and proposed a muscular fatigue model to evaluate muscle fatigue progress under several muscular force patterns.

Experiments to validate the proposed methods were conducted. The results of these experiments showed that the proposed methods were considered to successfully estimate ground reaction forces during a walking cycle, to estimate muscle forces during motion and to evaluate muscle fatigue progress under several muscular force patterns. Therefore, this study has improved computer human models for application to more realistic simulations.

# Contents

# 1. Introductory remarks

## 1.1 Background

In the field of manufacturing, a human centered system is recently getting attention to realize more flexibility for manufacturing of wide product variety and volume. If the production processes aim only at higher productivity in manufacturing without attention to humans, the efficiency of working is decreased and the potential of industrial injury is increased. Therefore, computer human models that duplicate the properties and the functions of human are required to be developed to realize more ergonomic working environments. Furthermore, in the fields of sport engineering and welfare engineering, the analysis and clarification of the properties and the functions of human are also necessary. These researches also contribute to improve sport techniques and rehabilitation procedures. Furthermore, they can allow a higher quality life in the aging society.

Previously, computer human models that duplicate the properties and the functions of human have been developed. They have traditionally attempted to simulate or predict the forces and motions. They can generally be separated into two categories: internal body structure and external gross motion body models. The first type deals with the detail structure of various body subsystems such as the head, thorax, spine, etc. and will predict stresses, stains and localized deformations. The latter model category deals with overall body response and generally provides as output motion data of body segments and interactive forces between body segments and external structural elements [1].

The development of complex and detailed human models has been particularly rapid and successful during the last 30 years. This growth can mostly be attributed to the developments

in computer technology including the development of sophisticated accessory software. This relatively new and powerful analysis capability has opened the door to the solution of analytical equations describing the complex and detailed mechanical structure of the human body [1]. The basic formulating equations for computer human models were already available in the 19th century. Current models applied in human models have used the same formalism, usually either the Newton-Euler or Lagrange technique, to formulate equations describing chains of coupled rigid bodies, and with current computer-based analysis techniques solutions to such systems have become possible [2]. Models depicting the articulated, three-dimensional human body structure have been developed by a number of investigators. Among these are models described by Young [3], Robbins *et al.* [4], Furusho *et al.* [5], Huston *et al.* [6, 7] and Fleck *et al.* [8, 9].

Computer human models such as Jack and RAMSIS contribute to the efficiency of the product design process. They have been utilized as an effective design tool to visualize the interaction of a human and workstation system such as passenger car interior and factory workspace and to evaluate the human-workstation interaction from an ergonomic perspective such as reach, visibility and comfort [10]. The ergonomic design methodology using the computer human models makes the iterative process of design evaluation, diagnosis and revision more rapid and economical [11]. Traditionally, human-vehicle interactions have been evaluated in the development process using physical mock-ups [12]. The integration of human factors is then carried out in laboratory and field experiments, which are often considered to be too expensive and time consuming [13].

Over the last 30 years, the utilization of human modeling tools has supported ergonomic evaluations in virtual environments. This has reduced the need for physical tests. Developers,

reviewers [11, 12] and users [14] of human simulation tools claim that they may reduce development time and costs. Furthermore, human modeling tools provide the opportunity to perform quick tests [14], which enable users to check the first rough designs and accelerate the initial design phase. Designers and engineers have requested such tools [15]. Furthermore, computer human modeling tools provide means for the development of a standardized evaluation methodology [14] and have the potential of becoming a standard validation and benchmarking method [16]. In car industry companies today, human modeling tools are used in a working process [17]. In the future, it may be necessary to develop a formal standardized process as the number of tool users in each company increases.

In addition, computer simulation of the dynamics of musculoskeletal systems is an important tool in biomechanics. It is useful for a wide range of problems, such as predicting the outcome of tendon transfers [18], understanding multijoint movements [19], evaluating ergonomics [20], optimizing biomechanical performance [21, 22], developing neural prostheses [23] and understanding the neural control of movement [24, 25]. Software for musculoskeletal simulation is widely available today, both from commercial vendors and open source software projects. Most musculoskeletal simulators are based on algorithms for multibody dynamics initially developed for simulating robots and engineering machinery. Examples of these types of simulators include software packages such as SIMM [18], AnyBody [20], MSMS [23] and OpenSim [26], and many research simulations, including those used in all the papers cited above [27].

Consequently, computer human models considering musculoskeletal model can serve as a valuable design and evaluation tool not only in the development of new systems, but also in evaluating the biomechanical stresses resulting from manual industrial work. Realistic

simulations can contribute significantly to the prevention and reduction of presently occurring injuries in the field of manufacturing. They can also contribute to the improvement of efficiency of rehabilitation procedures and performance analysis in sports in the fields of welfare engineering and sport engineering. Therefore, it is required to develop computer human models that can conduct realistic simulations.

## 1.2 Objectives

Software of computer human models is widely available today, both from commercial vendors and open source software projects. They are used for the evaluation of products designs and for improvements of working environments, rehabilitation procedures and performance analysis in sports. Many of computer human models have evaluated the motions, usually the open-loop motions, using the human rigid segment model that can only calculate physical values such as reach, net force and net moment. Some computer human models including musculoskeletal models also have been developed. They usually have used optimization methods in the evaluation of motions. The optimization methods suggested by Crowninshield *et al.* [28] are usually used to estimate muscle forces during motions. The method estimates muscle forces with the sum of the muscle forces across a joint that equal the net moment of force at the joint. Unfortunately, these methods usually do not consider the functions of antagonistic muscles and biarticular muscles. Furthermore, computer human models that can evaluate muscle fatigue progress have not been developed yet.

This study proposes a method to evaluate the walking cycle, which is a closed-loop motion, using a rigid segment model. This study also investigates the musculoskeletal model considering the roles of antagonistic muscles and biarticular muscles and proposes the method

to estimate muscle forces during motions. The method is applied to dynamic motions and validated. Furthermore, this study investigates a mechanism of muscle fatigue and proposes a muscular fatigue model to evaluate muscle fatigue progress under several muscular force patterns. Therefore, this study can contribute to improve computer human models that can conduct more realistic simulations.

### 1.3 Construction

This thesis consists of 6 chapters including this chapter as shown in Fig. 1.1.

Chapter 1 showed the background and the objectives of this study.

Chapter 2 showed a human rigid segment model and a method to analyze 3-dimensional motions. It is difficult to analyze walking motions in which both feet are on the ground simultaneously unless at least one force platform or preferably two are available. This study proposed a method that can calculate net forces at each joint during walking motions from only captured trajectories.

Chapter 3 develops a musculoskeletal model of lower limb that considers the role of antagonistic muscles and biarticular muscles. This study proposed a method to estimate muscle forces during motions considering these roles of muscles. Furthermore, this study validated the proposed model to estimate muscle forces by applying the model to vertical jumping as an example of a 2-dimensional dynamic motion and to a jogging motion as 3-dimensional example.

Chapter 4 outlines a musculoskeletal model of upper and lower limbs that includes the roles of antagonistic muscles and biarticular muscles to estimate muscle forces during lifting operations as an example of a working motion. Furthermore, various motion patterns in the

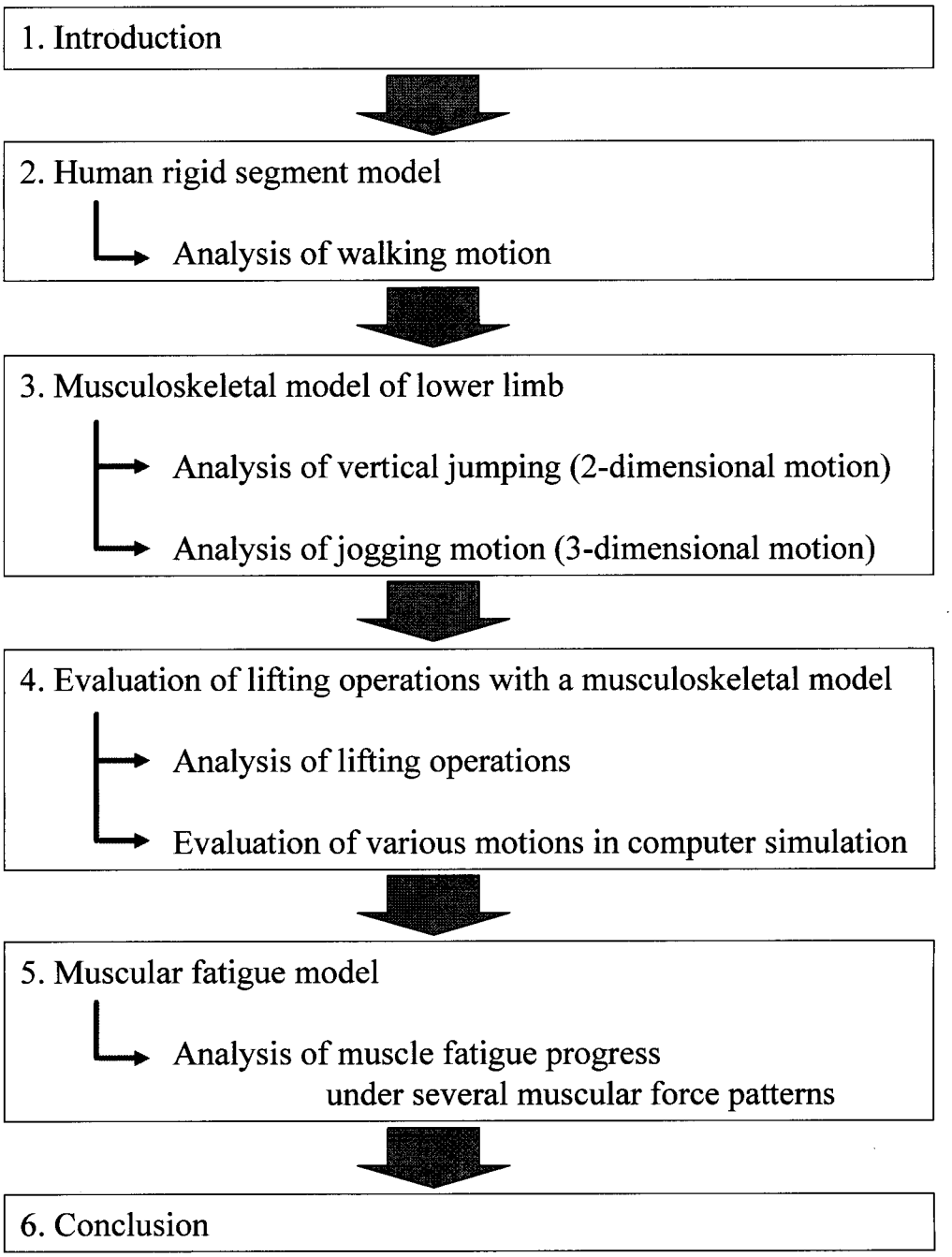


**Fig. 1.1** Construction of this thesis

lifting operations were created by a computer simulation based on the experimental lifting operation and evaluated considering the muscle forces of upper and lower limbs estimated with the musculoskeletal model.

Chapter 5 showed a mechanism of muscle fatigue. This study proposed a muscular fatigue

model to evaluate muscle fatigue progress under several muscular force patterns.

Finally, chapter 6 showed the conclusion of this dissertation.

**References**

[1] Freivalds A., Kaleps I. : Computer aided strength prediction using the articulated total body model, Computers & Industrial Engineering, 8(2), 107-118, 1984.

[2] Kaleps I. : Prediction of whole-body response to impact forces in flight environments. In: Gierke H. E. (Ed.), Models and Analogues for the Evaluation of Human Biodynamic Response, Performance and Protection, AGARD Conf., Proc. No. 253, 1979.

[3] Young R. D. : A three-dimensional mathematical model of an automobile passenger, Texas Transportation Institute Research Report, 140(2), 1970.

[4] Robbins D. H., Bennett R. O., Bowman B. M. : User-oriented mathematical crash victim simulator, 16th Stapp Car Crash Conf., Proc. 128-148, 1972.

[5] Furusho H., Yokoya K. : Analysis of occupant's movement in head-on collision, Trans. Society of Automotive Engineers Japan, 1, 145-155, 1970.

[6] Huston R. L., Hessel R., Passarello C. : A three-dimensional vehicle-man model for collision and high acceleration studies, Society of Automotive Engineers, Paper No. 740275, 1974.

[7] Huston R. L., Passarello C. E., Harlow M. W., Winger J. M. : The UCIN 3-D Aircraft-occupant, Aircraft Crashworthiness, University Press of Virginia, 1975.

[8] Fleck J. T., Butler F. E., Vogel S. L. : An improved three dimensional computer simulation of motor vehicle crash victims, 4 vols. Calspan Corp., Final Technical Report No. ZQ-5180-L-I, 1974.

[9] Fleck J. T. : Calspan three-dimensional crash victim simulation program, Aircraft Crashworthiness, University Press of Virginia, 1975.

[10] Jung K., Kwon O., You H. : Development of a digital human model generation method

for ergonomic design in virtual environment, International Journal of Industrial Ergonomics, 39(5), 744-748, 2009.

[11] Chaffin D. B. : Digital Human Modeling for Vehicle and Workplace Design, Society of Automotive Engineers, Inc., Warrendale, USA, 2001.

[12] Porter J. M., Case K., Freer M. T., Bonny M. C. : Computer aided ergonomics design of automobiles. In: Peacock B., Karwowski W. (Ed.), Automotive Ergonomics, Taylor & Francis, London, UK, 1993.

[13] Helander M. G. : Seven common reasons to not implement ergonomics, International Journal of Industrial Ergonomics, 25(1), 97-101, 1999.

[14] Bowman D. : Using digital human modeling in a virtual heavy vehicle development environment. In: Chaffin D. (Ed.), Digital Human Modeling for Vehicle and Workplace Design, Society of Automotive Engineers, Inc., Warrendale, USA, 2001.

[15] Haslegrave C. M., Holmes K. : Integrating ergonomics and engineering in the technical design process, Applied Ergonomics, 25(4), 211-220, 1994.

[16] Sundin A : Participatory ergonomics in product development and workplace design, Doctorial Thesis, Chalmers University of Technology, Gothenburg, Sweden, 2001.

[17] Blome M., Dukic T., Hanson L., Hogberg D. : Computer based protocol for human simulation report. In Proceedings of IEA 2003, Seoul, South Korea, 3, 30-33, 2003.

[18] Delp S., Loan J. : A computational framework for simulating and analyzing human and animal movement, Computer Science of Engineering, 2, 46-55, 2000.

[19] Hollerbach J.M., Flash T. : Dynamic interactions between limb segments during planar arm movement, Biol. Cybern., 44, 67-77, 1982.

[20] AnyBodyTech, Anybody Modeling System. Software package

<http://www.anybodytech.com/>, 2009.

[21] Pandy M. G., Zajac F. E., Sim E., Levine W. S. : An optimal control model for maximum-height human jumping, Journal of Biomechanics, 23, 1185-1198, 1990.

[22] Kargo W., Nelson F., Rome L. : Jumping in frogs: assessing the design of the skeletal system by anatomically realistic modeling and forward dynamic simulation, Journal of Experimental Biology, 205, 1683-1702, 2002.

[23] Davoodi R., Urata C., Hauschild M., Khachani M., Loeb G. E. : Model-based development of neural prostheses for movement. IEEE Transactions Biomedical Engineering, 54, 1909-1918, 2007.

[24] McKay J. L., Burkholder T. J., Ting L.H. : Biomechanical capabilities influence postural control strategies in the cat hindlimb, Journal of Biomechanics, 40, 2254-2260, 2007.

[25] Berniker M., Jarc A., Bizzi E., Tresch M. C. : Simplified and effective motor control based on muscle synergies to exploit musculoskeletal dynamics, Natl. Acad. Sci. USA, Proc. 106, 7601-7606, 2009.

[26] Delp S. L., Anderson F. C., Arnold A. S., Loan P., Habib A., John C. T., Guendelman E., Thelen D. G. : OpenSim: open-source software to create and analyze dynamic simulations of movement, IEEE Transactions Biomedical Engineering, 54, 1940-1950, 2007.

[27] Pai D. K : Muscle mass in musculoskeletal models, Journal of Biomechanics, 43, 2093-2098, 2010.

[28] Crowninshield R. D., Brand R. A. : A Physiologically Based Criterion of Muscle Force Prediction in Locomotion, Journal of Biomechanics, 14, 793-800, 1981.

# 2. Motion analysis using a rigid segment model

## 2.1 Introduction

Net forces and net moments acting on human joints are very important for human movement analysis. However it is impossible to measure net forces and net moments directly. Usually the human body is modeled as a system of interconnected rigid-bodies. This enables the calculation of net forces and net moments mathematically and physically. Previously, computer human models that duplicate the properties and the functions of human have been developed. They are used for the evaluation of product designs and for improvement of working environments, rehabilitation procedures and sport techniques. They can predict net forces accurately and make possible the prediction of movement patterns prior to real-life application.

It is impossible and unrealistic to define the human model considering all complicated human functions because the human consists of approximately 200 bones and 800 muscles. Thus, the human model should be simplified depending on the analysis objectives. In general, human models have been classified as follow.

1. Skeleton model and musculoskeletal model
2. Dynamics model and static model
3. 3-dimensional model and 2-dimensional model
4. Whole-body model and partial model

The skeleton model permits calculation of net forces and net moments whereas the musculoskeletal model considers the properties and the functions of muscles. Dynamic models consider inertial forces generated by the acceleration of the segments but static

models ignore the inertial forces.

This study investigated a 3-dimensional, whole-body, skeleton human model that included dynamics. Furthermore this study suggests a way to estimate net forces at all joints as well as the ground reaction forces throughout a walking cycle using only motion capture data and body segment parameters. It is difficult to analyze walking motions in which both feet are on the ground simultaneously unless at least one force platform or preferably two are available.

## 2.2 Human segment model

Numerous human rigid-body models have been developed to calculate net forces and net moments with inverse dynamics based on segment models of varying complexity from three [1] to 17 segments [2]. This study used a model that consists of 15 rigid-body segments (1-Foot, 2-Leg, 3-Thigh, 4-Lower trunk, 5-Torso, 6-Upper arm, 7-Forearm, 8-Hand, 9-Head) as shown in Fig. 2.1

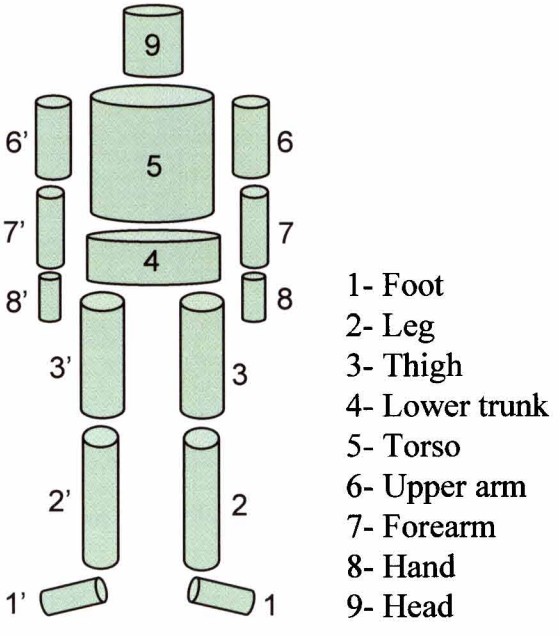


**Fig. 2.1** Human segment model

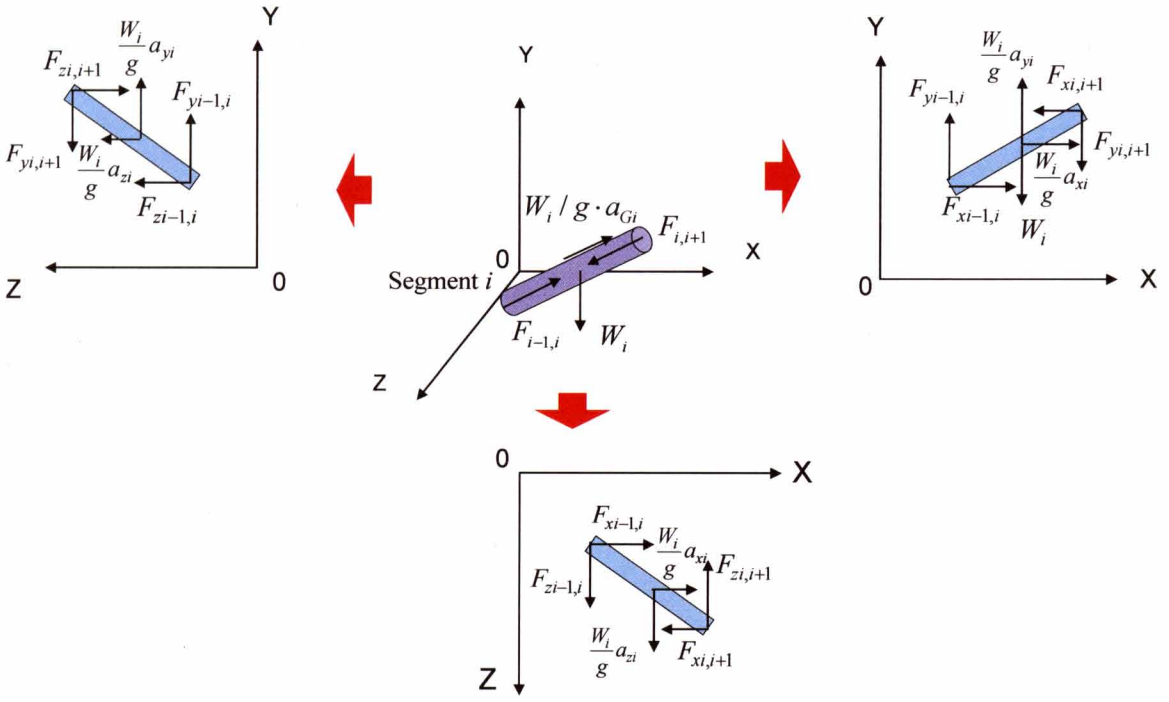


**Fig. 2.2** Net forces projected on each plane

Net forces from each segment can then be calculated with Newton-Euler equations [3, 4]. The weight of segment $i$ is represented by $W_i$, the acceleration of segment $i$ is represented by $a_{Gi}$ and the net force between each segment $i$ and $i$-1 is represented by $F_{i\text{-}1,\,i}$. Each rigid segment in 3-dimension is projected on the XY plane, the YZ plane and the ZX plane. Then net force $F_{i\text{-}1,\,i}$ is calculated for each plane in the static coordinate system as shown in Fig. 2.2. Newton's equation of each segment $i$ is defined as follows. Then, the weight of each segment $W_i$ is calculated from the mass of the participant with the distribution measured by Ae *et al.* [5].

$$\left(\frac{W_i}{g}\right)\underline{a}_{Gi} = \underline{F}_{i-1,i} - \underline{F}_{i,i+1} - W_i \cdot \underline{j} \qquad \underline{j} = \begin{pmatrix} 0 \\ 1 \\ 0 \end{pmatrix} \tag{2.1}$$

The net moment at each joint is also obtained with each rigid segment in 3-dimensions projected on the XY plane, the YZ plane and the ZX plane. The angles on each plane are represented by $\theta$ (on YZ plane), $\psi$ (on ZX plane) and $\phi$ (on XY plane). The angular

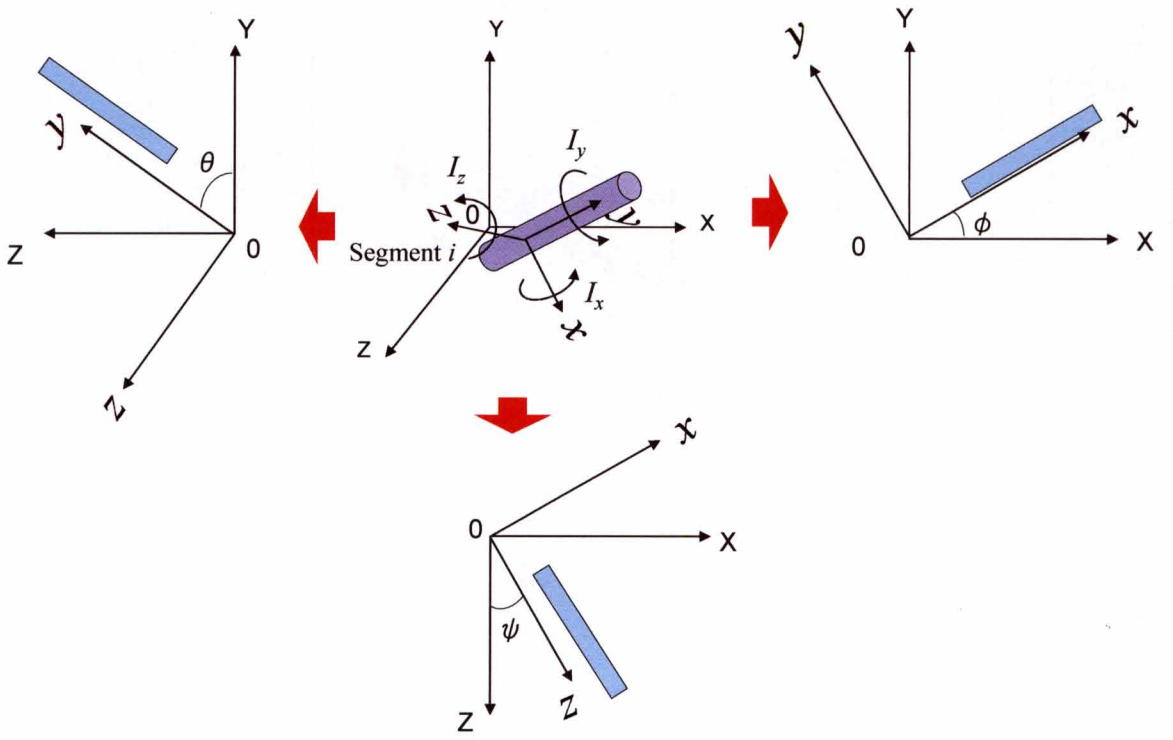


**Fig. 2.3** Segment of static and segment coordinate system

velocities are represented by $\omega_x$ (on YZ plane), $\omega_y$ (on ZX plane) and $\omega_z$ (on XY plane). The inertial moments that work around the main axis of segment as shown in Fig. 2.3 are represented by $I_x$, $I_y$, $I_z$. The external moments in the segment coordinate system are represented by $m_x$, $m_y$, $m_z$.

The external moments of segment coordinate system *m* is calculated as follow.

$$\begin{pmatrix} m_x \\ m_y \\ m_z \end{pmatrix} = \begin{pmatrix} I_x & 0 & 0 \\ 0 & I_y & 0 \\ 0 & 0 & I_z \end{pmatrix} \begin{pmatrix} \dot{\omega}_x \\ \dot{\omega}_y \\ \dot{\omega}_z \end{pmatrix} + \begin{pmatrix} I_z - I_y & 0 & 0 \\ 0 & I_x - I_z & 0 \\ 0 & 0 & I_y - I_x \end{pmatrix} \begin{pmatrix} \omega_y \omega_z \\ \omega_z \omega_x \\ \omega_y \omega_x \end{pmatrix} \tag{2.2}$$

Each segment is approximated and treated with the column. Then the inertial moment *I* is defined as follow.

$$I_x = I_z = \frac{W_i}{12g} \cdot (3r_i^2 + l_i^2)$$
$$I_y = \frac{W_i}{2g} \cdot r_i^2 \tag{2.3}$$

$W_i$ : *weight*
$r_i$ : *radius*
$l_i$ : *length*

The angular velocity $\omega$ is defined as follow.

$$\begin{pmatrix}\omega_x\\ \omega_y\\ \omega_z\end{pmatrix}=[\varphi][\psi]\begin{pmatrix}\dot{\theta}\\ 0\\ 0\end{pmatrix}+[\varphi]\begin{pmatrix}0\\ \dot{\psi}\\ 0\end{pmatrix}+\begin{pmatrix}0\\ 0\\ \dot{\varphi}\end{pmatrix}=[\pi]\begin{pmatrix}\dot{\theta}\\ \dot{\psi}\\ \dot{\varphi}\end{pmatrix} \tag{2.4}$$

Then, the matrixes are defined as follow.

$$[\pi]=\begin{bmatrix}\cos\varphi\cos\psi & \sin\varphi & 0\\ -\sin\varphi\cos\psi & \cos\varphi & 0\\ \sin\psi & 0 & 1\end{bmatrix},$$

$$[\theta]=\begin{bmatrix}1 & 0 & 0\\ 0 & \cos\theta & \sin\theta\\ 0 & -\sin\theta & \cos\theta\end{bmatrix},\ [\psi]=\begin{bmatrix}\cos\psi & 0 & -\sin\psi\\ 0 & 1 & 0\\ \sin\psi & 0 & \cos\psi\end{bmatrix},\ [\varphi]=\begin{bmatrix}\cos\varphi & \sin\varphi & 0\\ -\sin\varphi & \cos\varphi & 0\\ 0 & 0 & 1\end{bmatrix} \tag{2.5}$$

The angular acceleration $\dot{\omega}$ is defined as follow.

$$\begin{pmatrix}\dot{\omega}_x\\ \dot{\omega}_y\\ \dot{\omega}_z\end{pmatrix}=\frac{d}{dt}\left([\pi]\begin{bmatrix}\dot{\theta}\\ \dot{\psi}\\ \dot{\varphi}\end{bmatrix}\right)=[\pi]\begin{pmatrix}\ddot{\theta}\\ \ddot{\psi}\\ \ddot{\varphi}\end{pmatrix}+[\pi_1]\begin{pmatrix}\dot{\psi}\dot{\varphi}\\ \dot{\varphi}\dot{\theta}\\ \dot{\theta}\dot{\psi}\end{pmatrix},$$

$$[\pi_1]=\begin{pmatrix}\cos\varphi & -\sin\varphi\cos\psi & -\cos\varphi\sin\psi\\ -\sin\varphi & -\cos\varphi\cos\psi & \sin\varphi\sin\psi\\ 0 & 0 & \cos\psi\end{pmatrix} \tag{2.6}$$

Consequently, the net moment is calculated for each plane in the static coordinate system as shown in Fig. 2.4 where the link length of segment $i$ is represented by $l_i$, the inertial moment of static coordinate system of segment $i$ is represented by $IM_i$, the position vector of segment $i$ is represented by $\underline{\boldsymbol{r}}$ and the net moment between each segment $i$ and $i$-1 is represented by $M_{i\text{-}1,\,i}$. $IM_i$ is the inertial moments of the static coordinate system. Therefore, $IM_i$ must be calculated by multiplying the moment of the segment coordinate system $m_i$ by conversion matrix. The way to convert from segment coordinate system to static coordinate system is represented as follows.

$$\begin{bmatrix}M_x\\ M_y\\ M_z\end{bmatrix}=[\theta]^T[\psi]^T[\varphi]^T\begin{bmatrix}m_x\\ m_y\\ m_z\end{bmatrix} \tag{2.7}$$

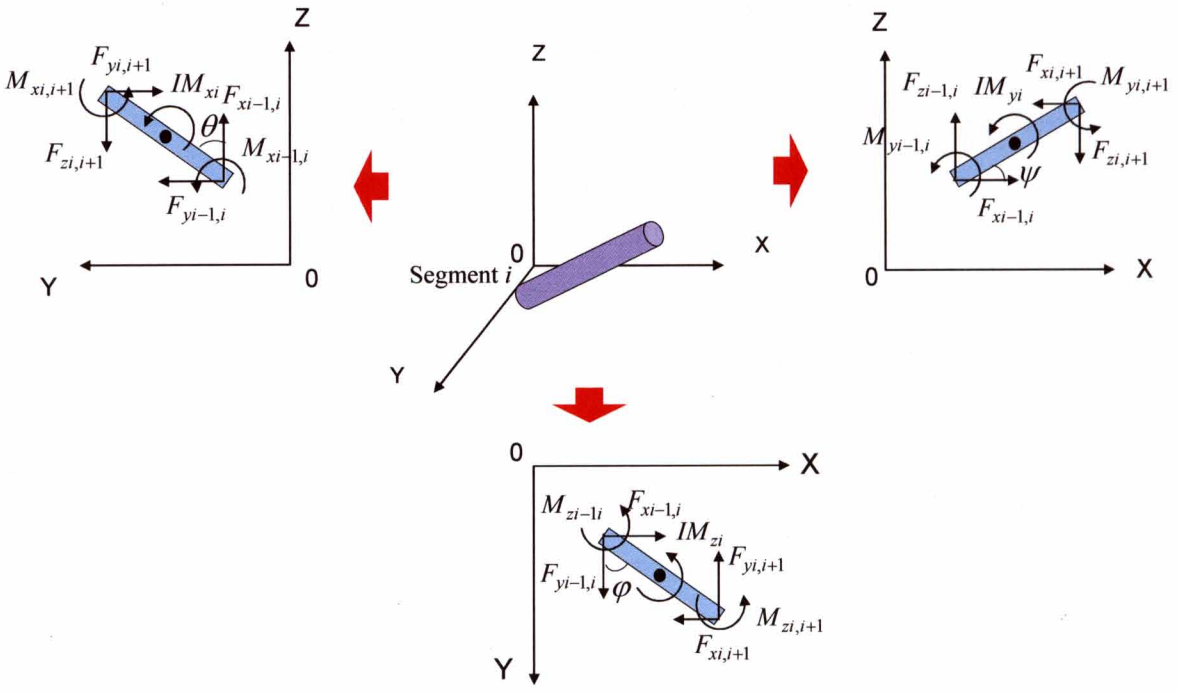


**Fig. 2.4** Net moments projected on each plane

Then the net moment in the static coordinate system is defined as follows.

$$\underline{IM}_i = \underline{M}_{i-1,i} - \frac{1}{2}\cdot l_i \cdot \underline{r} \times \underline{F}_{i-1,i} - \underline{M}_{i,i+1} - \frac{1}{2}\cdot l_i \cdot \underline{r} \times \underline{F}_{i,i+1} \tag{2.8}$$

For example, the net moment on the XY plane is,

$$\begin{aligned} IM_{zi} = M_{zi-1,i} - M_{zi,i+1} + \frac{1}{2} l_i \sin\varphi \cdot F_{xi-1,i} - \frac{1}{2} l_i \cos\varphi \cdot F_{yi-1,i} \\ + \frac{1}{2} l_i \sin\varphi \cdot F_{xi,i+1} - \frac{1}{2} l_i \cos\varphi \cdot F_{yi,i+1} \end{aligned} \tag{2.9}$$

## 2.3 Experimental data analysis method

The acceleration and angular acceleration of each segment are necessary to calculate net forces and net moments using Newton-Euler equations with the human segment model described in the preceding section. In this study, the positional data of the joints were obtained from the captured images with a motion capture system. The acceleration and the angular

acceleration are obtained with the positional data of the joints differentiated. In general, the acceleration and the angular acceleration obtained from the positional data have errors. The acceleration and the angular acceleration are required to be measured as accurately and noiselessly as possible because they effect the net forces and net moments directly. Therefore, the positional data of the joints obtained from the captured images are required to be smoothed to remove noises of positional data of the joints. This study smoothed the positional data of the joints using a Butterworth, zero-lag, low-pass filter [6, 7].

Low-pass digital filtering of noisy signals has for many years been an essential procedure for biomechanics. Probably, the most widely used filtering method in human movement analyses was first published by Winter *et al.* [6] and was later shown by Pezzack *et al.* [7] to successfully reduce the noise in kinematic signals and their derivatives. Butterworth filters are often chosen for smoothing movement data because they are optimally flat in their pass-band, have relatively high roll-offs and rapid response in the time domain. To make a zero-lag filter, the data were passed through the filter twice (once in the forward direction and once in reverse). To maintain the correct cutoff when using multiple passes of a filter (cascading) the cutoff frequency must be adjusted [8]. The following equations adjust the Butterworth filters.

$$C_{BW} = \frac{1}{\sqrt[4]{2^{\frac{1}{n}} - 1}} \tag{2.10}$$

$$f^*_{BW} = f_{BW} \times c_{BW} \tag{2.11}$$

where, $f_{BW}$ is the desired cutoff frequency and $f^*_{BW}$ is the adjusted cutoff frequency to produce the requested cutoff and $n$ is the number of filter passes. Notice that the Butterworth filter's cutoff is not adjusted when the data are passed once ($n$ = 1). The next step is to determine the corrected angular cutoff frequency of $\omega_c^*$ of the low-pass filter [9, 10] where *fsr* is the

sampling rate in hertz.

$$\omega_c^* = \tan\left(\frac{\pi f_{BW}^*}{f_{sr}}\right) \tag{2.12}$$

To compute the Butterworth filter coefficients let $K_1 = \sqrt{2}\omega_c^*$ and $K_2 = (\omega_c^*)^2$. The low-pass coefficients become:

$$a_0 = a_2 = \frac{K_2}{1 + K_1 + K_2}, a_1 = 2a_0 \tag{2.13}$$

$$b_1 = 2a_0\left(\frac{1}{K_2} - 1\right), b_2 = 1 - (a_0 + a_1 + a_2 + b_1) \tag{2.14}$$

The following equation is the second-order recursive filter:

$$y_j = a_0(x_j + 2x_{j-1} + x_{j-2}) + b_1 y_{j-1} + b_2 y_{j-2} \qquad j = \text{scene number} \tag{2.15}$$

On the other hand, the acceleration and the angular acceleration are obtained with the positional data of the joints differentiated. The mathematical differential formula is described as follows.

$$f'(t_i) = \lim_{\Delta t \to 0}\left(\frac{f(t_i + \Delta t) - f(t_i)}{\Delta t}\right) \tag{2.16}$$

However this equation can not apply to the human movement analysis because the positional data of the joints is discrete-time data. The differential formula for the discrete-time data is described as follows.

$$\dot{X}_1 = \frac{1}{2}(-3X_1 + 4X_2 - X_3) \cdot f_{sr} \tag{2.17}$$

$$\dot{X}_j = \frac{1}{2}(X_{j+1} - X_{j-1}) \cdot f_{sr} \tag{2.18}$$

$$\dot{X}_n = \frac{1}{2}(3X_n - 4X_{n-1} - X_{n-2}) \cdot f_{sr} \tag{2.19}$$

Then, $X_j$ is the data before derivation and $\dot{X}_j$ is the data after derivation. First, the

velocity is obtained from the positional data with the equations. Subsequently, the acceleration is obtained from the velocity with the equations.

Thus, the net forces and the net moments can be calculated with the positional data filtered from the obtained positional data and the human rigid segment model described above.

## 2.4 Estimation of ground reaction forces during 3-dimensional walking cycle

Ambulatory assessment is required in many applications of human movement analysis, including the evaluation of the impact of rehabilitation treatments in daily life [11, 12] and the ergonomic evaluation of working tasks and environments [13]. However, it is difficult to analyze ambulatory motions in which both feet are on the ground simultaneously unless at least one force platform or preferably two are available and positioned so that a participant's foot lands on no more than one force platform. Previously, net forces were calculated with ground reaction forces of each foot, measured by force platforms or pressure insoles [14] during ambulatory motions. But it is not always possible or affordable to have force platforms or pressure insoles under each foot. Furthermore, there are gait patterns that are not compatible with side-by-side force platforms or too large to permit single foot contacts, e.g., small children. Therefore, this study outlines a method that can calculate net forces at each joint during ambulatory motions from only captured trajectories and body segment parameters.

### 2.4.1 Method to estimate ground reaction forces during walking cycle

**Phases during walking cycle.** There are two phases during a walking cycle as shown in Fig. 2.5. The first is a single-support phase when only one leg is on the ground as shown in Fig.

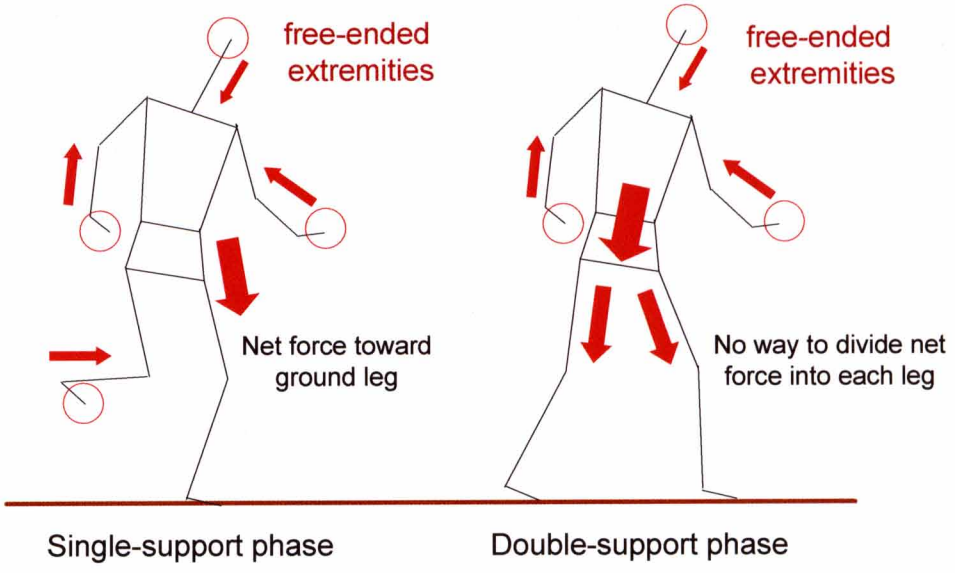


**Fig. 2.5** Support phase during a walking cycle

2.5 (left). In this case, it is possible to calculate net forces at each joint by proceeding from the free-ended extremity link-by-link toward the ground leg. The second is a double-support phase when both legs are on the ground as shown in Fig. 2.5 (right). In this case, the net forces of the joints of each leg are indeterminate because there is no way to divide the sum of net force on the hip joint from the free-ended extremities into each leg. If the net force on the hip joint can be divided into each leg, the net forces of the joints of each leg can be calculated with Newton-Euler equations on the thigh toward leg and foot. Then, the ground reaction forces of each leg can be obtained.

**Method to divide net force on the hip joint into each leg during double-support phases.** This study proposed a way to calculate net forces during double-support phases by assuming the sum of net forces on the hip joint from the free-ended extremities to be divided into each leg depending on the body gravity position. Then, the body gravity position can be calculated

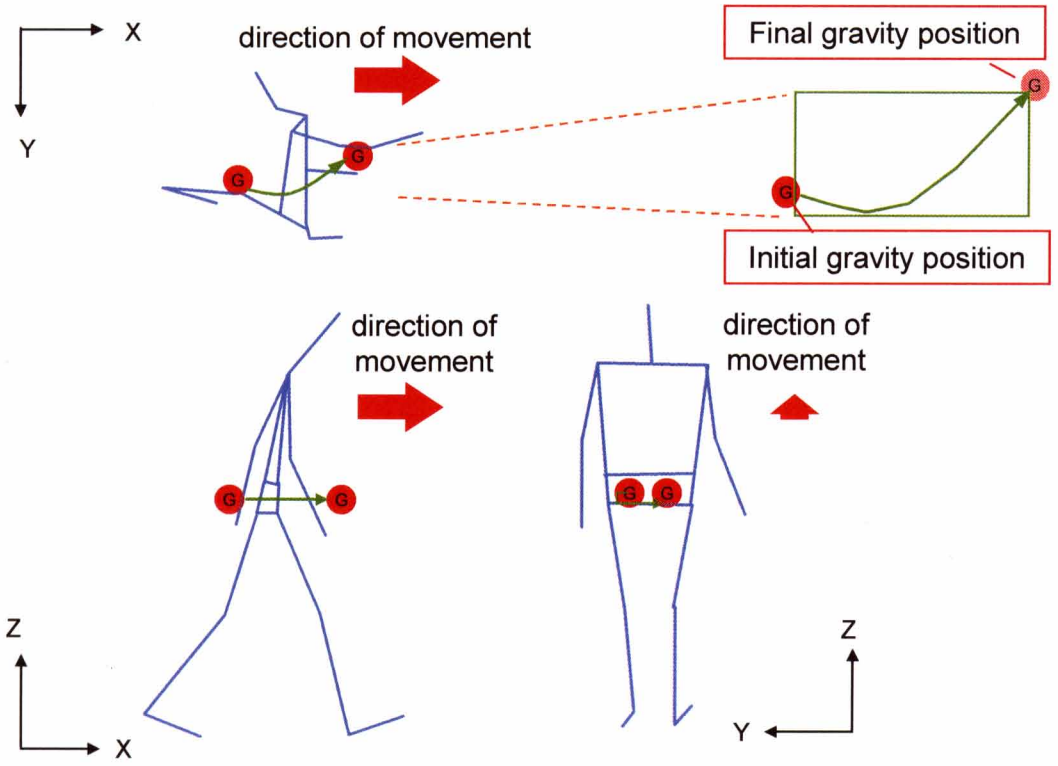


**Fig. 2.6** Behavior of the body gravity position during double-support phase

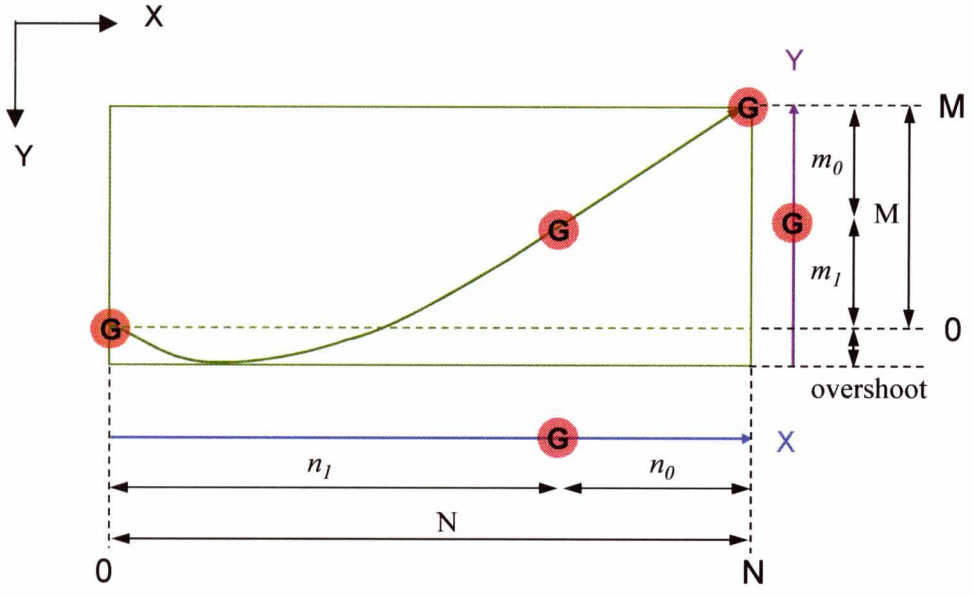


**Fig. 2.7** Determination of distribution of each leg

from the location of each body segment. Fig. 2.6 shows the behavior of the body gravity position when both legs are on the ground (from left foot touch-down to right foot toe-off). The distribution of the net force immediately before left foot touch-down has the right leg at

100% and that of left leg at 0%. Likewise the distribution of the net force on left leg is 100% and that of right leg is 0% at the moment when the right foot leaves the ground at its toe-off event. So the distribution of the net force is assumed to be determined by the rectangle on the XY plane that the trajectory of the centre of gravity makes as shown in Fig. 2.7. In the X direction, the distribution of right leg is 100% and that of left leg is 0% in the initial position. On the other hand, that of right leg is 0% and that of left leg is 100% in the final position. When the initial gravity position in X direction is assumed to be 0 and the final gravity position in X direction is assumed to be N, the distribution of right leg is $n_0 / N \times 100\%$ and that of left leg is $n_1 / N \times 100\%$ when the gravity position is $n_1$ as shown in Fig. 2.7. Similarly, in Y direction, when the initial gravity position is assumed to be 0 and the final gravity position is assumed to be M, the distribution of right leg is $m_0 / M \times 100\%$ and that of left leg is $m_1 / M \times 100\%$ when the gravity position is $m_1$ as shown in Fig. 2.7. However in Y direction, the gravity usually moves to the left after it moves to the right once. In this overshoot the distribution of right leg is assumed to be $(1 + overshoot/M) \times 100\%$ and that of left leg is assumed to be $(0 - overshoot/M) \times 100\%$. This overshoot is so small that the distribution of each leg will not become over 100% or under 0% when combined with both X direction and Y direction. So combined with both X direction and Y direction, the distribution of the net force on the hip joint into each leg is determined as follows. Then, the effects of the lengths of N and M are considered because the longer the length is, the more the effect is.

$$D_{right} = \left( \frac{M}{M+N} \times \frac{m_0}{M} + \frac{N}{M+N} \times \frac{n_0}{N} \right) \times 100 = \frac{m_0 + n_0}{M+N} \times 100\% \tag{2.20}$$

$$D_{left} = \left( \frac{M}{M+N} \times \frac{m_1}{M} + \frac{N}{M+N} \times \frac{n_1}{N} \right) \times 100 = \frac{m_1 + n_1}{M+N} \times 100\% \tag{2.21}$$

### 2.4.2 Experimental method

**Experimental protocol.** To validate the proposed method, data from a gait laboratory equipped with three force platforms were collected. Three participants (heights: 173.3±7.1 cm, masses: 85.0 ± 13.3 kg), after informed consent, participated in the study. Each participant was recorded (at 200 Hz) walking across the floor-mounted force platforms (Kistler) while the trajectories of reflective markers were captured by a Vicon MX infrared motion capture system at 200 frames per second.

**Data analysis.** The positional data of the joints obtained from the captured images were smoothed using a Butterworth low-pass filter (cutoff frequency 6 Hz) [6, 7]. The ground reaction forces were calculated with the proposed method and compared against the measured ground reaction forces obtained from the force platforms. In this study, the analysis programs were made with Borland C++ Builder 6 to calculate the ground reaction forces from the positional data with the proposed method.

### 2.4.3 Results and discussion

**Results.** The ground reaction forces of the three participants for the proposed method and the force platforms during gait cycle are shown in Fig. 2.8 to Fig. 2.10. The analysis range is from left foot initial contact to right foot toe-off. The double-support phase from initial contact by the foot to the other foot toe-off is represented by D1. The single-support phase by the foot is represented by S. The double-support phase from initial contact by the other foot to the foot toe-off is represented by D2. The correlations of the three participants between the estimated ground reaction forces and the force platforms for each phase are shown in Table 2.1 to Table 2.3. The root-mean-squared differences of the three participants between the

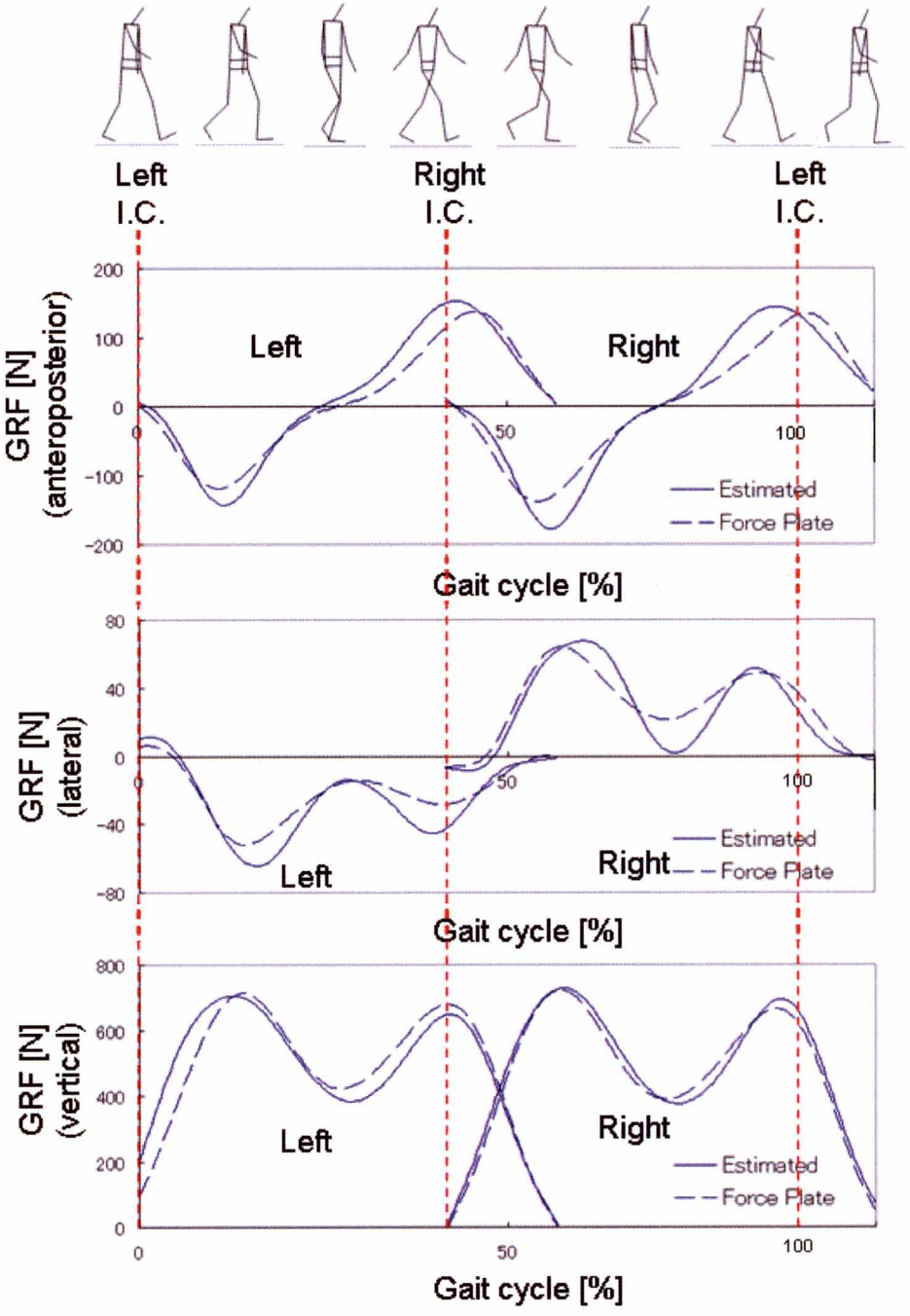


**Fig. 2.8** Ground reaction forces compared between the proposed method and the force platforms during gait cycle: Participant 1 (I.C. = initial contact)

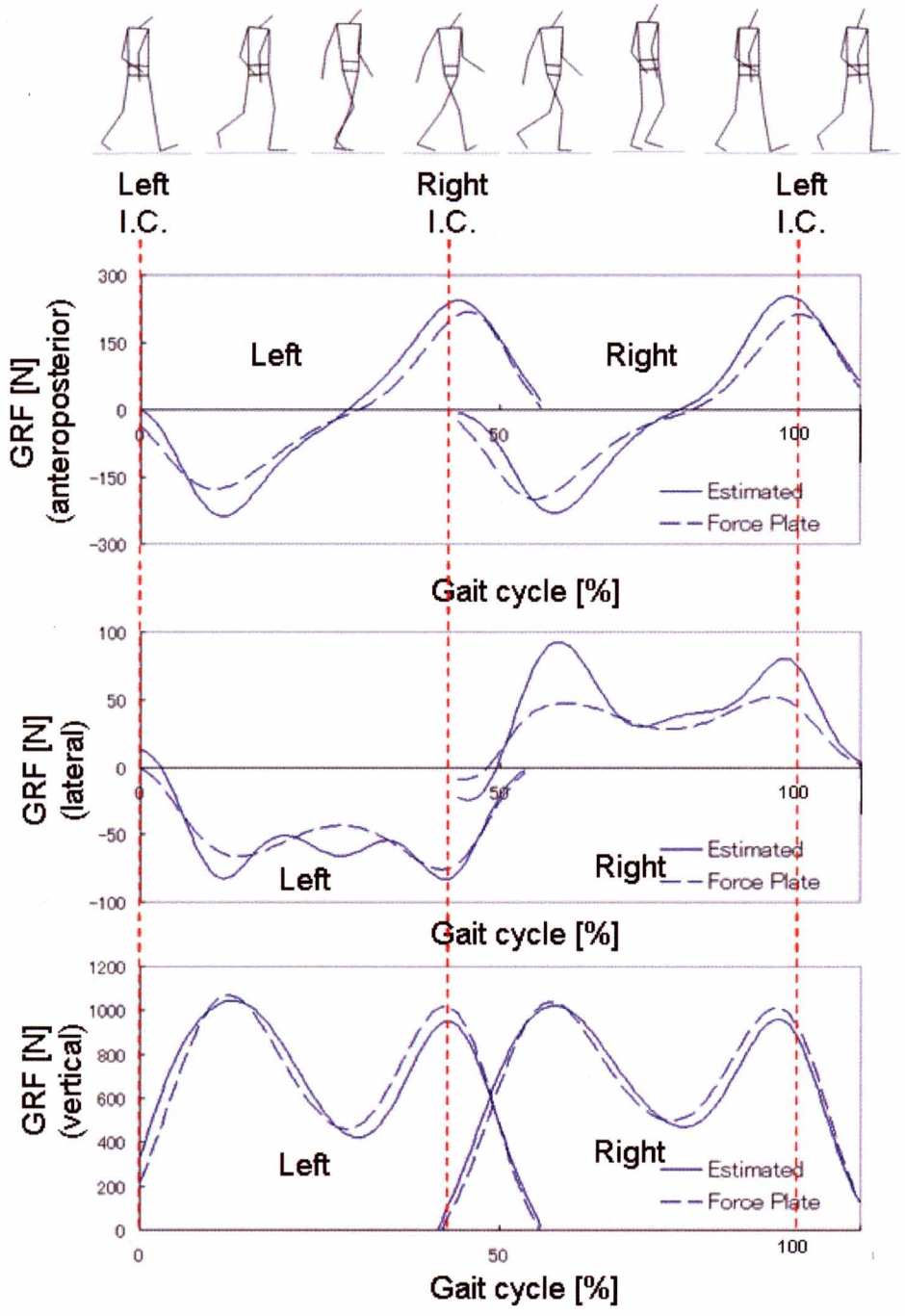


**Fig. 2.9** Ground reaction forces compared between the proposed method and the force platforms during gait cycle: Participant 2 (I.C. = initial contact)

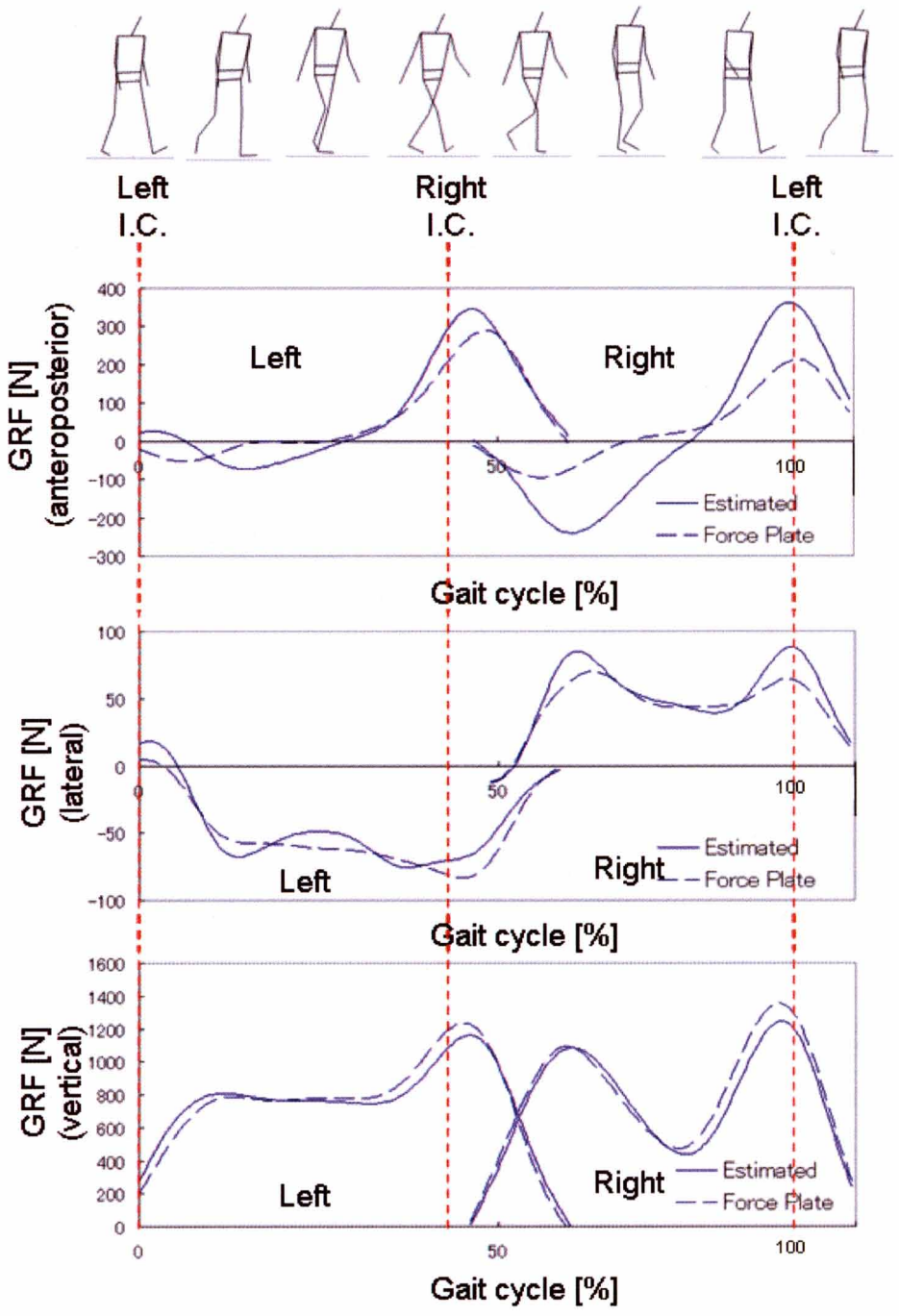


**Fig. 2.10** Ground reaction forces compared between the proposed method and the force platforms during gait cycle: Participant 3 (I.C. = initial contact)

**Table 2.1** Correlations between the estimated ground reaction forces and force platforms for each phase (D1 = first double-support phase, S = single-support phase, D2 = second double-support phase): Participant 1 (X=anteroposterior, Y=mediolateral, Z=vertical)

| | Left foot | | | Right foot | | |
|---|---|---|---|---|---|---|
| Phase | D1 | S | D2 | D1 | S | D2 |
| x | 0.99 | 0.99 | 0.98 | 0.97 | 0.99 | 0.98 |
| y | 0.99 | 0.93 | 0.96 | 0.99 | 0.91 | 0.96 |
| z | 0.99 | 0.98 | 0.99 | 0.99 | 0.98 | 0.99 |

**Table 2.2** Correlations between the estimated ground reaction forces and force platforms for each phase: Participant 2 (X=anteroposterior, Y=mediolateral, Z=vertical)

| | Left foot | | | Right foot | | |
|---|---|---|---|---|---|---|
| Phase | D1 | S | D2 | D1 | S | D2 |
| x | 0.99 | 0.99 | 0.99 | 0.97 | 0.99 | 0.99 |
| y | 0.99 | 0.61 | 0.99 | 0.99 | 0.84 | 0.99 |
| z | 0.99 | 0.96 | 0.99 | 0.99 | 0.97 | 0.99 |

**Table 2.3** Correlations between the estimated ground reaction forces and force platforms for each phase: Participant 3 (X=anteroposterior, Y=mediolateral, Z=vertical)

| | Left foot | | | Right foot | | |
|---|---|---|---|---|---|---|
| Phase | D1 | S | D2 | D1 | S | D2 |
| x | 0.11 | 0.99 | 0.99 | 0.92 | 0.98 | 0.99 |
| y | 0.99 | 0.54 | 0.99 | 0.99 | 0.91 | 0.99 |
| z | 0.99 | 0.98 | 0.99 | 0.99 | 0.97 | 0.99 |

**Table 2.4** Root means squared differences between the estimated ground reaction forces and force platforms for each phase (D1 = first double-support phase, S = single-support phase, D2 = second double-support phase): Participant 1 (X=anteroposterior, Y=mediolateral, Z=vertical) (%Yields = RMS divided by the value from minimum to maximum of the estimated ground reaction forces)

| | Left foot [N] (%Yields) | | | Right foot [N] (%Yields) | | |
|---|---|---|---|---|---|---|
| Phase | D1 | S | D2 | D1 | S | D2 |
| x | 11.4 (3.7 %) | 24.6 (8.0 %) | 10.2 (3.3 %) | 18.9 (5.7 %) | 30.8 (9.3 %) | 19.5 (5.9 %) |
| y | 4.0 (5.1 %) | 10.5 (13.5 %) | 2.5 (3.2 %) | 5.6 (7.1 %) | 11.2 (14.2 %) | 7.8 (9.9 %) |
| z | 129.9 (17.5 %) | 38.8 (5.2 %) | 19.4 (2.6 %) | 26.0 (3.5 %) | 26.9 (3.6 %) | 28.5 (3.8 %) |

**Table 2.5** Root means squared differences between the estimated ground reaction forces and force platforms for each phase: Participant 2 (X=anteroposterior, Y=mediolateral, Z=vertical)

| | Left foot [N] (%Yields) | | | Right foot [N] (%Yields) | | |
|---|---|---|---|---|---|---|
| Phase | D1 | S | D2 | D1 | S | D2 |
| x | 32.5 (6.9 %) | 38.8 (8.2 %) | 15.4 (3.3 %) | 46.2 (9.7 %) | 39.9 (8.4 %) | 11.2 (2.4 %) |
| y | 10.7 (11.6 %) | 11.7 (12.7 %) | 3.5 (3.8 %) | 13.6 (11.9 %) | 22.5 (19.7 %) | 14.2 (12.5 %) |
| z | 122.1 (12.1 %) | 66.3 (6.6 %) | 33.1 (3.3 %) | 61.0 (6.1 %) | 52.7 (5.3 %) | 40.2 (4.0 %) |

**Table 2.6** Root means squared differences between the estimated ground reaction forces and force platforms for each phase: Participant 2 (X=anteroposterior, Y=mediolateral, Z=vertical)

| | Left foot [N] (%Yields) | | | Right foot [N] (%Yields) | | |
|---|---|---|---|---|---|---|
| Phase | D1 | S | D2 | D1 | S | D2 |
| x | 49.4 (11.9 %) | 48.7 (11.8 %) | 10.9 (2.6 %) | 67.2 (11.3 %) | 121.0 (20.4 %) | 63.4 (10.7 %) |
| y | 10.5 (11.2 %) | 9.4 (10.0 %) | 10.0 (10.6 %) | 6.0 (6.1 %) | 11.9 (12.0 %) | 10.5 (10.6 %) |
| z | 80.0 (7.0 %) | 56.4 (4.9 %) | 54.9 (4.8 %) | 45.9 (3.8 %) | 83.4 (6.8 %) | 54.9 (4.5 %) |

estimated ground reaction forces and the force platforms for each phase are shown in Table 2.4 to Table 2.6.

**Discussion.** The results showed that the correlations between the estimated ground reaction forces and the force platforms during single-support phases were weaker than those during double-support phases. Furthermore, the root-mean-squared differences between the estimated ground reaction forces and the force platforms during single-support phases were larger than those during double-support phases. The reason for this is considered to be measurement error. The movements of many segments during single-support phases are faster than those of double-support phases. The number of moving segments during single-support phases is also larger than that during double-support phases such as non-support leg. The accelerations of each segment are quite different from the actual ones when the measurement error of the joint position is not negligible. That is why the net forces of each segment are quite different from actual ones.

The results also showed that the correlations of mediolateral direction were weaker than those of another direction. Furthermore, the root-mean-squared differences of mediolateral direction were larger than those of another direction. Generally, ground reaction forces during walking work for mainly vertical and anteroposterior directions. On the contrary, ground reaction forces working for mediolateral direction are small. Then the error of the net forces

distributed by the proposed method is considered to affects the results of the correlations and the yield of root-mean-squared differences a lot. These reasons are considered to make the correlations of mediolateral direction weaker and the root-mean-squared differences of mediolateral direction larger.

The results also showed that the differences between the estimated ground reaction forces and the force platforms of participant 3 were larger than those of another participant. The differences of anteroposterior and mediolateral directions were conspicuously large though those of vertical direction were small. Generally, the yields of root-mean-square differences of anteroposterior and mediolateral directions are easily affected by the measurement error because the values from minimum to maximum of the ground reaction forces of those directions are small. However, the differences of especially anteroposterior direction of participant 3 were relatively large. The reason for this is considered to be incorrect distribution of the participants' mass to each segment. The net forces estimated on each segment are quite different from the actual ones when the mass of each segment is different from the actual one. Another reason is considered to be forces derived from muscles. Forces derived from muscles can work on the force platforms even if the segments are static. Forces derived from muscles cannot be evaluated while the segments are static because the human segment model cannot consider the role of muscles. Then, the walking motion pattern of participant 3 may be different from another participant. Thus, the proposed method is

considered to be difficult to estimate ground reaction forces precisely during walking that the forces derived from muscles work greatly.

However, the results of this study showed that the patterns of the ground reaction forces estimated by the proposed method were similar to those of the force platforms especially on the anteroposterior and vertical directions that have a great effect on the walking. The correlations between the estimated ground reaction forces and the force platforms were also strong. The averages of the correlations throughout the walking cycle of participant 1 of the left foot were 0.98 on the anteroposterior direction and 0.92 on the vertical direction. Those of the right foot were 0.97 and 0.99. Those of participant 2 of the left foot were 0.99 on the anteroposterior direction and 0.96 on the vertical direction. Those of the right foot were 0.98 and 0.98. Those of participant 3 of the left foot were 0.95 on the anteroposterior direction and 0.99 on the vertical direction. Those of the right foot were 0.96 and 0.98. Furthermore, the results of this study showed that the root-mean-squared differences between the estimated ground reaction forces and the force platforms were not so large. The averages of the yields of the root-mean-squared differences throughout the walking cycle of participant 1 of the left foot were 5.0 % on the anteroposterior direction and 8.4 % on the vertical direction. Those of the right foot were 7.0 % and 3.7 %. Those of participant 2 of the left foot were 6.1 % on the anteroposterior direction and 7.3 % on the vertical direction. Those of the right foot were 6.8 % and 5.2 %. Those of participant 3 of the left foot were 8.7 % on the anteroposterior

direction and 5.6 % on the vertical direction. Those of the right foot were 14.1 % and 5.0 %. Then the reasons that the yields of participant 3 were relatively large were mentioned as above.

Therefore the proposed method was considered to successfully estimate the net forces at the joints as well as the ground reaction forces throughout a walking cycle. Thus, the methods proposed in this study permit inverse dynamics analyses of locomotor activities without the necessity of imbedded force platforms. Such situations include the following: studies with very small or very tall people, studies with blind people who cannot target the force platforms and studies where force platforms cannot be positioned to record two consecutive landings. This study applied the proposed method only to the walking cycle under the standard condition. Then, one of the future works of this study is considered to be validation whether the proposed method can be applied to the walking cycle under another condition such as slop.

## 2.5 Conclusion

This study investigated the whole-body human rigid segment model to calculate the net forces and the net moments from the captured images obtained with motion capture system. Previously, the human segment model has been usually applied to only open-loop motions. Then, this study proposed a way to estimate net forces at all joints as well as the ground

reaction forces throughout a walking cycle using only with motion capture data and body segment parameters. Several walking trials were conducted to validate the proposed method. The results of this study showed that the correlations between the estimated ground reaction forces and force platforms were very strong. Furthermore, the root-mean-squared differences between the estimated ground reaction forces and the measured ones especially on the anteroposterior direction and the vertical direction that have a great effect on the walking were relatively small. Therefore the proposed method was considered to successfully estimate the net forces at the joints as well as the ground reaction forces throughout a walking cycle.

Previously, the net forces and net moments during walking motion created by the computer simulation could not be estimated because double-support phase during walking needs at least one force platform or preferable two. When the ground reaction forces can be estimated only with the captured motions as this study, the walking motion created by the computer simulation can be evaluated in the computer. Then the variety of motions that the computer human model can evaluate will be growing with the help of this study.

**References**

[1] McMahon T. A. : Muscles, Reflexes, and Locomotion, Princeton, NJ: Princeton University Press, 1984.

[2] Hatze H. : Quantitative analysis, synthesis and optimization of human motion, Human Movement Science, 3, 5-25, 1981.

[3] Stepanenko Y., Vukobratovic M. : Dynamics of articulated open-chain active mechanisms, Mathematical Biosciences, 28, 137-170, 1976.

[4] Orin D. E., McGhee R. B., Vukobratovic M., Hartoch G. : Kinematic and kinetic analysis of open-chain linkage utilizing Newton-Euler method, Mathematical Biosciences, 43, 107-130, 1979.

[5] Ae M., Tang H., Yokoi T. : Estimation of inertia properties of the body segments in Japanese athletes, Society of Biomechanisms Japan, 11, 23-33, 1992.

[6] Winter D. A., Sidwall H. G., Hobson D. A. : Measurement and reduction of noise in kinematics of locomotion, Journal of Biomechanics, 7, 157–159, 1974.

[7] Pezzack J. C., Winter D. A., Norman R. W. : An assessment of derivative determining techniques for motion analysis, Journal of Biomechanics, 10, 377–382, 1977.

[8] Robertson D. G. E., Dowling J. J : Design and responses of Butterworth and critically damped digital filters, Journal of Electromyography and Kinesiology, 13, 569-573, 2003.

[9] Winter D.A. : Biomechanics and Human Movement, Wiley Interscience, Toronto, 1979.

[10] Murphy S. D., Robertson D. G. E. : Construction of a high-pass digital filter from a low-pass digital filter, Journal of Applied Biomechanics, 10, 374–381, 1994.

[11] Bussmann J. B. J., Veltink P. H., Koelma F., Lummel R. C. V., Stam H. J. : Ambulatory monitoring of mobility-related activities: The initial phase of the development of an activity monitor, European Journal of Physical Medicine and Rehabilitation, 5, 2–7, 1995.

[12] Buschmann H. B., Reuvekamp P. J., Veltink P. H., Martens W. L., Stam H. J. : Validity and reliability of measurements obtained with an "activity monitor" in people with and without a transtibial amputation, Phys. Therapy, 78, 989–998, 1998.

[13] Baten C. T. M., Oosterhoff P., Kingma I., Veltink P. H., Hermens H. J. : Inertial sensing in ambulatory load estimation, Proc. 18th Annual International Conference of the IEEE Engineering, Medical and Biological Society, Amsterdam, Netherlands, 1996.

[14] Cordero A. F., Koopman H. J. F. M., Helm F. C. T. : Inverse dynamics calculations during gait with restricted ground reaction force information from pressure insoles, Gait and Posture, 23(2), 189-199, 2006.

# 3. Motion analysis with a musculoskeletal model of lower limb that considers the roles of antagonistic muscles and biarticular muscles

## 3.1 Introduction

The method to calculate net forces and net moments at each joint during motions from captured images using the human rigid segment model was described in chapter 2. Furthermore this study proposed a way to estimate net forces at all joints as well as the ground reaction forces throughout a walking cycle using only with motion capture data and body segment parameters and validated the proposed method in the experiments in chapter 2.

However, estimation of muscle forces during human motions is important in the fields of sport, ergonomics and bioengineering in order to improve sport techniques, rehabilitation procedures, product designs and work environments, and so on. In general, in the musculoskeletal models that have been developed, the roles of antagonistic muscles and biarticular muscles are not considered to estimate muscle forces. Antagonistic muscles are the muscles that act in opposition to the prime movers or agonists of a movement. Biarticular muscles are the muscles that work simultaneously on two joints. Then this study investigated a musculoskeletal model that considers the roles of antagonistic muscles and biarticular muscles. Furthermore this study validated the proposed model to estimate muscle forces by applied to vertical jumping and jogging motion as exsamples of dynamic motions.

### 3.2 Estimation of muscle forces using a musculoskeletal model

#### 3.2.1 Muscle arrangements at the lower limb

As there are many muscles in the lower limb, it is difficult to model all the contributory muscles. So this study used a musculoskeletal model that includes nine representative muscles in sagittal plane as shown in Fig. 3.1. The following muscles are included: 1-tibialis anterior (TA), 2-gastrocnemius (GAS), 3-soleus (SOL), 4-rectus femoris (RF), 5-vastus lateralis (VAS), 6-semimembranosus (SM), 7-biceps femoris and short head (BFSH), 8-iliopsoas (IL) and 9-gluteus maximus (GMAX). Then, GAS, RF and SM are biarticular muscles and others are monoarticular muscles.

#### 3.2.2 Optimization method

Crowninshield *et al.* [1] outlined an optimization method to estimate muscle forces.

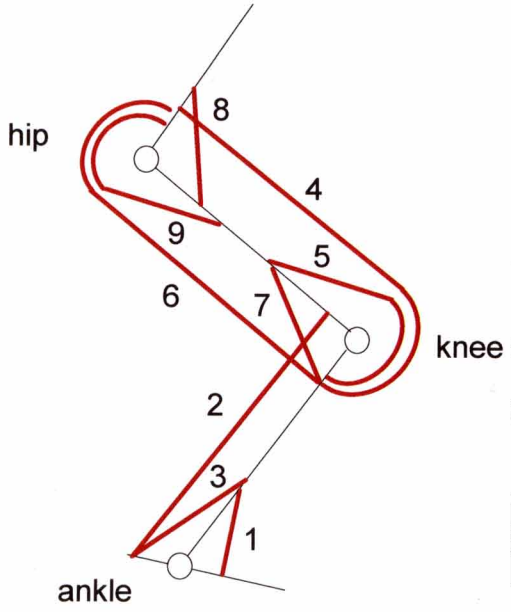


| No. | Muscle actuator |
|---|---|
| 1 | Tibialis anterior (TA) |
| 2 | Gastrocnemius (GAS) |
| 3 | Soleus (SOL) |
| 4 | Rectus femoris (RF) |
| 5 | Vastus lateralis (VAS) |
| 6 | Semimenbranosus (SM) |
| 7 | Biceps femoris and short head (BFSH) |
| 8 | Iliopsoas (IL) |
| 9 | Gluteus masimus (GMAX) |

**Fig. 3.1** Muscle arrangements at the human lower limb

They suggested that the formula (3.1) shown below is assumed to be the equality condition and the formula (3.2) is assumed to be the inequality condition. Muscle forces are determined by minimizing the objective function, $u$, in formula (3.3).

$$M_j = \sum_i r_i \times F_i \tag{3.1}$$

$$F_{i\min} \le F_i \le F_{i\max} \tag{3.2}$$

$$u = \sum_{i=1}^{m} (\frac{F_i}{A_i})^n \tag{3.3}$$

Then the net moment acting on a joint $j$ is represented by $M_j$. Moment arm and force of muscle $i$ are represented by $r_i$ and $F_i$. $m$ is the number of muscles in the model. They investigated that coefficient $n$=2 or 3 was effective. Minimum force and maximum force of muscle $i$ are represented by $F_{imin}$ and $F_{imax}$. This method can estimate muscle forces from the net moments at the joints. However, these methods unfortunately usually do not consider the functions of antagonistic muscles and biarticular muscles. If musculoskeletal models do not consider these roles of muscles, they are unlikely to accurately portray the magnitudes of the agonistic muscles.

### 3.2.3 Coordination-control model that considers the roles of antagonistic muscles and biarticular muscles

Oshima *et al.* [2] suggested a coordination-control model that considers the roles of the antagonistic muscles and biarticular muscles. The model including three pairs of the

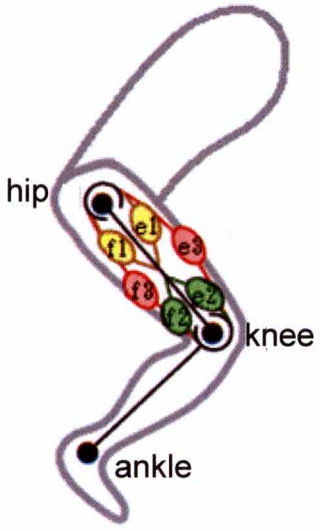


**Fig. 3.2** Model including three pairs of the antagonistic muscles [2]

antagonistic muscles in lower limb suggested by Oshima *et al.* [2] is shown in Fig. 3.2.

The model consists of 6 muscles, muscle f1 substituted for GMAX, muscle e1 substituted for IL, muscle f2 substituted for BFSH, muscle e2 substituted for VAS, muscle f3 substituted for SM and muscle e3 substituted for RF. Then the muscle f1 and the muscle e1 are the antagonistic monoarticular muscles pair, which works on the hip joint. The muscle f2 and the muscle e2 are also the antagonistic monoarticular muscles pair, which works on the knee joint. The muscle f3 and the muscle e3 are the antagoni stic biarticular muscles pair, which works simultaneously on both the hip and knee joints. Oshima *et al.* [2] defined that these muscles act on the distal extremity and the maximum force of each muscle acts on the distal extremity as $F'_{mf1}$, $F'_{me1}$, $F'_{mf2}$, $F'_{me2}$, $F'_{mf3}$, $F'_{me3}$ as shown in Fig. 3.3. Then the maximum output force distribution on the distal extremity is geometrically a hexagon from maximum force of each muscle. They also verified the maximum output force distribution on the distal extremity was

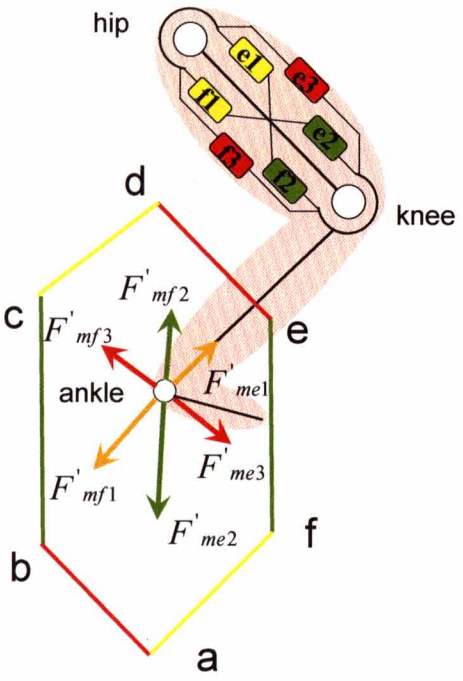


**Fig. 3.3** Coordination-control model of the lower limb [2]

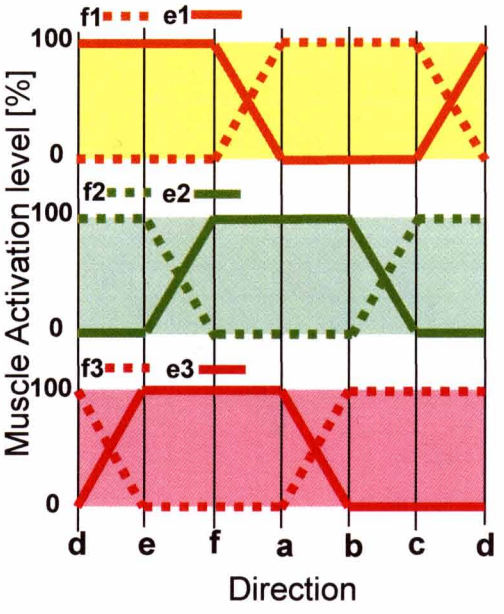


**Fig. 3.4** Muscle activation pattern of each output force direction [2]

a hexagon in the experiment. The position of this hexagon changes depending on the posture or arrangement of the joints. This is that the side *ab* and *de* is parallel to the thigh segment, the side *af* and *cd* is parallel to the leg segment and the side *bc* and *ef* is parallel to the line from the hip joint to the ankle joint. They also investigated the vector of the output force on the distal extremity is related to a muscle activation pattern as shown in Fig. 3.4. For example, when the vector of the output force is direction *a* as maximum in Fig. 3.3, the muscle forces are defined as 100% of maximum muscle force for muscles f1, e2 and e3 and 0% of maximum muscle force for muscles e1, f2 and f3. Therefore the distribution of each muscle force is determined by the vector of the output force on the distal extremity and the muscle

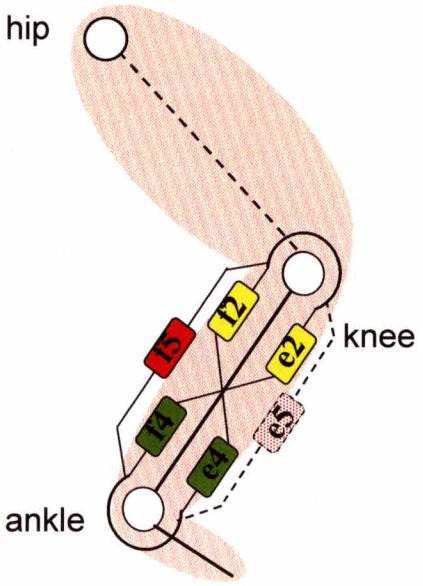


**Fig. 3.5** Adaptation of coordination-control model to the lower leg

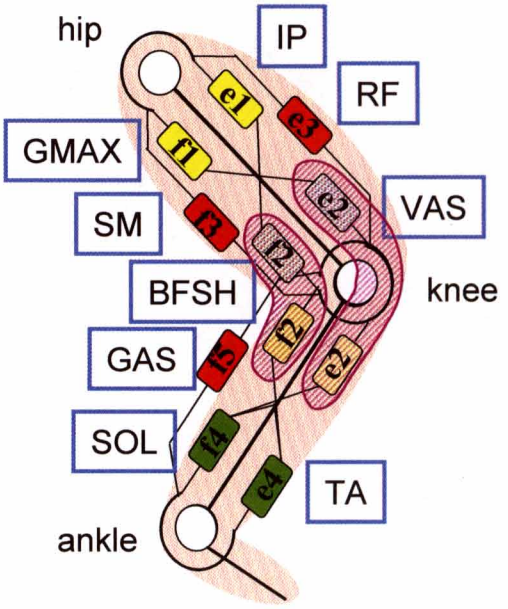


**Fig. 3.6** Extended musculoskeletal model of the lower limb

activation pattern.

The distribution of each muscle force can be calculated with the model mentioned as above. However this model is not enough to apply to dynamic motions in which muscles existing on the lower leg work effectively such as vertical jumping and jogging motion because this model has only been applied to the muscles existing on the thigh. For this study, this problem was overcome by applying the former model to the lower leg as shown in Fig. 3.5. This study considered the lower leg same as the former thigh model by including muscles f2 and e2, which act on the knee joint, and by existing temporary biarticular muscle e5 that has slight muscle force. Thus, the muscle forces of the lower leg could be calculated with the same method as the thigh model. Then the muscles f2 and e2 are determined with the thigh model

and the lower leg model because these muscles exist in both models. In this study, muscle forces of muscle f2 and e2 estimated with the lower leg model were used because muscle forces estimated with the lower leg model were not so different from those estimated with the thigh model in the experiments as described later. Then the thigh model has 6 muscles and the lower leg model has 6 muscles. In these muscles, muscle f2 and muscle e2 are overlapping the both model and muscle e5 in the lower leg model is existing temporarily. So the extended model has 9 muscles in the lower limb, Tibialis anterior(e4), Gastrocnemius (f5), Soleus (f4), Rectus femoris (e3), Vastus lateralis (e2),Semimenbranosus (f3), Biceps femoris and short head (f2), Iliopsoas (e1) and Gluteus maximus (f1) as shown in Fig. 3.6.

The maximum force of each muscle is necessary to be clarified preliminarily to estimate the muscle forces during motions with the proposed musculoskeletal model. In this study, the maximum force of each muscle was determined by references. Maximum muscle force $F_{i\max}$ can be described by $F_{i\max} = A_i \times \sigma$ because $F_{i\max}$ is proportional to the physical cross-sectional area $A_i$ (Spector *et al.* [3]). $\sigma$ is the magnitude of the force that can be generated in unit area and was investigated by many researches [4, 5, 6]. In this study, $\sigma$ was assumed to be $\sigma = 50\ [N/cm^2]$ and maximum muscle force $F_{i\max}$ was determined. This study used physical cross-sectional area $A_i$ measured by Akima *et al.* [7]. The physical cross-sectional area of each muscle is shown in Fig. 3.7.

However, the proposed musculoskeletal model can not use the maximum muscle force $F_{i\max}$

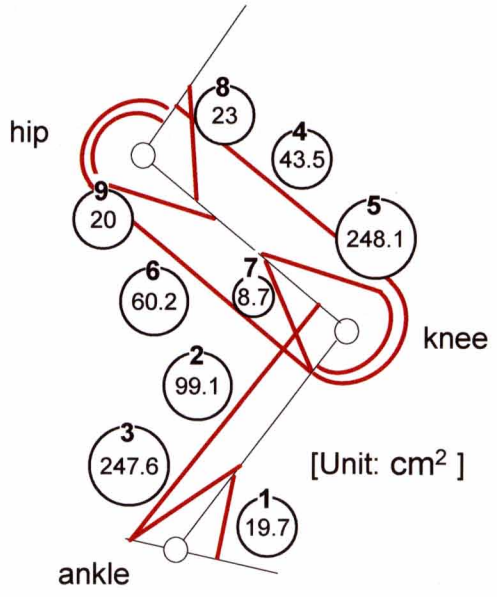


**Fig. 3.7** Estimated values of physical cross-sectional areas [7]

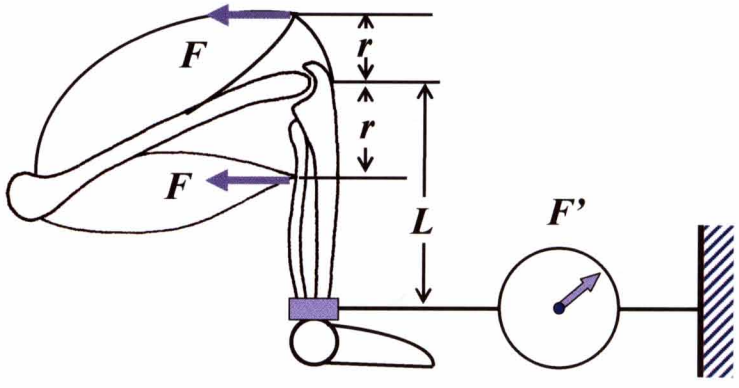


**Fig. 3.8** The mechanism of muscle levers

directly because the maximum muscle force is different from the maximum output force on the distal extremity. Then this study defined the maximum output force on the distal extremity $F'_{imax}$ with the muscle levers as shown in Fig. 3.8. The muscle force represented by $F$ is always larger than the output force on the distal extremity represented by $F'$ because the link length $L$ is always longer than the moment arm $r$. Then the relationship between $F$ and $F'$ is

described as follow.

$$F' = F \times r / L \tag{3.4}$$

This study used the moment arm $r_i$ measured by Hoy *et al.* [8]. Thus, this study converted the maximum force $F_{i\max}$ to the maximum output force $F'_{i\max}$.

The vector of the output force on the distal extremity is necessary to be calculated to estimate the distribution of each muscle using the coordination-control model described as above. The vector of the output force on the distal extremity can be calculated from the net moments at the hip and knee joints. The output force of x axis is represented by $f_x$, that of y axis is represented by $f_y$, the angle of the ankle and knee joints are represented by $\theta_{ankle}$ and $\theta_{knee}$, the link length of the thigh and the leg are represented by $l_{thigh}$ and $l_{leg}$ and the net moments of the hip and knee joints are represented by $M_{hip}$ and $M_{knee}$ as shown in Fig. 3.9. The relationship between the output force and the net moments is represented as follows. The vector of the output force can be calculated by solving the simultaneous equations.

$$M_{hip} = (l_{leg} \sin\theta_{ankle} + l_{thigh} \sin\theta_{knee}) f_x - (l_{leg} \cos\theta_{ankle} + l_{thigh} \cos\theta_{knee}) f_y \tag{3.5}$$

$$M_{knee} = (l_{leg} \sin\theta_{ankle}) f_x - (l_{leg} \cos\theta_{ankle}) f_y \tag{3.6}$$

Similarly, the vector of the output force on the distal extremity in the lower leg model can be calculated from the net moments at the knee and ankle joints.

The distribution of each muscle force can be estimated with the obtained output force on the distal extremity ($f_x$, $f_y$) applied to the model in Fig. 3.3. Then the muscle forces can be

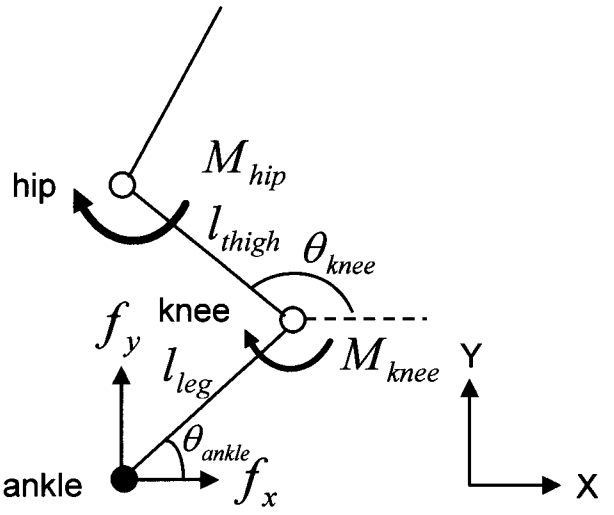


**Fig. 3.9** Relationship between output force on the distal extremity and net moments

estimated with the scale of the vector of the output force.

### 3.3 Hill muscle model

Each muscle force existing on the lower limb can be calculated with the model described in preceding section. In general, electromyograms (EMGs) are usually used to validate the estimated muscle forces because muscle forces can not be measured directly. However, strictly speaking, the estimated muscle forces can not be validated with the electromyograms during dynamic motions in which the muscle contraction rate is not negligible such as vertical jumping and jogging motion because electromyograms measure the muscle activation level, not muscle forces. Then this study calculated the muscle activation level from the estimated muscle forces using Hill muscle model. Many muscle model based on Hill muscle model have been suggested. This study used the muscle model suggested by Delp *et al.* [9] as shown

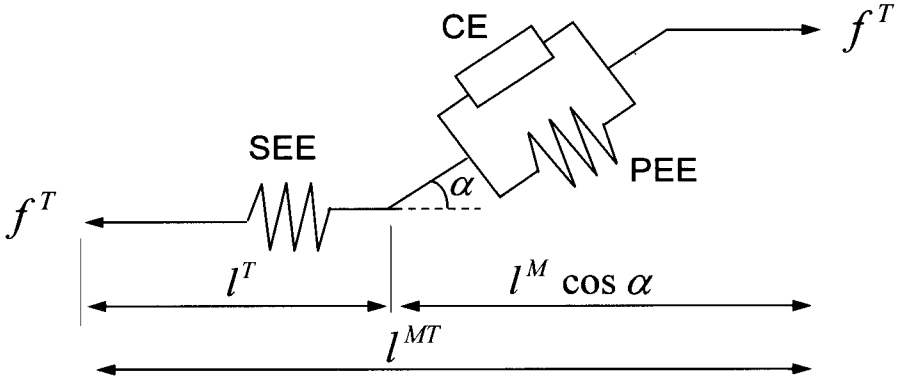


**Fig. 3.10** Hill muscle model suggested by Delp *et al.* [9]

in Fig. 3.10. This model consists of three components, contraction element (CE), parallel elastic element (PEE), sinew elastic element (SEE). This model can calculate the muscle activation level from the estimated muscle forces during dynamic motions as vertical jumping and jogging motion. The parameter of the pinnate angle is represented by $\alpha$, the natural length of muscle fiber is represented by ${l_0}^M$ and the natural length of tendon is represented by ${l_s}^T$. This study used these parameters measured by Hoy *et al.* [8]. The forces of CE, PEE and SEE in Fig. 3.10 are represented by $f^{ce}$, $f^{pe}$, $f^T$. The forces of CE, PEE and SEE normalized by the maximum muscle forces are represented by $\tilde{f}^{ce}$, $\tilde{f}^{pe}$, $\tilde{f}^T$. The length of CE, PEE and SEE are represented by $l^{ce}$, $l^{pe}$, $l^T$. The length of the muscle-tendon represented by $l^{MT}$ consists of the sum of the length of the muscle fiber and the tendon. When it is assumed to be $l^M = l^{ce} = l^{pe}$, the length of the muscle-tendon ($l^{MT}$) can be calculated with the pinnate angle $\alpha$ as follow.

$$l^{MT} = l^M \cos\alpha + l^T \tag{3.7}$$

The relationship of muscle forces among the elements are described as follow.

$$f^T = (f^{ce} + f^{pe})\cos\alpha \tag{3.8}$$

The coefficient of extension of the tendon represented by $\tilde{\varepsilon}$ is defined as follow.

$$\tilde{\varepsilon} = \frac{l^T - {l_s}^T}{{l_s}^T} \tag{3.9}$$

Delp *et al.* [9] investigated the relationship between the normalized force and the coefficient of extension of the tendon, the relationship between the normalized force and the normalized length and the relationship between the normalized force and the normalized velocity in the experiment. These relationships are shown in Fig. 3.11. The maximum contraction velocity of contraction element represented by $v^0$ is assumed to be $10{l_0}^M$ m/s ($ {l_0}^M$ : natural length of muscle fiber) [10]. The muscle activation level is represented by $a$, the relationship between the normalized force and the coefficient of extension of the tendon is represented by $\tilde{f}^T(\tilde{\varepsilon})$, the relationship between the normalized force and the normalized length is represented by $\tilde{f}^{ce}(\tilde{l}^M)$ and $\tilde{f}^{pe}(\tilde{l}^M)$ and the relationship between the normalized force and the normalized velocity is represented by $g^{ce}(v^{ce}/v^0)$. Then the formulas are defined as follows.

$$f^{ce} = f_{i\max} \cdot \tilde{f}^{ce}(\tilde{l}^M) \cdot g^{ce}(v^{ce}/v^0) \cdot a \tag{3.10}$$

$$f^{pe} = f_{i\max} \cdot \tilde{f}^{pe}(\tilde{l}^M) \tag{3.11}$$

$$f^T = f_{i\max} \cdot \tilde{f}^T(\tilde{\varepsilon}) \tag{3.12}$$

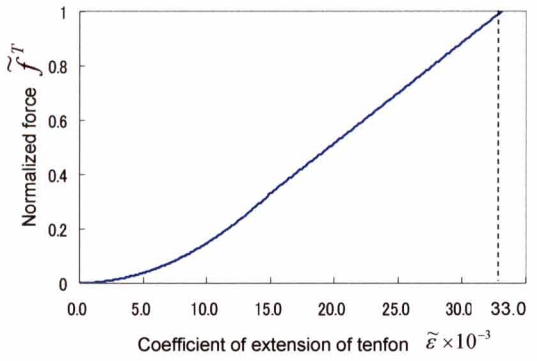


(a) Relationship between normalized force and ratio of tendon length

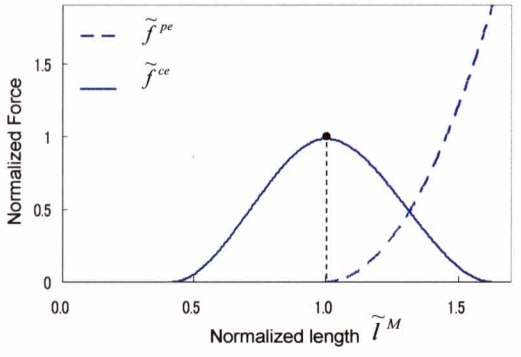


(b) Relationship between normalized force and normalized length

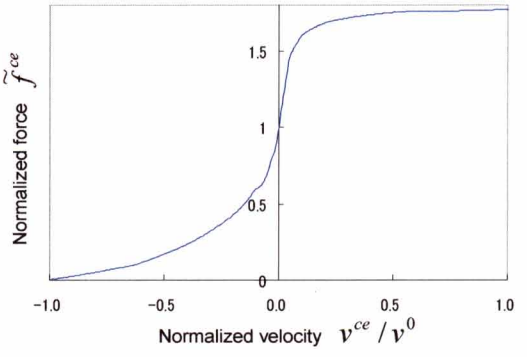


(c) Relationship between normalized force and normalized velocity

**Fig. 3.11** Properties of each element of muscle investigated by Delp *et al.* [9]

The contraction velocity represented by $v^{ce}$ is calculated as follow. ${l^M}_{prev}$ is the previous $l^M$. $\Delta t$ is the scale of timestep.

$$v^{ce} = \frac{l^M - {l^M}_{prev}}{\Delta t} \tag{3.13}$$

First, the tendon length $l^T$ is calculated with the estimated muscle force $f^T$, formula (3.12), Fig. 3.10(a) and formula (3.9). Subsequently, the length of muscle fiber $l^M$ is calculated with formula (3.7). Then the length of the muscle-tendon $l^{MT}$ is calculated from the posture of the body geometrically. Subsequently, the force of PEE $f^{pe}$ is calculated with

formula (3.11) and Fig. 3.10(b). Subsequently, the force of CE $f^{ce}$ is calculated with formula (3.8). Consequently, the muscle activation level $a$ is calculated with formula (3.10), formula (3.13) and Fig. 3.10(c).

### 3.4 Estimation and validation of muscle forces of lower limb during vertical jumping

The method to estimate the muscle forces and the muscle activation levels with the proposed musculoskeletal model have been describe in the preceding section. Fig. 3.12 showed the flowchart to estimate the muscle activation levels from the measured data during 2-dimensional motions. First, the position of each joint and the ground reaction forces are obtained from the experiment. Subsequently, the net moment of each joint is calculated by Newton-Euler equation with the human rigid segment model from the measured data. The output forces at the distal extremity are calculated from the net moments. On the other hand,

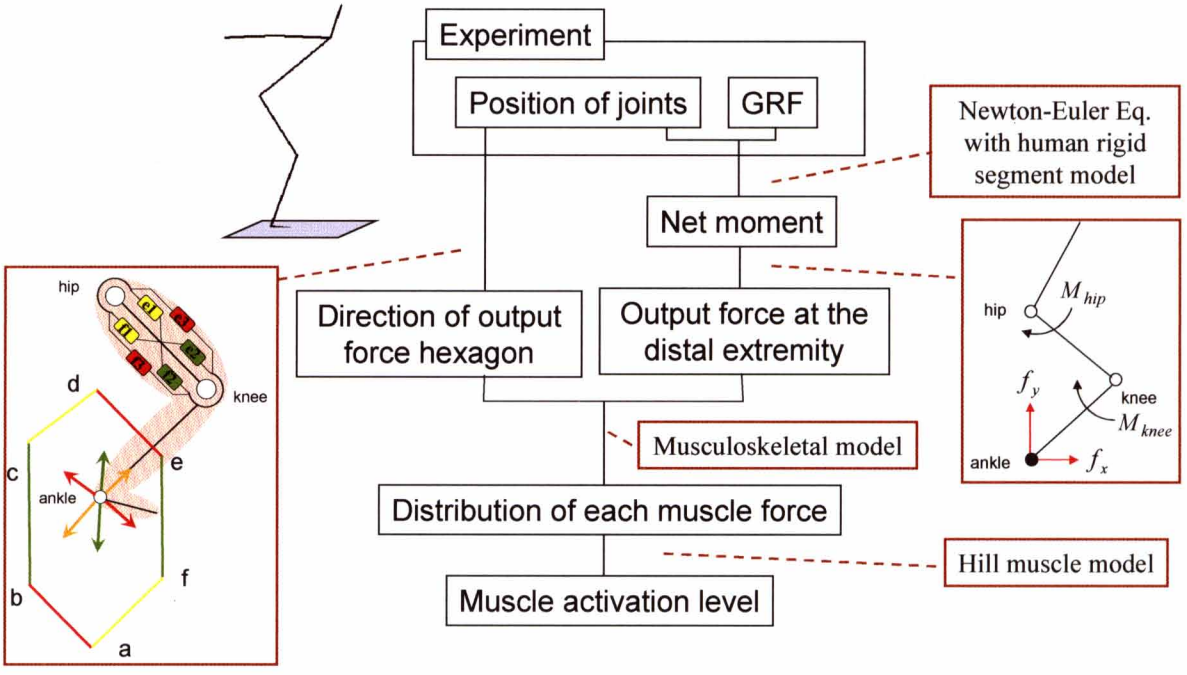


**Fig. 3.12** Flowchart to estimate muscles activation levels during 2-dimensional motions

the direction of the hexagon of the output force distribution at the distal extremity with the musculoskeletal model is determined with the posture of the lower limb. Then the distribution of each muscle force is estimated from the output forces and the hexagon of the output force distribution at the distal extremity with the musculoskeletal model. Finally, the muscle activation level of each muscle is estimated from the estimated muscle forces with Hill muscle model. In this section, vertical jumping as an example of a 2-dimensional dynamic motion was conducted to validate the proposed method to estimate muscle forces and muscle activation levels. Surface electromyograms (EMGs) of tibialis anterior (TA), gastrocnemius (GAS), soleus (SOL), rectus femoris (RF), vastus lateralis (VAS), semimembranosus (SM), biceps femoris and short head (BFSH) and gluteus maximus (GMAX) were measured to compare with the estimated muscle activation levels.

### 3.4.1 Experimental methods

**Experimental protocol.** One participant (height: 181.0 cm, mass: 86.6 kg), after informed consent, participated in the study. Each jump trial was recorded at 250 frames per second using the Vicon MX infrared motion capture system with the ground reaction forces measured from a floor-mounted force platforms (Kistler) at 1000 Hz. Simultaneously, eight electromyograms (EMGs) of tibialis anterior (TA), gastrocnemius (GAS), soleus (SOL), rectus femoris (RF), vastus lateralis (VAS), semimembranosus(SM), biceps femoris, short head (BFSH) and gluteus maximus (GMAX) were recorded at 1000 Hz. Then eight muscles except iliopsoas (IL) were measured because muscle IL that is the antagonistic muscle of muscle GMAX, which works for the flexion of the hip joint, is difficult to be measured by EMG.

**Data analysis.** The net forces and the net moments of the lower limb were calculated from the obtained positional data of the joints using the human rigid segment model described in chapter 2. Then in this study, vertical jumping was analyzed only in the sagittal plane. The positional data of the joints obtained from the captured images were smoothed using a Butterworth filter (cutoff frequency 6 Hz) described in chapter 2. The muscle forces were calculated from the positional data and the net moments with the proposed musculoskeletal model. Furthermore, the muscle activation levels were calculated from the calculated muscle forces with Hill muscle model. The measured EMGs full-wave rectified and filtered with a low-pass, critically-damped digital filter (cutoff frequency 6 Hz) [11]. The measured EMGs were normalized by their maximums under the maximum voluntary contraction. The analysis programs were made with Borland C++ Builder 6 to calculate the muscle forces from positional and force plate data.

### 3.4.2 Results and discussion

The muscle activation levels of muscle VAS and BFSH estimated by both of the thigh model and the lower leg model of the proposed musculoskeletal model are shown in Fig. 3.13. The comparison between the muscle forces estimated by the musculoskeletal model and the muscle activation level estimated from the muscle forces with Hill muscle model in the muscle GAS and SOL, which had conspicuously great differences between the muscle force and the muscle activation level, is shown in Fig 3.14.The net moments of the ankle joint (extension as a positive direction), the knee joint (flexion as a positive direction) and the hip joint (extension as a positive direction) calculated with the human rigid segment model are shown in Fig. 3.15. Each muscle activation level estimated by the proposed method and that

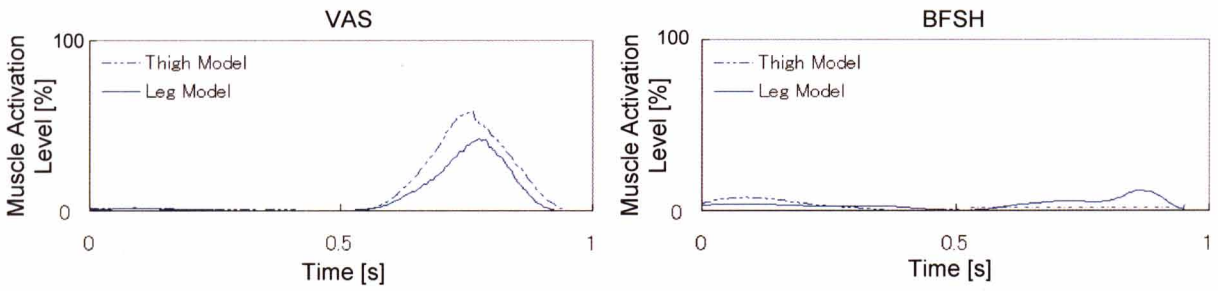


**Fig. 3.13** Comparison of muscle activation levels of VAS and BFSH between thigh model and lower leg model

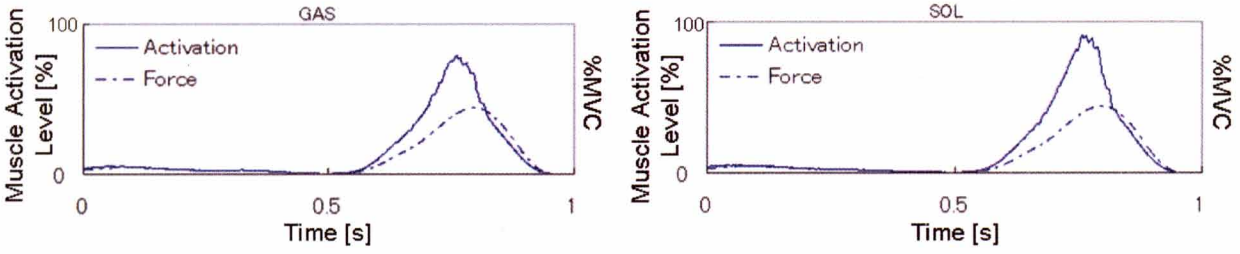


**Fig. 3.14** Comparison between the muscle activation level and %MVC

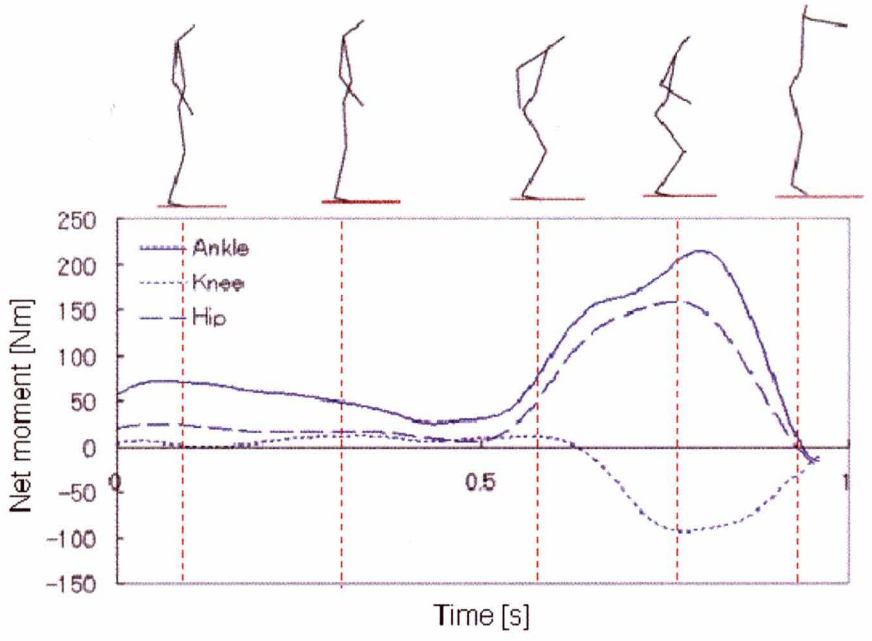


**Fig. 3.15** Net moments of the ankle, knee and hip joints

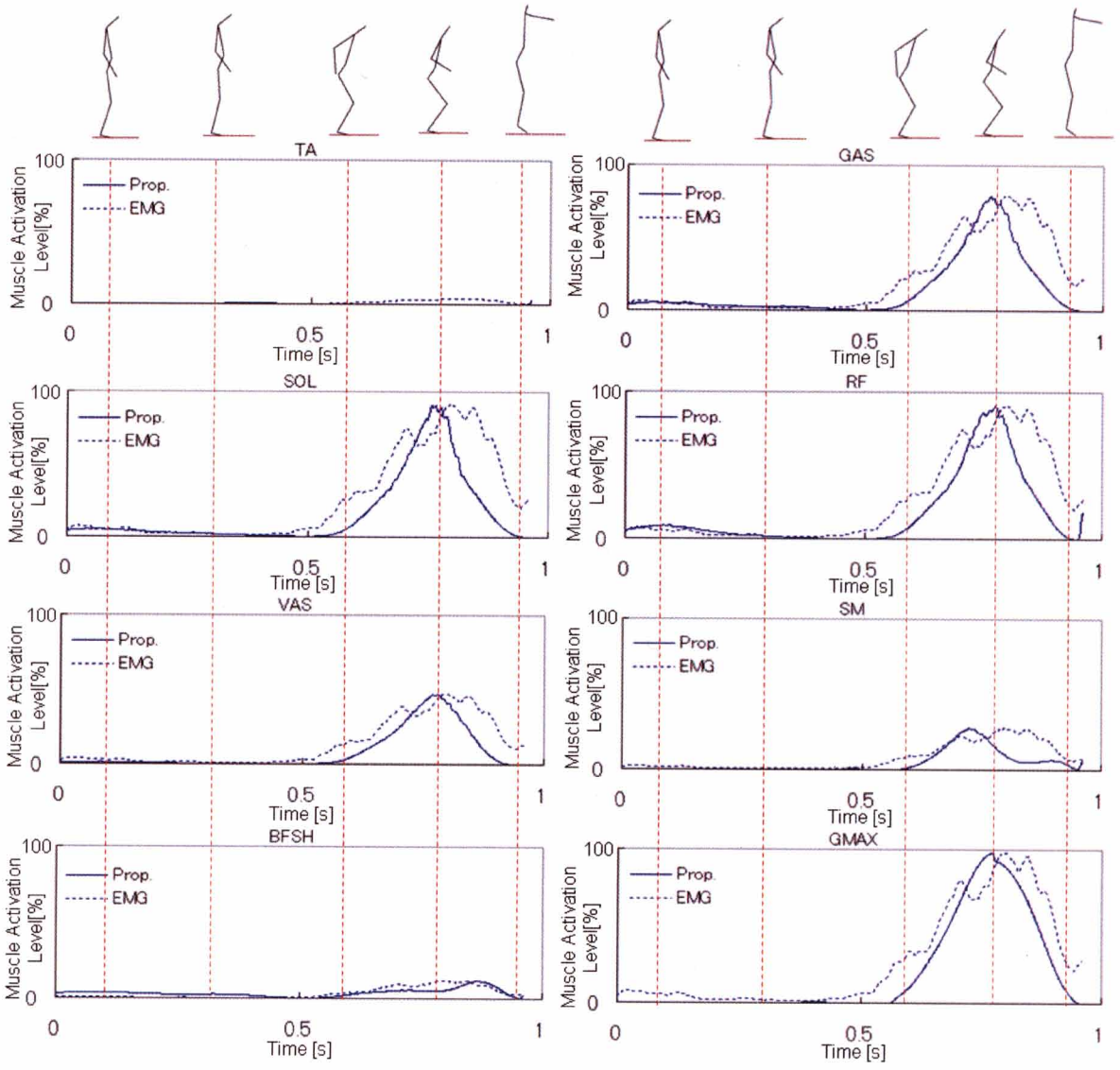


**Fig. 3.16** Comparison of muscle activation levels between the proposed method and the EMG

**Table 3.1** Correlations between the proposed method and the EMG

| Muscle | Correlation |
|---|---|
| TA | 0.40 |
| GAS | 0.87 |
| SOL | 0.86 |
| RF | 0.87 |
| VAS | 0.90 |
| SM | 0.79 |
| BFSH | 0.77 |
| GMAX | 0.95 |

measured by EMG are shown in Fig. 3.16. The correlations between the proposed method and EMGs are shown in Table 3.1.

Fig. 3.13 showed that the muscle activation level of muscle VAS estimated by the lower leg model of the proposed musculoskeletal model was similar to that estimated by the thigh model. Furthermore, the root-means-squared difference between the lower leg model and the thigh model was small (7.03%) and the correlation was strong (0.98) in muscle VAS. In muscle BFSH, the correlation between the lower leg model and the thigh model was weak (0.09) because muscle BFSH was little activated during motion as shown in Fig. 3.13. However, the root-means-squared difference was small (4.25%). Therefore, in muscles VAS and BFSH, this study used the muscle activation levels estimated by the lower leg model because those estimated by both models did not have great differences.

Fig. 3.14 showed that the differences between the muscle forces estimated by the musculoskeletal model and the muscle activation level estimated from the muscle forces with Hill muscle model in the muscle GAS and SOL were conspicuously large. The root-means-squared differences between the muscle force and the muscle activation level were 9.0 % in the muscle GAS and 11.6 % in the muscle SOL throughout vertical jumping. Furthermore, those were 12.7 % in the muscle GAS and 16.4 % in the muscle SOL during the scene from squat to takeoff of vertical jumping when the muscles were activated strongly. The results of this is considered that it is necessary to calculate the muscle activation level from the muscle forces to validate with the electromyograms especially for the analysis of vertical jumping in which the muscle contraction rate is not negligible.

Fig. 3.15 showed that the net moments of the ankle, knee and hip joints worked for the extension of the joints during vertical jumping.

According to the results shown in Fig.3.16, at the ankle joint, muscle TA, which works for the flexion of the ankle joint, contributed very little force to the vertical jumping. Muscles GAS and SOL, which work for the extension of the ankle joint, contributed to the vertical jumping. These results showed that muscles GAS and SOL mainly worked for the extension of the ankle joint.

At the knee joint, muscles RF and VAS, which work for the extension of the knee joint, contributed to the vertical jumping. So these muscles mainly worked for the extension of the knee joint. However, muscles SM and BFSH, which work for the flexion of the knee joint, and muscle GAS, which is the biarticular muscle and works for the flexion of the knee joint, contributed to the vertical jumping though muscle BFSH contributed small force. So these muscles worked in opposition to the prime movers or agonists of the knee joint. Therefore, these results showed that the proposed method to estimated muscle forces could consider the role of the antagonistic muscles at the knee joint.

At the hip joint, muscles GMAX and SM, which work for the extension of the hip joint, contributed to the vertical jumping. So these muscles mainly worked for the extension of the hip joint. Furthermore, muscle RF, which is the biarticular muscle and works on the knee and hip joints simultaneously, worked in opposition to the prime movers or agonists of the hip joint. Therefore, these results also showed that the proposed method to estimated muscle forces could consider the role of the antagonistic muscles at the hip joint.

Thus, the results of this study showed that the patterns of the muscle activation levels by the proposed method were similar to those of the EMGs. Consequently, the results showed that the proposed method had stronger correlations with EMGs. Therefore, the proposed method effectively used both the monoarticular and the biarticular muscles at the hip, knee and ankle

joints. The proposed method was considered to successfully estimate the patterns of activation of the muscles during vertical jumping. Then, the antagonistic muscles are the muscles that act in opposition to the prime movers or agonists of a movement. The role of these muscles contributes to realize the control function responding flexibility to disturbance. The role of these muscles also contributes to control accurately the direction of the output force. Biarticular muscles are the muscles that work simultaneously on two joints. These muscles, which look redundancy, can realize robust stability by constructing the control system coordinating with other muscles. Therefore, the antagonistic muscles and the biarticular muscles are considered to work mainly for the control of the direction of the output force and for keeping up the body balance during vertical jumping. The consideration of these muscles is considered to be necessary to provide athletes with motions that they can give the best performance and unprecedented technical advices during vertical jumping.

In conclusion of this section, vertical jumping as an example of a 2-dimensional dynamic motion was conducted to validate the proposed method to estimate muscle forces and the muscle activation levels. Surface electromyograms (EMGs) of tibialis anterior (TA), gastrocnemius (GAS), soleus (SOL), rectus femoris (RF), vastus lateralis (VAS), semimembranosus (SM), biceps femoris and short head (BFSH) and gluteus maximus (GMAX) were measured to compare with the estimated muscle activation levels. The results of this study showed that the patterns of the muscle activation levels by the proposed method were similar to those of the EMGs. Therefore, the proposed method was considered to successfully estimate the patterns of activation of the muscles during vertical jumping.

### 3.5 Estimation of muscle forces of lower limb during 3-dimensional jogging motion

The method to estimate the muscle forces and the muscle activation levels with the proposed musculoskeletal model have been describe in the preceding section. However the proposed method described in the preceding section can be applied to only 2-dimensional motion. This section proposed the method to estimate muscle forces during 3-dimensional motion. Furthermore, jogging motion as an example of a 3-dimensional dynamic motion was conducted to validate the proposed method to estimate muscle forces and the muscle activation levels. Surface electromyograms (EMGs) of tibialis anterior (TA), gastrocnemius (GAS), soleus (SOL), rectus femoris (RF), vastus lateralis (VAS), semimembranosus (SM), biceps femoris and short head (BFSH) and gluteus maximus (GMAX) were measured to compare with the estimated muscle activation levels.

#### 3.5.1 Method to estimate muscle forces during 3-dimensional motion

To estimate muscle forces of the lower limb existing in the sagittal plane during 3-dimensional motion, the lower limb in 3-dimensional is necessary to be matrix-transformed to 2-dimensional as shown in Fig. 3.17. Then, the sagittal plane of the lower limb was defined to be the plane described by the thigh, leg and foot segment by assuming the knee joint and the ankle joint to move only extension and flexion in 3-dimensional motion. This study reconstructed the positional data of the joints in 2-dimensional plane with the angles of the ankle, knee and hip joints obtained from the positional data of the joints in 3-dimensional space and the link length of each segment. The net moments of the ankle, knee and hip joints calculated with the human rigid segment model described in chapter 2 are also necessary to be transformed to the local coordinate system in sagittal plane of lower limb because these

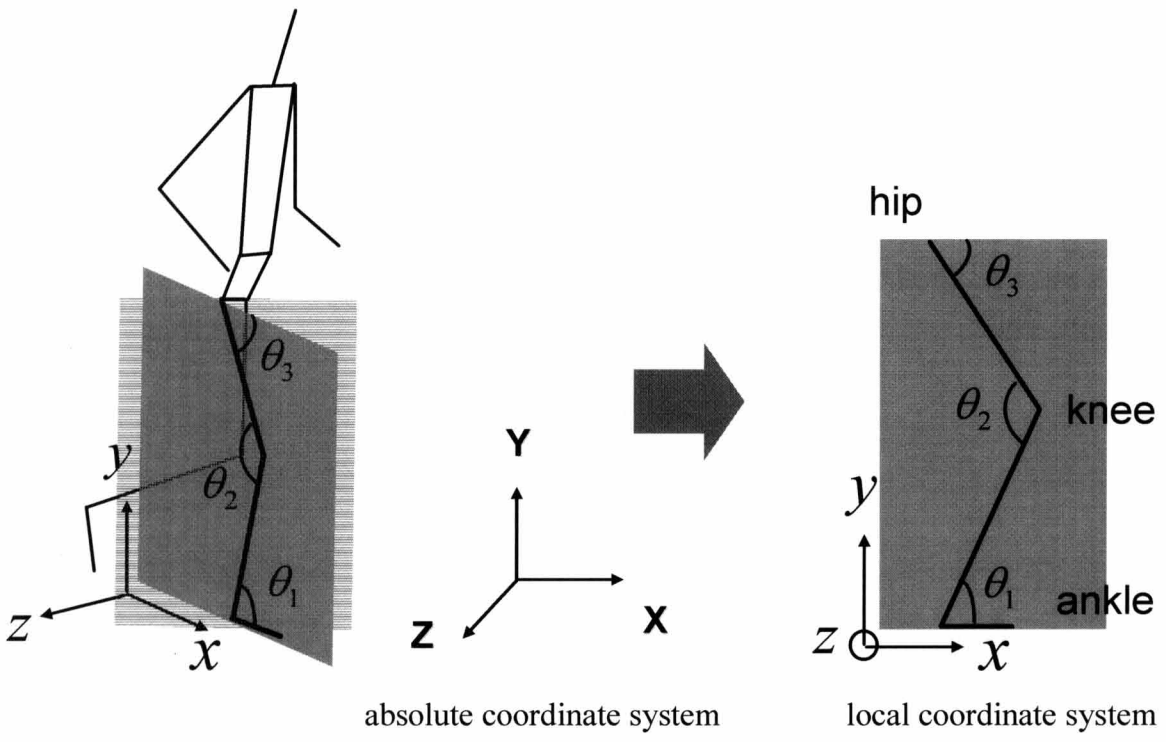


**Fig. 3.17** Matrix-transformation of 3-dimensinal space to 2-dimensional plane

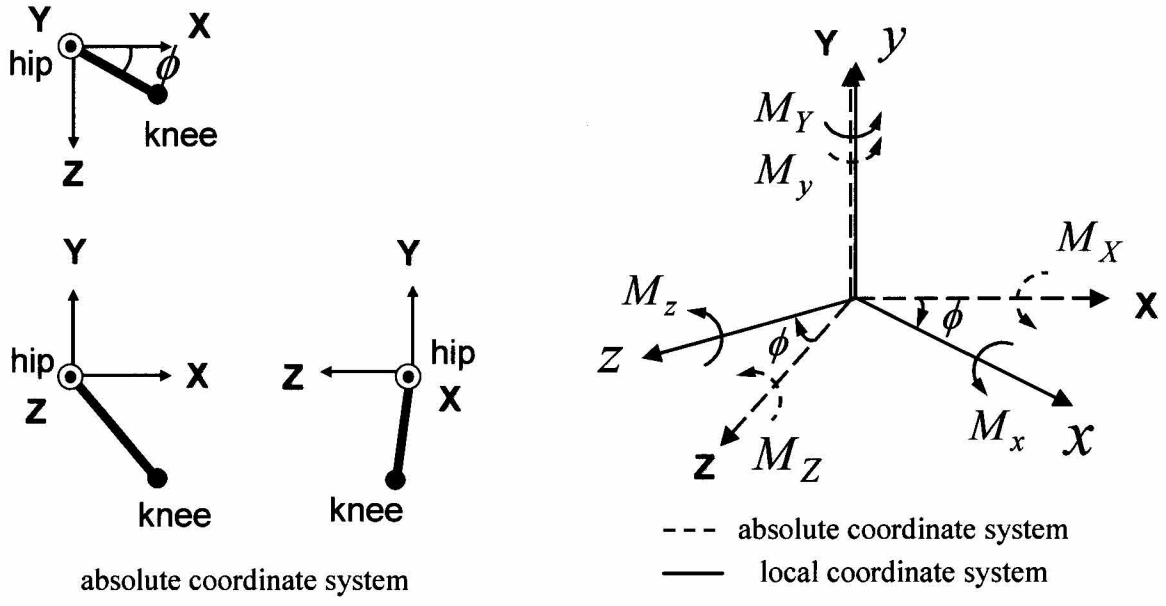


**Fig. 3.18** Rotation of net moments to the local coordinate system

form the local coordinate system

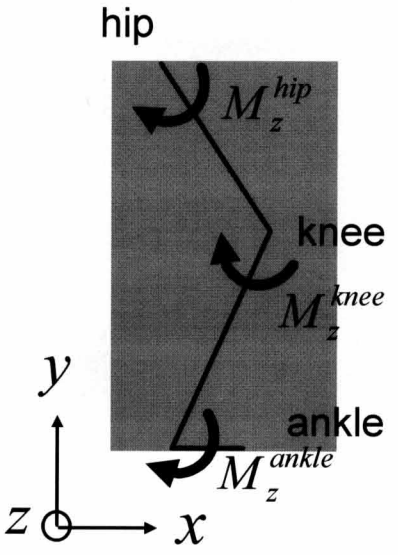


**Fig. 3.19** Net moment of each joint in the sagittal plane of the lower limb

calculated net moments work around each axis in the absolute coordinate system. Then, the anteroposterior direction is assumed to be X axis, the mediolateral direction is assumed to be Y direction and the vertical direction is assumed to be Z direction in the absolute coordinate system of jogging motion. Furthermore, the anteroposterior direction is assumed to be x axis, the mediolateral direction is assumed to be y axis and the vertical direction is assumed to be z axis in the local coordinate system in sagittal plane of the lower limb. The net moment working around each axis of the absolute coordinate system is assumed to be $M_X$, $M_Y$ and $M_Z$. That working around each axis of the local coordinate system is assumed to be $M_x$, $M_y$ and $M_z$. For example, when the thigh segment is rotated by $\phi$ from the absolute coordinate system as shown in Fig. 3.18, the net moments in the local coordinate system as shown in Fig. 3.19 can be calculated by matrix-transformation with the transformation matrix described as follow. The net moment of each joint working around z axis of the local coordinate system can be calculated by matrix-transformation in the hip, knee and ankle

joints.

$$\begin{bmatrix} M_x \\ M_y \\ M_z \end{bmatrix} = \begin{bmatrix} \cos\phi & 0 & -\sin\phi \\ 0 & 1 & 0 \\ \sin\phi & 0 & \cos\phi \end{bmatrix} \begin{bmatrix} M_X \\ M_Y \\ M_Z \end{bmatrix} \tag{3.14}$$

Thus, the muscle forces of lower limb during 3-dimensional motion can be estimated with the proposed method described in the preceding section. Fig. 3.20 showed the flowchart to estimate the muscle activation levels from the measured positional data of the joints during motions. First, the position of each joint and the ground reaction forces are obtained from the experiment. Subsequently, the net force and net moment of each joint are calculated by Newton-Euler equation with the human rigid segment model from the measured data. Then the position of each joint of lower limb in 2-dimensional plane is reconstructed from the position in 3-dimensinoal space and the net moment of each joint of lower limb working for

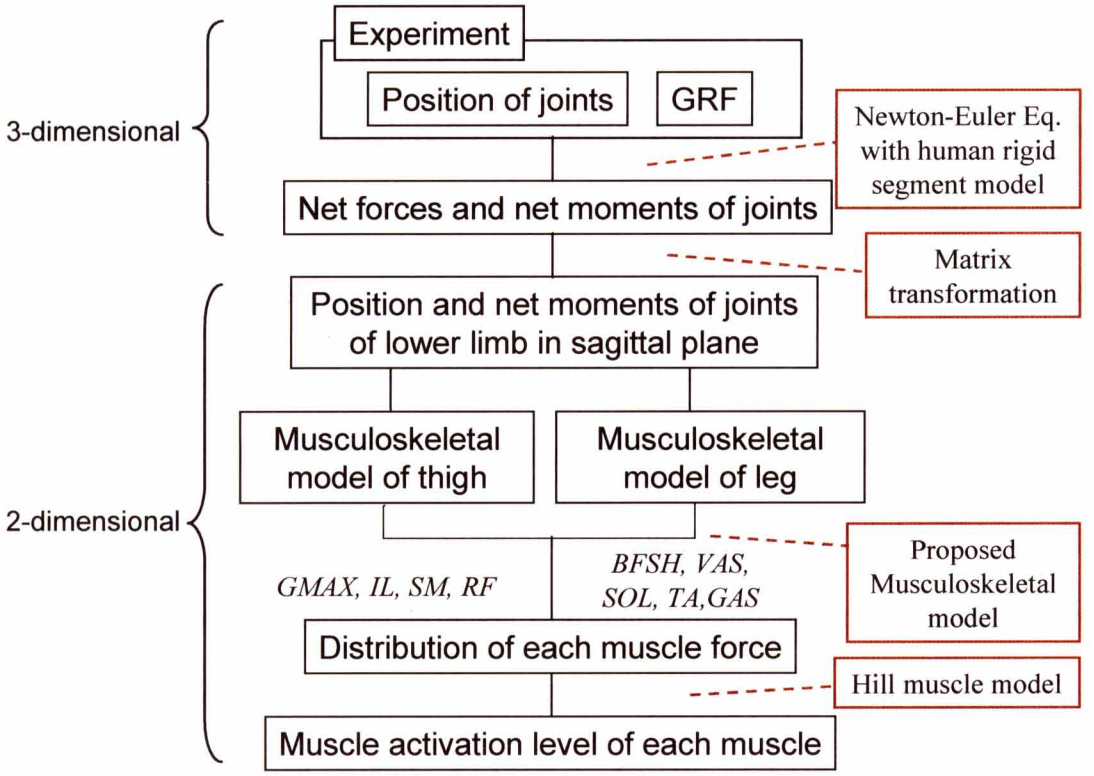


**Fig. 3.20** Flowchart to estimate muscle activation levels during 3-dimensional motions

sagittal plane with matrix transformation. Then the muscle forces can be estimated with the proposed method to estimate muscle forces during 2-dimensional motions. Finally, the muscle activation level of each muscle can be estimated from the estimated muscle forces with Hill muscle model.

### 3.5.2 Experimental methods

**Experimental protocol.** One participant (height: 161.0 cm, mass: 81.6 kg), after informed consent, participated in the study. Each jogging trial was recorded at 250 frames per second using the Vicon MX infrared motion capture system with the ground reaction forces measured from a floor-mounted force platforms (Kistler) at 1000 Hz. Simultaneously, eight electromyograms (EMGs) of tibialis anterior (TA), gastrocnemius (GAS), soleus (SOL), rectus femoris (RF), vastus lateralis (VAS), semimembranosus(SM), biceps femoris and short head (BFSH) and gluteus maximus (GMAX) on the dominate leg were recorded at 1000 Hz. Then eight muscles except iliopsoas (IL) were measured because muscle IL that is the antagonistic muscle of muscle GMAX, which works for the flexion of the hip joint, is difficult to be measured by EMG.

**Data analysis.** The net forces and the net moments of the lower limb were calculated from the obtained positional data of the joints using the human rigid segment model described in chapter 2. The positional data of the joints obtained from the captured images were smoothed using a Butterworth filter (cutoff frequency 6 Hz) described in chapter 2. The muscle forces were calculated with the proposed method. Furthermore, the muscle activation levels were calculated from the calculated muscle forces with Hill muscle model. The measured EMGs

full-wave rectified and filtered with a low-pass, critically-damped digital filter (cutoff frequency 6 Hz) [11]. The measured EMGs were normalized by their maximums under the maximum voluntary contraction. The analysis programs were made with Borland C++ Builder 6 to calculate the muscle forces from positional and force platform data.

### 3.5.3 Results and discussion

The net moments of the ankle joint (extension as a positive direction), the knee joint (flexion as a positive direction) and the hip joint (extension as a positive direction) in the sagittal plane obtained by matrix-transformation from those calculated with the human rigid segment model in 3-dimension are shown in Fig. 3.21. The muscle activation level of each muscle estimated by the proposed method and that measured by EMGs are shown in Fig. 3.22. The correlations between the proposed method and EMGs are shown in Table 3.2. Then the analysis range is from the undominant foot toe-off to the undominant foot touch-down.

At the ankle joint, the net moment worked for the extension of the joint. Muscle TA, which works for the flexion of the ankle joint, contributed very little force to the jogging. However, muscle TA worked in opposition to the prime movers or agonists of the ankle joint because it was activated slightly. So these results showed that the proposed method could consider the role of the antagonistic muscles. Muscles GAS and SOL, which work for the extension of the ankle joint, contributed to the jogging. These results showed that muscles GAS and SOL mainly worked for the extension of the ankle joint. Furthermore, the correlations between the proposed method and the EMGs of muscles TA, GAS and SOL were 0.67, 0.82 and 0.63 respectively. So the proposed method was considered to be validated on these muscles at the ankle joint.

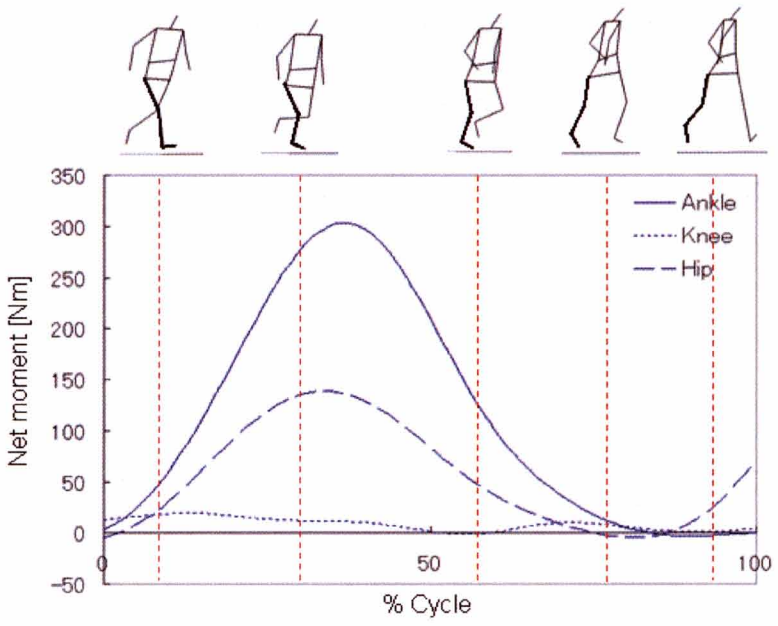


**Fig. 3.21** Net moment of each joint of lower limb in sagittal plane

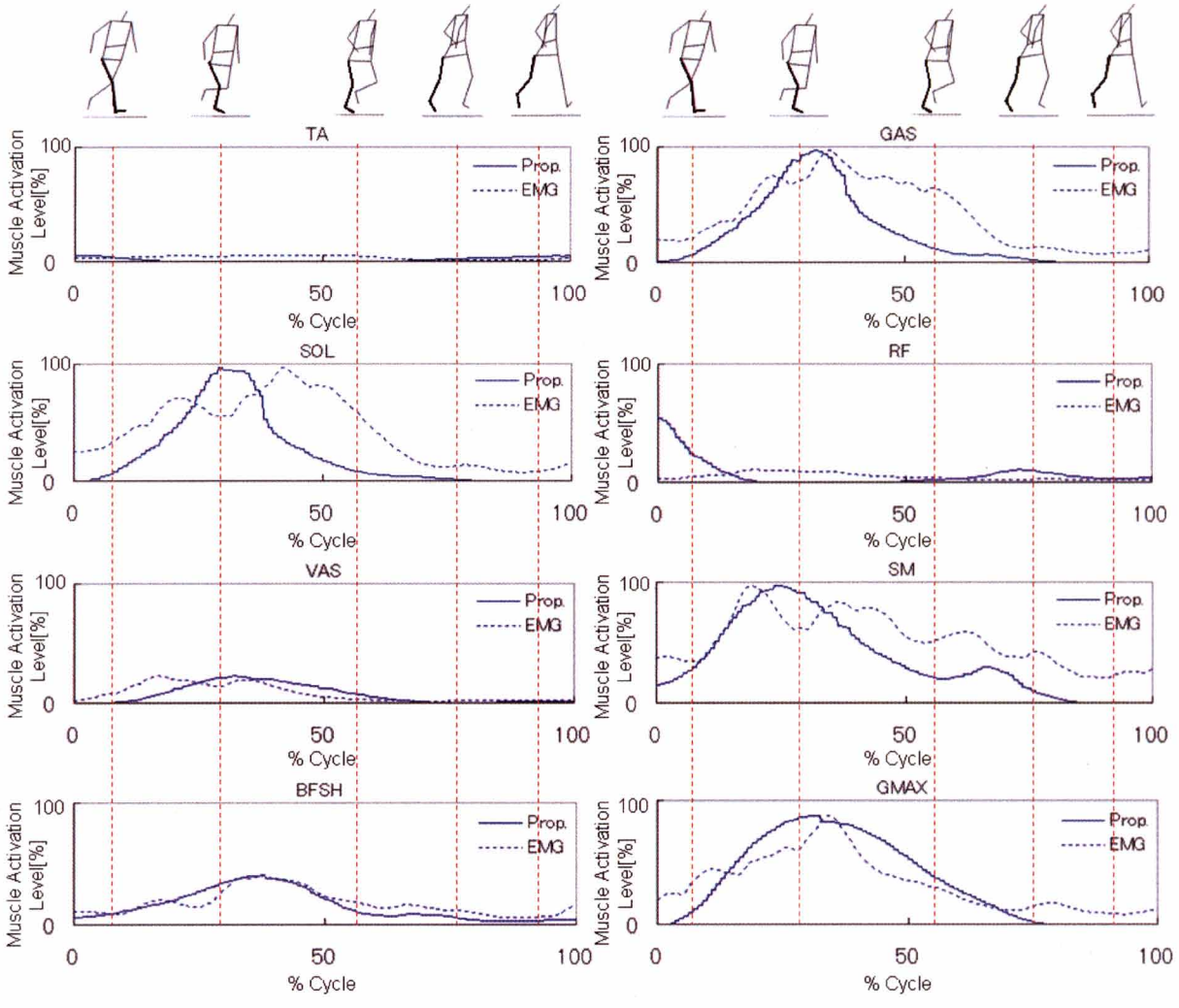


**Fig. 3.22** Comparison of muscle activation levels between the proposed method and the EMGs

**Table 3.2** Correlations between the proposed method and the EMGs

| Muscle | Correlation |
|---|---|
| TA | 0.67 |
| GAS | 0.82 |
| SOL | 0.63 |
| RF | 0.28 |
| VAS | 0.69 |
| SM | 0.85 |
| BFSH | 0.92 |
| GMAX | 0.92 |

At the knee joint, though the net moment worked for the extension of the joint, the net moment was not so large. Muscles RF and VAS, which work for the extension of the knee joint, contributed to the jogging. So these muscles mainly worked for the extension of the knee joint. In muscle VAS, the pattern of the muscle activation level estimated by the proposed method was similar to that measured by the EMG and the correlation between the proposed method and the EMG were 0.69. So the proposed method was considered to be validated on this muscle. In muscle RF, though the pattern of the muscle activation level estimated by the proposed method was similar to that measured by the EMG after the undominant foot touch-down (Cycle = 20 ~ 100%), that by the proposed method was different from that by the EMG before the undominant foot touch-down (Cycle = 0 ~ 20%). The cause of this was considered that the great changing of the posture of the lower limb and the acceleration of each segment before the foot touch-down made the net moments calculated by the human rigid segment model different from actual ones. So the errors of the muscle forces estimated from the net moments were a little large. However, the proposed method was considered to be validated on this muscle except for before the undominant foor touch-down because the correlation between the proposed method and the EMG after the undominant foot

touch-down (Cycle = 20 ~ 100%) was 0.71.

Muscle BFSH, which is the monoarticular muscle and works for the flexion of the knee joint, muscle SM, which is the biarticular muscle and works for the flexion of the knee joint, and muscle GAS, which is the biarticular muscle and works for the flexion of the knee, contributed to the jogging. These results showed that these muscles worked in opposition to the prime movers or agonists of the knee joint. So these results showed that the proposed method could consider the role of the antagonistic muscles. Furthermore, in muscles BFSH and SM, the patterns of the muscle activation levels estimated by the proposed method were similar to those measured by the EMGs and the correlations between the proposed method and the EMGs of muscles BFSH and SM were 0.92 and 0.85 respectively. So the proposed method was considered to be validated on these muscles at the knee joint.

At the hip joint, the net moment worked for the extension of the joint. Muscle GMAX, which works for the extension of the hip joint, and muscle SM, which is the biarticualr muscle and works for the extension of the hip joint, contributed to the jogging. These results showed that these muscles mainly worked for the extension of the hip joint. Furthermore, in muscle GMAX, the pattern of the muscle activation level estimated by the proposed method was similar to that measured by the EMG and the correlation between the proposed method and the EMG was 0.92. So the proposed method was considered to be validated on this muscle at the hip joint.

Thus, the results of this study showed that the patterns of the muscle activation levels by the proposed method were similar to those of the EMGs. Consequently, the results showed that the proposed method had stronger correlations with EMGs. Therefore, the proposed method effectively used both the monoarticular and the biarticular muscles at the hip, knee and ankle

joints. The proposed method was considered to successfully estimate the patterns of muscle activation during 3-dimensional jogging motion. Then, the antagonistic muscles are the muscles that act in opposition to the prime movers or agonists of a movement. The role of these muscles contributes to realize the control function responding flexibility to disturbance. The role of these muscles also contributes to control accurately the direction of the output force. Biarticular muscles are the muscles that work simultaneously on two joints. These muscles, which look redundancy, can realize robust stability by constructing the control system coordinating with other muscles. Therefore, the antagonistic muscles and the biarticular muscles are considered to work mainly for the control of the direction of the output force and for keeping up the body balance during jogging. The consideration of these muscles is considered to be necessary to provide athletes with motions that they can give the best performance and unprecedented technical advices during jogging.

In conclusion of this section, this study proposed the method to estimate muscle forces during 3-dimensional motion. Furthermore, jogging motion as an example of a 3-dimensional dynamic motion was conducted to validate the proposed method to estimate muscle forces and the muscle activation levels. Surface electromyograms (EMGs) of tibialis anterior (TA), gastrocnemius (GAS), soleus (SOL), rectus femoris (RF), vastus lateralis (VAS), semimembranosus (SM), biceps femoris and short head (BFSH) and gluteus maximus (GMAX) were measured to compare with the estimated muscle activation levels. The results of this study showed that the patterns of the muscle activation levels by the proposed method were similar to those of the EMGs. Therefore, the proposed method was considered to successfully estimate the patterns of muscle activation during jogging motion.

### 3.6 Conclusion

Estimation of muscle forces during human motions is important in the fields of sport, ergonomics and bioengineering in order to improve sport techniques, rehabilitation procedures, product designs and work environments, and so on. Therefore, this study investigated a musculoskeletal model of lower limb that considers the roles of antagonistic muscles and biarticular muscles. Furthermore this study proposed the method to estimate muscle forces and muscle activation levels during motions using the musculoskeletal model.

Vertical jumping as an example of a 2-dimensional dynamic motion was conducted to validate the proposed method. Jogging motion as an example of a 3-dimensional dynamic motion was also conducted to validate the proposed method. Surface electromyograms (EMGs) of tibialis anterior (TA), gastrocnemius (GAS), soleus (SOL), rectus femoris (RF), vastus lateralis (VAS), semimembranosus (SM), biceps femoris and short head (BFSH) and gluteus maximus (GMAX) were measured to compare with the estimated muscle activation levels. The results of this study showed that the patterns of the muscle activation levels by the proposed method were similar to those of the EMGs. Therefore, the proposed method was considered to successfully estimate the patterns of muscle activation during dynamic motions.

**References**

[1] Crowninshield R. D., Brand R. A. : A Physiologically Based Criterion of Muscle Force Prediction in Locomotion, Journal of Biomechanics, 14, 793-800, 1981.

[2] Oshima T., Fujikawa T., Kumamoto M. : Functional Evaluation of Effective Muscle Strength Based on a Muscle Coordinate System Consisted of Biarticular and Monoarticular Muscles - Contractile Forces and Output Forces of Human Limbs, Journal of the Japan Society of Precision Engineering, 65(12), 1772-1777, 1999.

[3] Spector S. A., Gardiner P. F., Zernicke R. F., Roy R. R., Edgerton V. R. : Muscle architecture and force-velocity characteristics of cat soleus and medial gastrocnemius: implications for neural control, Journal of Neuro-physiol, 44, 951-960, 1980.

[4] Wickiewicz T. L., Roy R. R., Powell P. L., Edgerton V. R. : Muscle architecture of the human lower limb, Clin. orthop. Rel. Res, 179, 275-283, 1983.

[5] Brad R. A., Pedersen D. R., Frienderich J. A. : The sensitivity of muscle force predictions to changes in physiologic cross-sectional area, Journal of Biomechanics, 19, 589-596, 1986.

[6] Chang Y. W., Hughes R. E., Su F. C., Itoi E., An K. N. : Prediction of muscle force involved in shoulder internal rotation, Journal of Shoulder and Elbow Surgery, 9(3), 188–195, 2000.

[7] Akima H., Kuno S., Fukunaga T., Katsuta S. : Architectural Properties and Specific Tension of Human Knee Extensor and Flexor Muscles Based on Magnetic Resonance Imaging, Japanese journal of physical fitness and sports medicine, 44(2), 267-278, 1995.

[8] Hoy M. G., Zajac F. E., Gordon M. E. : A Musculoskeletal Model of the Human Lower Extremity: The Effect of Muscle, Tendon, and Moment Arm on the Moment-Angle

Relationship of Musculotendon Actuators at the Hip, Knee, and Ankle, Journal of Biomechanics, 23(2), 157-169, 1990.

[9] Delp S., Loan P., Hoy M., Zajac F. E., Fisher S., Rosen J. : An interactive graphics-based model of the lower extremity to study orthopaedic surgical procedures, IEEE Trans. on Biomedical Engineering, 37(8), 757-767, 1990.

[10] Pandy M. G., Zajac F. E., Sim E., Levine W. S. : An optimal control model for maximum-height human jumping, Journal of Biomechanics, 23(12), 1185-1198, 1990.

[11] Robertson D. G. E., Dowling J. J. : Design and responses of Butterworth and critically damped digital filters, Journal of Electromyography and Kinesiology, 13, 569-573, 2003.

# 4. Evaluation of lifting operations with a musculoskeletal model

## 4.1 Introduction

For several decades, productivity preferred unmanned factory or factory automation has been the major trend in manufacturing. However, human centered manufacturing system is getting attention to realize much more flexibility of product variety and volume for manufacturing. Previously, computer human models that duplicate the properties and the functions of human have been developed. Some commercial software such as Jack [1] and RAMSIS [2] has been produced. They are used for the evaluation of product designs and for the improvement of working environments, rehabilitation procedures. However, unfortunately they are not enough to evaluate the workload of muscles because they have only analyzed with a human rigid segment model. On the other hand, the computer human models that can evaluate the workload of muscles such as AnyBody [3] have been developed. But this has not usually considered the roles of antagonistic muscles and biarticular muscles. Furthermore, the evaluation of various motion patterns for human considering muscle forces has not been investigated sufficiently. Then, this study investigated a musculoskeletal model of upper and lower limbs including the roles of antagonistic muscles and biarticular muscles. This study also proposed the method to estimate muscle forces during lifting operations as an example of a working motion. Furthermore, this study proposed the method to create various motions in computer simulation and evaluate the motions with the musculoskeletal model that considers the roles of antagonistic muscles and biarticular muscles.

## 4.2 Estimation of muscle forces of the upper and lower limbs during lifting operations

This section conducted lifting operations to estimate muscle forces of the upper and lower limbs with the musculoskeletal model that considers the roles of antagonistic muscles and biarticular muscles. Surface electromyograms (EMGs) of deltoid anterior (Da), deltoid posterior (Dp), brachialis (Br), lateral head of triceps brachii (Tla), long head of biceps (Blo) and long head of triceps brachii (Tlo) were measured to compare with the estimated muscle forces.

### 4.2.1 Method to estimate muscle forces of the upper and lower limbs

**Muscle arrangements at the upper and lower limbs.** This study assumed lifting operations to be 2-dimensional motion. This study used a human rigid segment model that consists of 8 rigid body segments (1-Foot, 2-Leg, 3-Thigh, 4-Body, 5-Upper arm, 6-Forearm, 7-Hand, 8-Head) as shown in Fig. 4.1. As there are many muscles in the upper and lower limbs, it is difficult to model all the contributory muscles. So this study used a musculoskeletal model that includes 6 representative muscles of the upper limb and 6 representative muscles of the lower limb in sagittal plane as shown in Fig. 4.1. The following muscles are included: 1-deltoid anterior (Da), 2-deltoid posterior (Dp), 3-brachialis (Br), 4-lateral head of triceps brachii (Tla), 5-long head of biceps (Blo) and 6-long head of triceps brachii (Tlo) at the upper limb and i-gluteus maximus (GMAX), ii-iliopsoas (IL), iii-biceps femoris and short head (BFSH), iv-vastus lateralis (VAS), v-semimembranosus (SM), vi-rectus femoris (RF) at the lower limb.

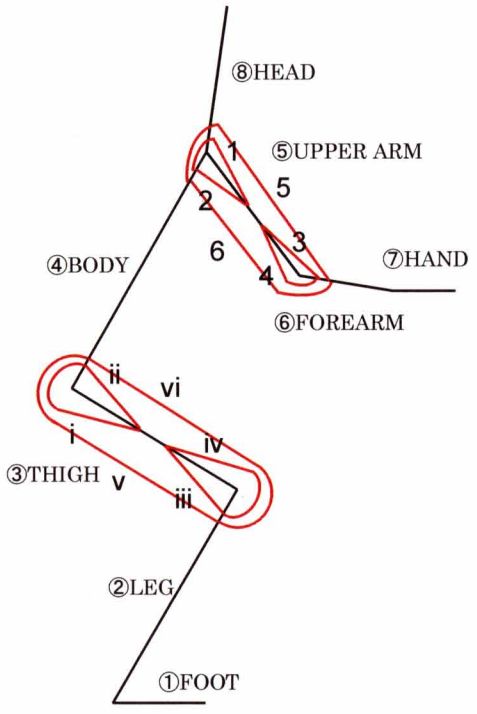


**Fig. 4.1** Muscle arrangements at the human upper and lower limbs

**Method to estimate muscle forces that considers the roles of antagonistic muscles and biarticular muscles.** Oshima *et al.* [4] suggested a coordination-control model that considers the roles of the antagonistic muscles and biarticular muscles of the upper limb. The model including three pairs of the antagonistic muscles in the upper limb suggested by Oshima *et al.* [4] is shown in Fig. 4.2a.

The model consists of 6 muscles, muscle f1 substituted for Da, muscle e1 substituted for Dp, muscle f2 substituted for Br, muscle e2 substituted for Tla, muscle f3 substituted for Blo and muscle e3 substituted for Tlo. Then the muscle f1 and the muscle e1 are the antagonistic monoarticular muscles pair, which works on the shoulder joint. The muscle f2 and the muscle e2 are also the antagonistic monoarticular muscles pair, which works on the elbow joint. The muscle f3 and the muscle e3 are the antagonistic biarticular muscles pair, which works simultaneously on both the shoulder and elbow joints. Oshima *et al.* [4] defined that these

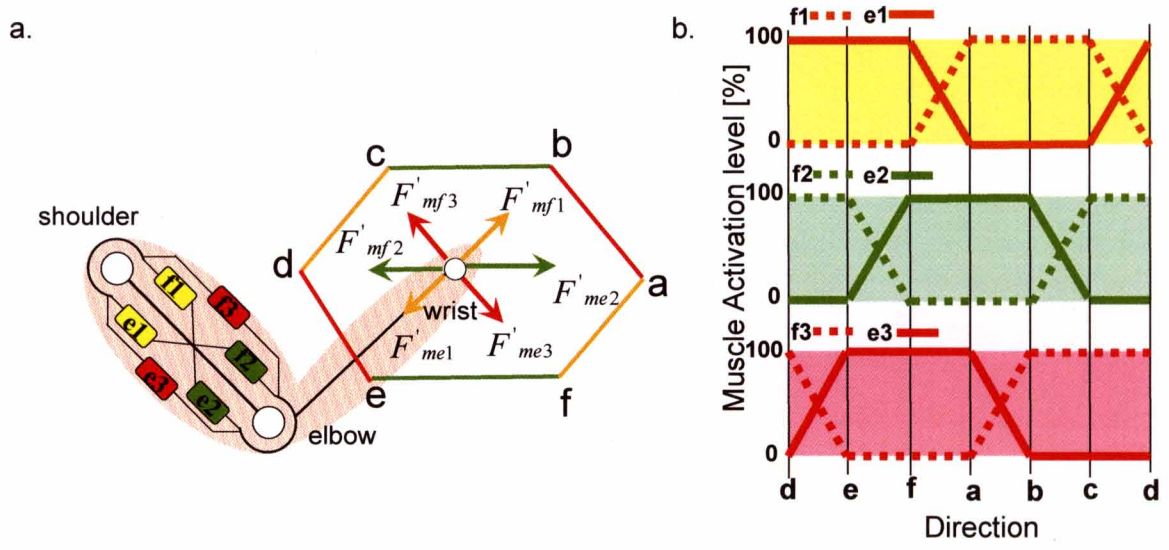


**Fig. 4.2** Coordination-control model of the upper limb that considers the roles of antagonistic muscles and biarticular muscles

muscles act on the distal extremity and the maximum force of each muscle acts on the distal extremity as $F'_{mf1}$, $F'_{me1}$, $F'_{mf2}$, $F'_{me2}$, $F'_{mf3}$, $F'_{me3}$ as shown in Fig. 4.2a. Then the maximum output force distribution on the distal extremity is geometrically a hexagon from maximum force of each muscle. They also verified the maximum output force distribution on the distal extremity is a hexagon in the experiment. The position of this hexagon changes depending on the posture or arrangement of the joints. This is that the side *ab* and *de* is parallel to the upper limb segment, the side *af* and *cd* is parallel to the forearm segment and the side *bc* and *ef* is parallel to the line from the shoulder joint to the wrist joint. They also investigated the vector of the output force on the distal extremity is related to the muscles activation pattern as shown in Fig. 4.2b. For example, when the vector of the output force is direction *a* as maximum in Fig. 4.2a, the muscle forces are defined as 100% of maximum muscle force for muscles f1, e2 and e3 and 0% of maximum muscle force for muscles e1, f2 and f3. Therefore the distribution of each muscle force is determined by the vector of the output force on the distal extremity

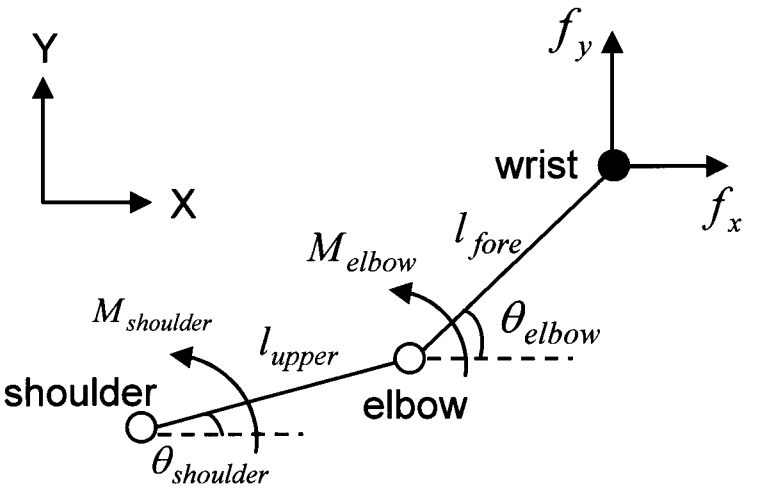


**Fig. 4.3** Relationship between output force on the distal extremity and net moments

and the muscle activation pattern.

The vector of the output force on the distal extremity is necessary to be calculated to estimate the distribution of each muscle using the coordination-control model described as above. The vector of output force on the distal extremity can be calculated from the net moments at the shoulder and elbow joints. The output force of x axis is represented by $f_x$, that of y axis is represented by $f_y$, the angle of the shoulder and the elbow joints are represented by $\theta_{shouler}$ and $\theta_{elbow}$, the link length of the upper arm and the forearm are represented by $l_{upper}$ and $l_{fore}$ and the net moments of the shoulder and elbow joints are represented by $M_{shoulder}$ and $M_{elbow}$ as shown in Fig. 4.3. The relationship between the output force and the net moments is represented as follows. The vector of the output force can be calculated by solving the simultaneous formulas.

$$\begin{aligned} M_{shoulder} = &(l_{fore}\sin\theta_{elbow} + l_{upper}\sin\theta_{shoulder})f_x \\ &-(l_{fore}\cos\theta_{elbow} + l_{upper}\cos\theta_{shoulder})f_y \end{aligned} \tag{4.1}$$

$$M_{elbow} = (l_{fore}\sin\theta_{elbow})f_x - (l_{fore}\cos\theta_{elbow})f_y \tag{4.2}$$

The distribution of each muscle force can be estimated with the obtained output force on the distal extremity ($f_x$, $f_y$) applied to the model in Fig. 4.2a. Then the muscle forces can be estimated with the scale of the vector of the output force.

Then the muscle forces of the lower limb can be estimated with the proposed method described in chapter 3.

The maximum output force distribution derived from the maximum force of each muscle is necessary to be clarified preliminarily to estimate the muscle forces during motions with the proposed musculoskeletal model. The participants need to output all directions with the maximum forces to measure the maximum output force distribution. But the results of these trials are susceptible to error due to their fatigue. Then, this study used the method of measuring the maximum output force distribution suggested by Oshima *et al.* [5]. The method can describe the maximum output force distribution in the shape of hexagon geometrically with the measured forces of only four directions. The aluminum frame with a hand grip on a three component dynamometer (KYOWA Corp. LSM-B-SAI) shown in Fig. 4.4a was used to

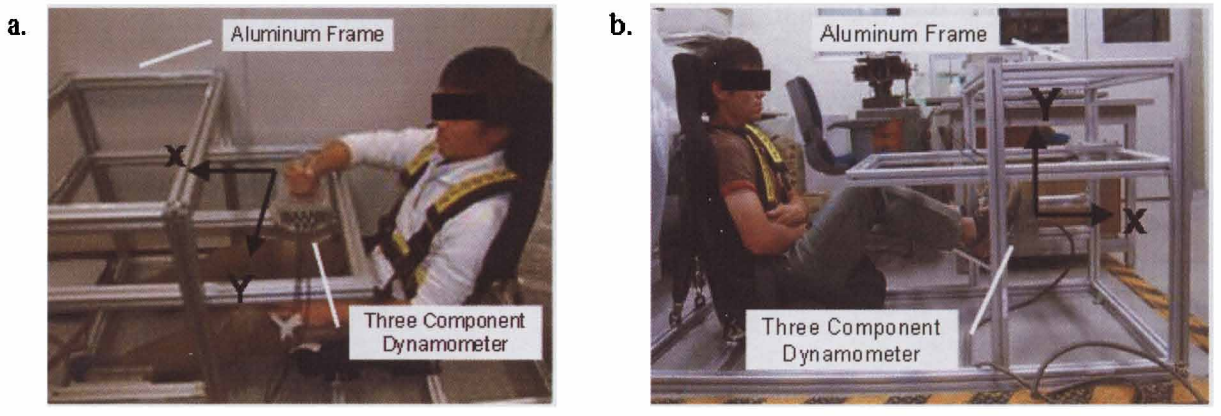


**Fig. 4.4** Measuring equipment of the output force distribution on the distal extremity

(a = Upper limb, b = Lower limb)

measure the maximum output forces of the upper limb. The aluminum frame with the jig fixing a foot on a three component dynamometer (KISTLER Corp. 9257B) shown in Fig. 4.4b was used to measure the maximum output forces of the lower limb. The posture of the upper and lower limbs of participants can be adjusted with the three component dynamometers and seat changed.

The flowchart to estimate the muscle forces from the measured data during lifting operations is shown in Fig. 4.5. First, the maximum output force distributions in the shape of hexagon at the upper and lower extremities are measured preliminarily with the devices shown in Fig. 4.4. Subsequently, the position of each joint and the external forces of the upper extremity derived from the mass of the object measured with the force platform are obtained from the experiment of lifting operation. The net moment of each joint is calculated by Newton-Euler equation with the human rigid segment model from the measured data. The output forces at the upper and lower extremities are calculated from the net moments. On the other hand, the direction of the hexagon of the output force distribution at the upper and lower extremities with the musculoskeletal model is determined with the posture of the upper and lower limb.

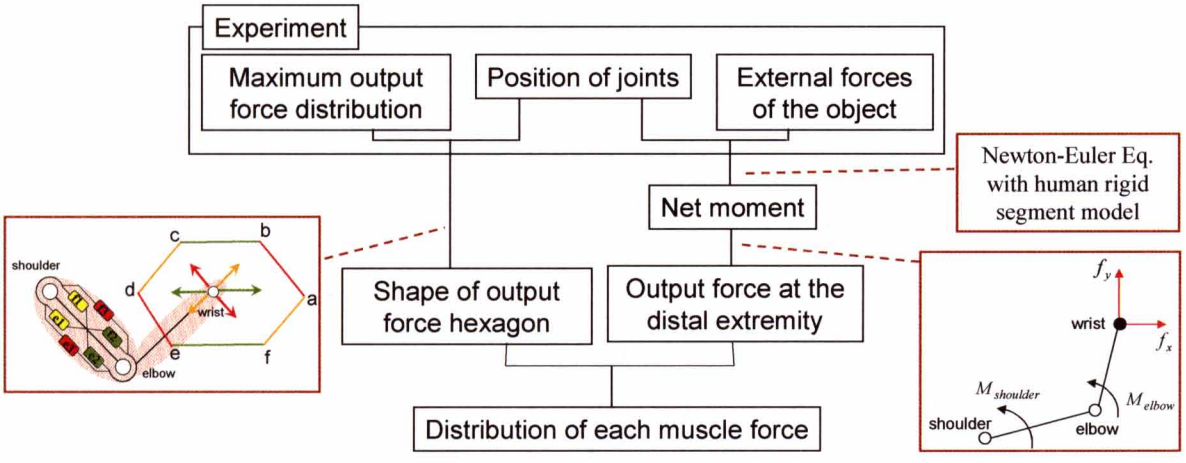


**Fig. 4.5** Flowchart to estimate muscle forces during lifting operations

Then the distribution of each muscle force is estimated from the output forces and the hexagon of the output force distribution at the distal extremity with the musculoskeletal model.

### 4.2.2 Experimental methods

**Experimental protocol.** Three participants (height: 171.3±3.3 cm, mass: 63.0±5.7 kg), after informed consent, participated in this study to validate the proposed method. First, the maximum output force distribution of the upper and lower limbs of each participant was measured with the method described in the preceding section. Subsequently, each lifting operation was recorded at 125 frames per second using the CCD camera (SONY Corp. XC-009). Simultaneously, six surface electromyograms (EMGs) of deltoid anterior (Da), deltoid posterior (Dp), brachialis (Br), lateral head of triceps brachii (Tla), long head of biceps (Blo) and long head of triceps brachii (Tlo) were recorded at 1000 Hz. Furthermore, to measure the external forces of the upper extremity derived from the mass of the object before the object gets off the ground, a floor-mounted force platform (Kistler) under the object was measured at 1000Hz. The conditions of the lifting operations were that the height of lifting was 1.0 m and the mass of the object was 10 kg.

**Data analysis.** The positional data of the joints obtained from the captured images were smoothed using a Butterworth filter (cutoff frequency 6 Hz) [6, 7]. The net forces and the net moments of the joints were calculated from the obtained positional data of the joints using the human rigid segment model described in chapter 2. Then this study analyzed the lifting operations as a motion in the sagittal plane. Subsequently, the muscle forces were calculated

from the positional data and the net moments with the proposed method. The calculated muscle forces were normalized by their maximums. The measured EMGs full-wave rectified and filtered with a low-pass, critically-damped digital filter (cutoff frequency 6 Hz) [8]. The measured EMGs were normalized by their maximums under the maximum voluntary contraction. Strictly speaking, it is impossible to compare the calculated muscle force and the measured EMG because the measured EMG represents the muscle activation level which has the property that the muscle activation level is larger as the muscle contraction velocity is larger under the same muscle force [9]. However, this study assumed to neglect the effects of the muscle contraction velocity and compared the calculated muscle forces and the measured EMGs to validate the proposed model. The analysis programs were made with Borland C++ Builder 6 to calculate the muscle forces from positional and force plate data.

### 4.2.3 Results and discussion

The results of the maximum output force distributions of three participants of the upper limb are shown in Fig. 4.6a and those of the lower limb are shown in Fig. 4.6b. Using these results, the muscle forces during the lifting operations can be estimated with the proposed method considering the physical characteristics such as the maximum muscle forces. The net moments of each participant calculated from the obtained positional data with the human rigid segment model are shown in Fig. 4.7a to Fig. 4.7c.Then, the net moments of the knee joint (flexion as a positive direction), the hip joint (extension as a positive direction), the shoulder joint (flexion as a positive direction) and the elbow joint (flexion as a positive direction) that have a great effect on the lifting operations are shown in the Figures. The normalized muscle forces of each participant of the upper and lower limbs estimated by the proposed method

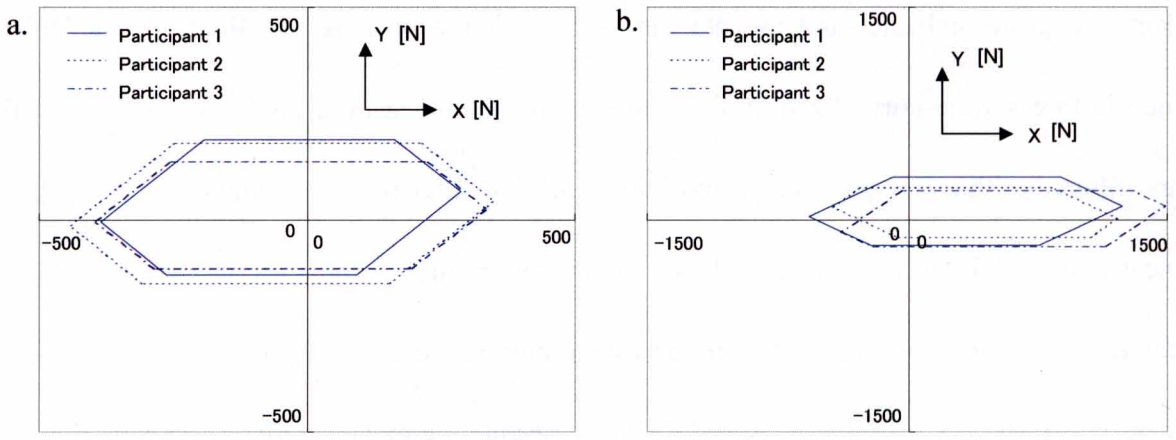


**Fig. 4.6** Measured maximum output force distribution on the distal extremity

(a = Upper limb, b = Lower limb)

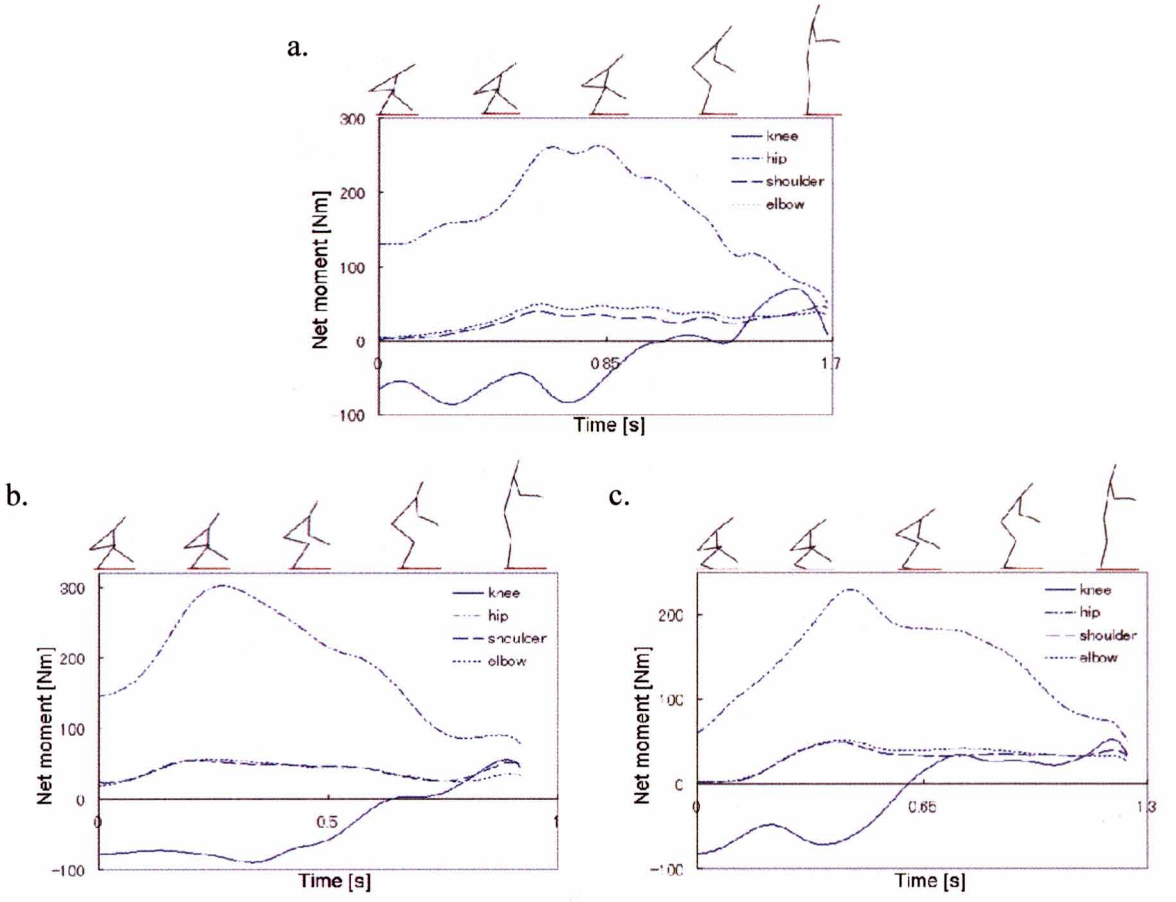


**Fig. 4.7** Net moments of the knee, hip, shoulder and elbow joints

(a = Participant 1, b = Participant 2, c = Participant 3)

a.

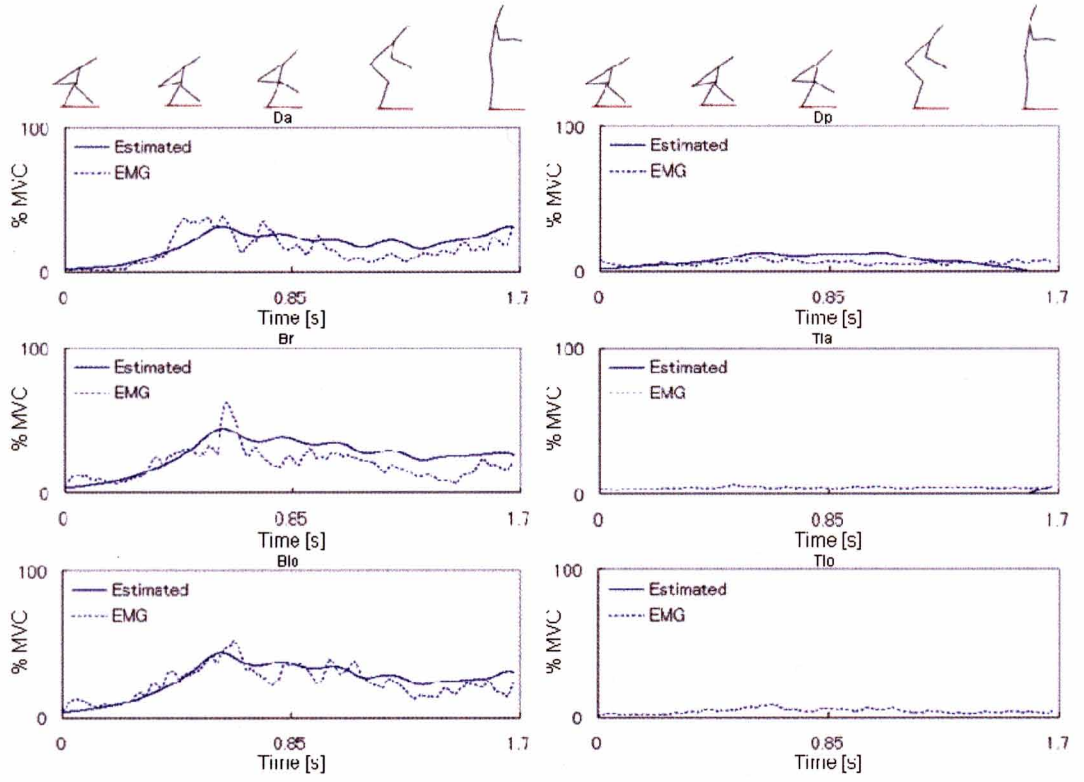


b.

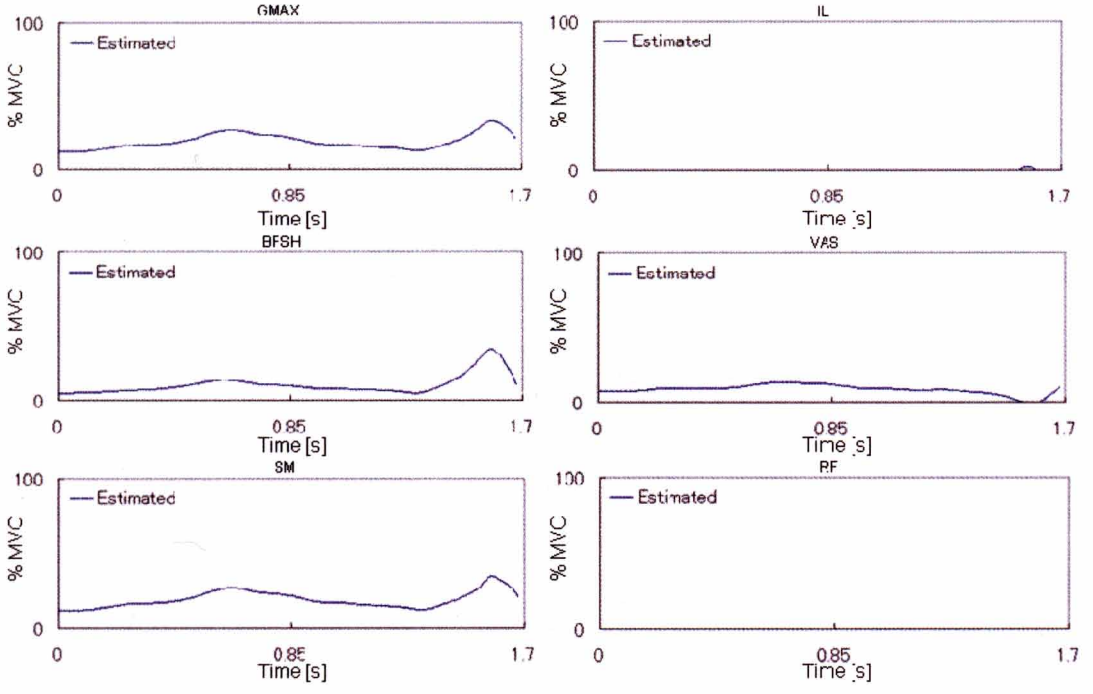


**Fig. 4.8** Normalized muscle forces estimated by the proposed method and the EMG

(a = Upper limb, b = Lower limb) (Participant 1)

a.

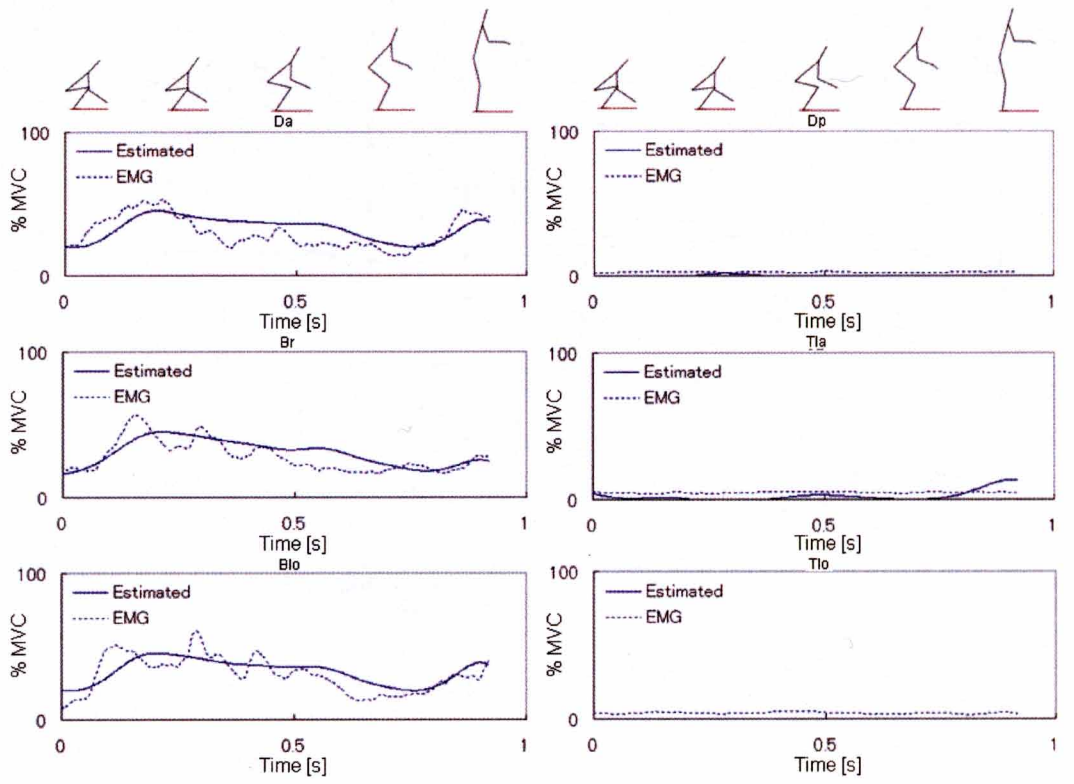


b.

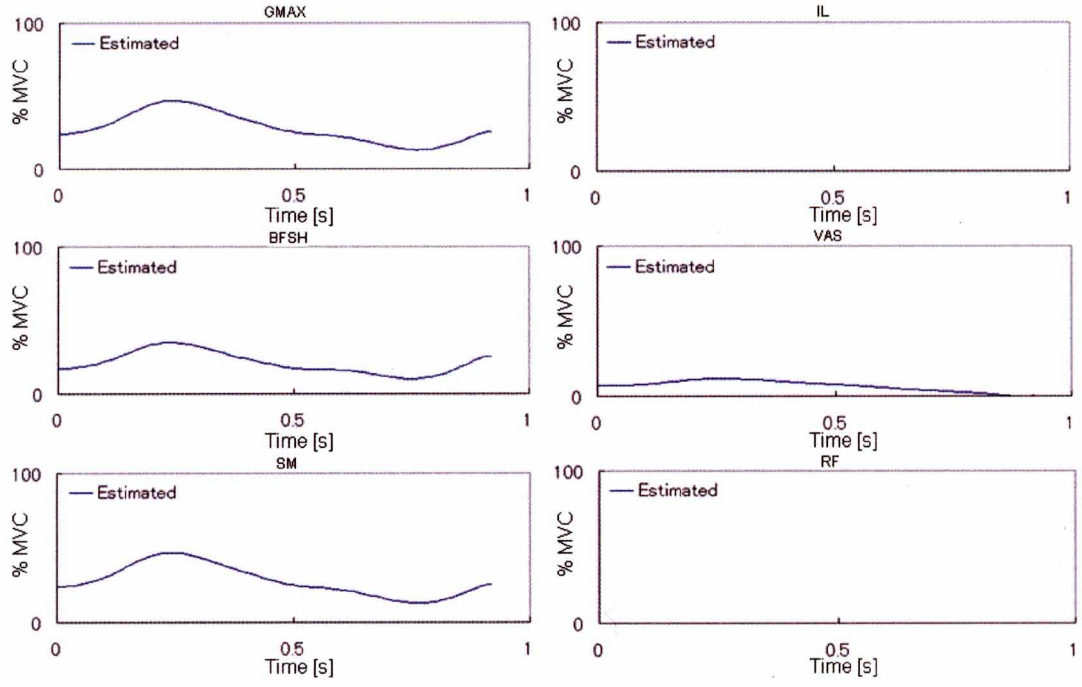


**Fig. 4.9** Normalized muscle forces estimated by the proposed method and the EMG

(a = Upper limb, b = Lower limb) (Participant 2)

a.

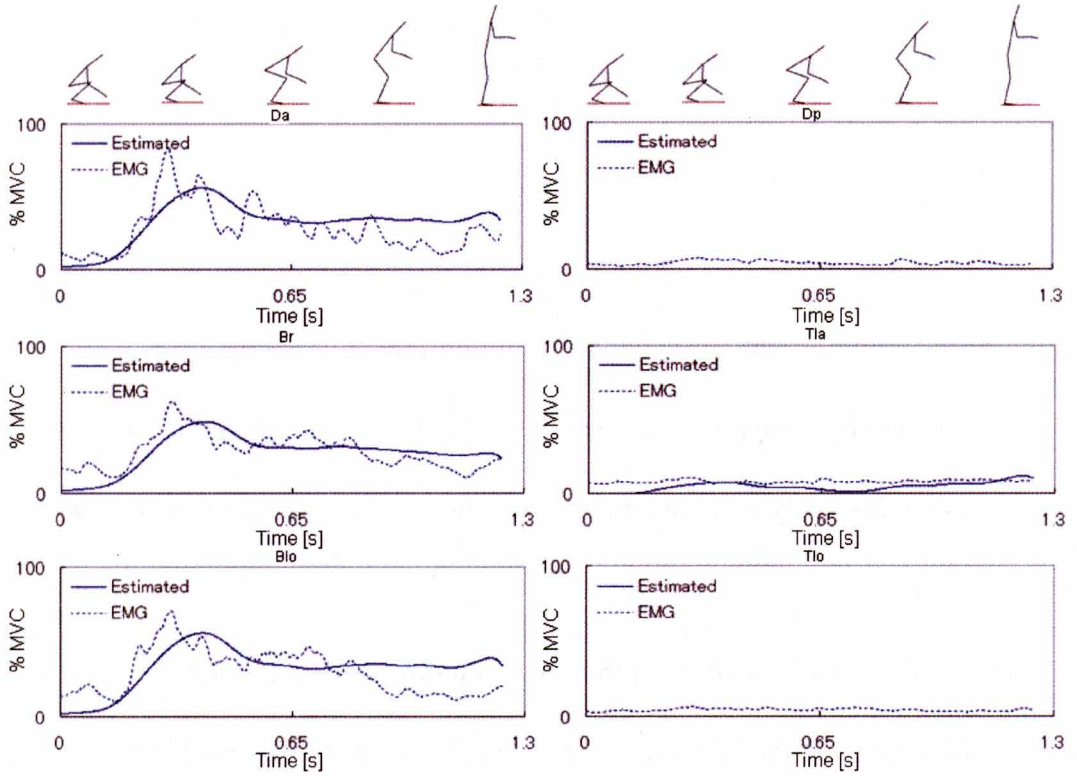


b.

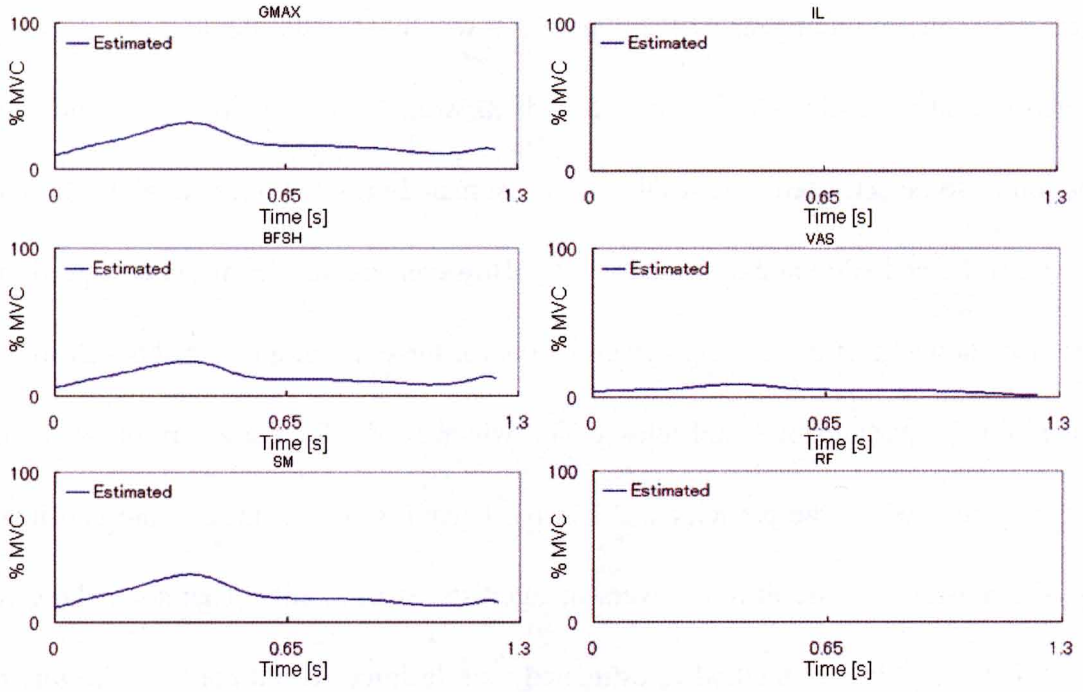


**Fig. 4.10** Normalized muscle forces estimated by the proposed method and the EMG

(a = Upper limb, b = Lower limb) (Participant 3)

during the lifting operations are shown in Fig. 4.8 to Fig. 4.10. Then the results of the EMGs were compared with the estimated muscle forces to validate the proposed method on the upper limb. On the other hand, only the results of the estimated muscle forces are shown on the lower limb. In chapter 3, this study proposed the extended musculoskeletal model including 9 muscles on the lower limb to estimate muscle forces and applied this model to dynamic motion such as vertical jumping. Furthermore, this study verified the proposed model was validated by comparing between the estimated muscle forces and the EMGs in the experiment. Then this study assumed not to need the EMGs to validate the proposed method on the lower limb.

The results of the upper limb showed that the net moments of the shoulder and elbow joints worked for the flexion of the joints and these were larger as the external forces of the upper extremity derived from the mass of the object were large before the object gets off the ground. The results of the net moments of the upper limb working for the flexion of the joints were expected to make muscles Da, Br and Blo, which work for the flexion of the shoulder and elbow joints, to be activated. The results of the estimated muscle forces certainly showed that muscles Da, Br and Blo were activated greatly. However, the results of the estimated muscle forces also showed that muscle Dp, which works for the extension of the shoulder joint, was activated on the participant 1 and muscle Tla, which works for the extension of the elbow joint, was activated on the participant 2 and participant 3. These muscles are considered to work in opposition to the prime movers or agonists of the joints. Therefore, these results showed that the proposed method to estimated muscle forces could consider the role of the antagonistic muscles on the upper limb. Furthermore, the correlations between the proposed method and the EMGs of muscles Da, Br and Blo, which have a great effect on the lifting

operations, were 0.74, 0.73 and 0.85 on participant 1, 0.61, 0.75 and 0.77 on participant 2 and 0.67, 0.70 and 0.53 on participant 3, respectively. Though the correlations of participant 3 were a little weak, the activation patterns of the muscle forces of the proposed method were similar to those of the EMGs. So the proposed method was considered to successfully estimate the activation patterns of the muscles during lifting operations on the upper limb.

The results of the lower limb showed that the net moments of the knee and hip joints worked for the extension of the joints. The results of the net moments of the lower limb working for the extension of the joints were expected to make muscles VAS, which works for the extension of the knee joint, and muscle GMAX, which works for the extension of the hip joint, to be activated. The results of the estimated muscle forces showed that muscles GMAX, BFSH, VAS and SM were activated greatly. Then muscle SM was plausible to be activated because muscle SM, which is the biarticular muscle and works on the knee and hip joints simultaneously, works for the extension of the hip joint. But muscle BFSH works for the flexion of the knee joint. This muscle is considered to work in opposition to the prime movers or agonists of the joint. Therefore, these results showed that the proposed method to estimated muscle forces could consider the role of the antagonistic muscles during the lifting operations.

The results of the lifting operations to estimate muscle forces showed that muscles Da, Br and Blo worked for the flexion of the shoulder and elbow joints mainly and muscle Dp or Tla worked in opposition to the prime movers or agonists of the joints on the upper limb. Furthermore, the results also showed that muscles GMAX and SM worked for the extension of the hip joint mainly, muscle VAS worked for the extension of the knee joint mainly and muscle BFSH worked in opposition to the prime movers or agonists of the joint on the lower limb. The results of this study found the workload of the upper limb relatively large

considering the effects of the muscles though the workload of the upper limb seemed to be small on the evaluation of the net moments because the net moment of the hip joint was especially large and the net moments of the shoulder and elbow joints were relatively small.

Then, the antagonistic muscles are the muscles that act in opposition to the prime movers or agonists of a movement. The role of these muscles contributes to realize the control function responding flexibility to disturbance. The role of these muscles also contributes to control accurately the direction of the output force. Biarticular muscles are the muscles that work simultaneously on two joints. These muscles, which look redundancy, can realize robust stability by constructing the control system coordinating with other muscles. Therefore, the antagonistic muscles and the biarticular muscles are considered to work mainly for the control of the direction of the output force, especially for the control of the object, and for keeping up the body balance during lifting operation. The consideration of these muscles is considered to be necessary to not only evaluate operations considering the physical characteristics but also provide workers with the optimal motions and environments that they can work safely, efficiently and comfortably

In conclusion of this section, this study investigated a musculoskeletal model of the upper and lower limbs including the roles of antagonistic muscles and biarticular muscles to estimate muscle forces during the lifting operations as an example of a working motion. The lifting operations were conducted to estimate muscle forces of upper and lower limbs with the proposed model. Surface electromyograms (EMGs) of deltoid anterior (Da), deltoid posterior (Dp), brachialis (Br), lateral head of triceps brachii (Tla), long head of biceps (Blo) and long head of triceps brachii (Tlo) were measured to compare with the estimated muscle forces. The results of this study showed that the proposed method was considered to successfully estimate

the muscle activation patterns during the lifting operations. Thus, the proposed musculoskeletal model can provide the environments where humans can work efficiently and safely considering their physical characteristics.

## 4.3 Verification of workload of muscles on various motion patterns in computer simulation

In this section, various motion patterns in the lifting operations were created in computer simulation based on the experimental lifting operations and evaluated considering the muscle forces of the upper and lower limbs estimated with the musculoskeletal model that considers the roles of antagonistic muscles and biarticular muscles.

### 4.3.1 Method to evaluate lifting operations on various motion patterns in computer simulation

**Human rigid segment model.** This study assumed lifting operations to be 2-dimensional motion. This study used a human rigid segment model that consists of 8 rigid body segments (1-Foot, 2-Leg, 3-Thigh, 4-Body, 5-Upper arm, 6-Forearm, 7-Hand, 8-Head) as shown in Fig. 4.11, where the link length of segment $i$ is represented by $l_i$, the contact point between segment $i$ and $i$-1 is represented by $O_i$ and the angle between segment $i$ and horizontal direction is represented by $\theta_i$.

**Motion patterns in computer simulation.** The variations of the angles of the joints during the lifting operations were suggested to be approximated by the function described as follow [10].

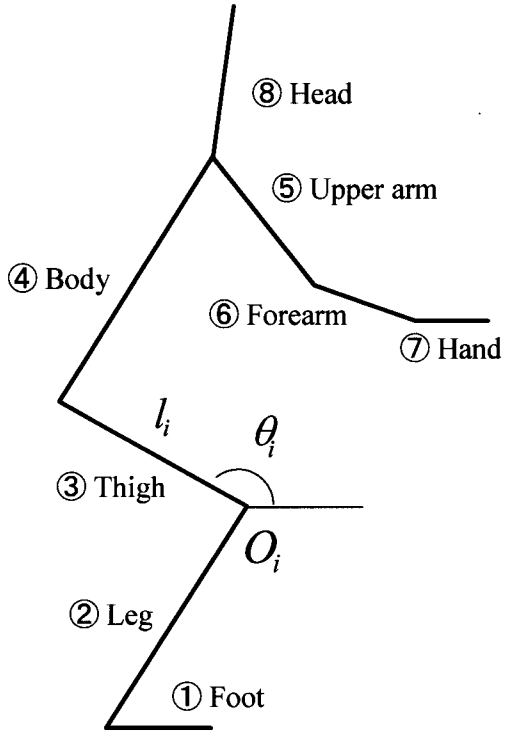


**Fig. 4.11** 2-dimensional human rigid segment model

$$f(t) = f_0 + (f_1 - f_0)\left[\frac{t}{pT} - \frac{1}{2\pi}\sin(\frac{2\pi t}{pT})\right] \tag{4.3}$$

Then, $T$ is the duration of the angle variation, $f_0$ is the angle at $t$=0 [s] and $f_1$ is the angle at $t$=$T$ [s]. $p$ is the variable that changes the duration of the angle variation. The variable $p$ is 1 during the standard lifting operations. For example, when the value of the variable $p$ is changed to 1/2, the duration of the angle variation is changed to 1/2 and the velocity of the angle variation is changed to be doubled. When the value of the variable $p$ of all joints is changed to 1/2 during the lifting operations, the lifting operations is conducted at twice the speed. Furthermore, when the value of the variable $p$ of the angle of lower body, $\theta_1$, $\theta_2$, $\theta_3$ is changed to 1/2 and that of upper body, $\theta_4$, $\theta_5$, $\theta_6$, $\theta_7$, $\theta_8$ is still 1, the motion pattern that human gets off his hip before lifting up the object can be created. Thus, the function of the angle variation can change the relationship among the joints and create various motion

patterns of lifting operations.

This study created various motion patterns of the lifting operations with the motion of the human body separated to the upper and lower bodies. The motion pattern that human gets off his hip before lifting up the object is assumed to be pattern A and the motion pattern that human gets off his hip after lifting up the object is assumed to be pattern B. Then the pattern A can be created by changing the variable $p$ of each joint, which is assumed to be $1/2 \le p \le 1$, with the function (4.3) and determining the angle variation of each joint described as follows.

On the angles of the upper body, $\theta_4$, $\theta_5$, $\theta_6$, $\theta_7$, $\theta_8$:

$$\begin{aligned} \theta_i &= f_0 \quad \text{when } 0 \le t \le (1-p)T \\ \theta_i &= f(t) \quad \text{when } (1-p)T < t \le T \end{aligned} \tag{4.4}$$

On the angles of the lower body, $\theta_1$, $\theta_2$, $\theta_3$:

$$\begin{aligned} \theta_i &= f(t) \quad \text{when } 0 \le t \le pT \\ \theta_i &= f_1 \quad \text{when } pT < t \le T \end{aligned} \tag{4.5}$$

On the other hand, the pattern B can be created by determining the angle variation on the upper body, $\theta_4$, $\theta_5$, $\theta_6$, $\theta_7$, $\theta_8$, with the formula (4.5) and that on the lower body, $\theta_1$, $\theta_2$, $\theta_3$, with the formula (4.4). As the value of the variable $p$ is changed to approaching 1/2, the motion pattern is approaching to the pattern A or the pattern B. As the value of the variable $p$ is changed to approaching 1, the motion pattern is approaching to the standard motion pattern. Then the control variable is assumed to be $s$ ($0 \le s \le 1$). The variable $p$ is defined as follows to create the pattern A as the control variable $s$ is changed to approaching 0 and the pattern B as the control variable $s$ is changed to approaching 1.

$$\begin{aligned} p &= s + 0.5 \quad \text{when } s \le 0.5 \\ p &= 1.5 - s \quad \text{when } s > 0.5 \end{aligned} \tag{4.6}$$

When the control variable $s$ is 0.5, the standard motion pattern is created.

Then the lifting operations were conducted to validate the method to create various motion patterns with the formula as described above. One participant (height: 172.0 cm, mass: 66.0 kg), after informed consent, participated in this study. Participant conducted three motions, the standard motion, the motion where human gets off his hip before lifting up the object (pattern A) and the motion where human gets off his hip after lifting up the object (pattern B).

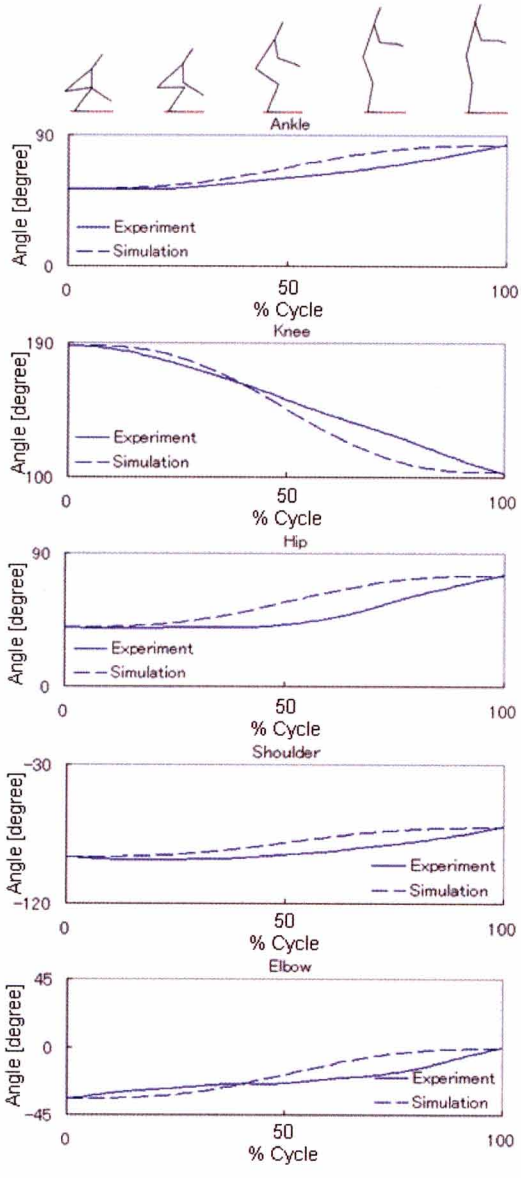


**Fig. 4.12a** Comparison of the joint angles between the experiment and the functional approximation (Standatd)

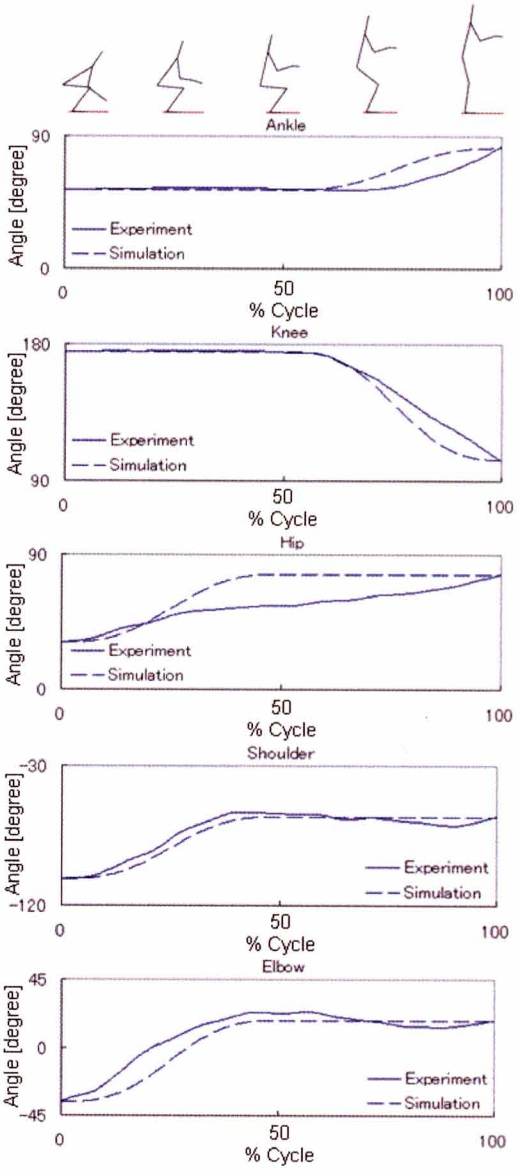


**Fig. 4.12b** Comparison of the joint angles between the experiment and the functional approximation (Pattern A)

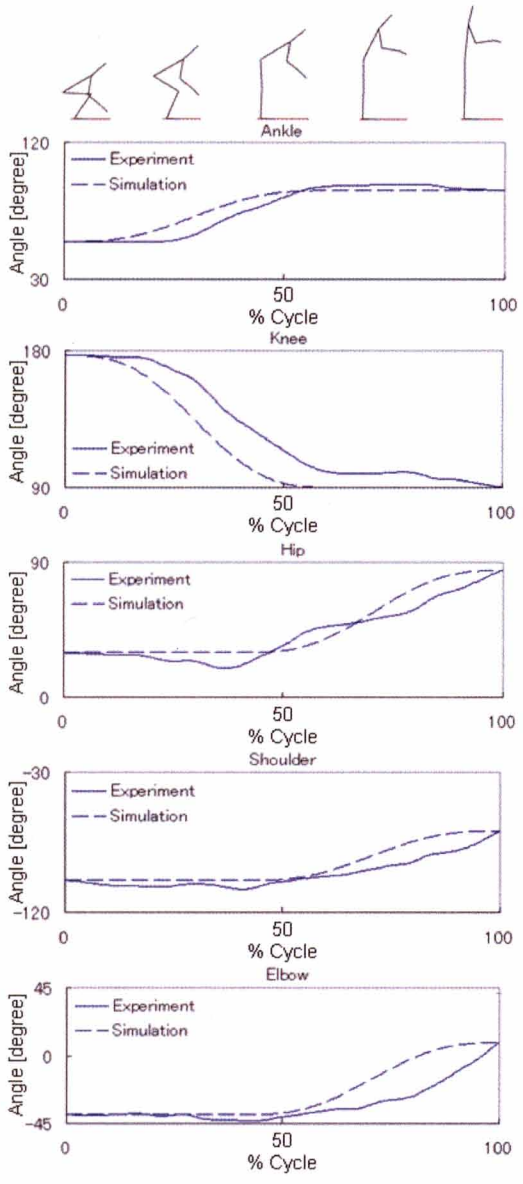


**Fig. 4.12c** Comparison of the joint angles between the experiment and the functional approximation (Pattern B)

Each lifting operations was recorded at 125 frames per second using the CCD camera (SONY Corp. XC-009). The conditions of the lifting operations were that the height of lifting was 1.0 m and the mass of the object was 10 kg. The positional data of the joints obtained from the captured images were smoothed using a Butterworth filter (cutoff frequency 6 Hz) [6, 7]. Then the angel variation calculated from the captured images was compared with that created by the formulas. The results of the angle variation of the standard motion, the pattern A and the pattern B are shown in Fig. 4.12. Then the angles of the ankle, knee, hip, shoulder and elbow joints that have a great effect on the lifting operations are shown in the Figures. The motion pictures in the Figures are the motions created by the formulas.

The results showed that the patterns of the angle variation calculated from the captured images were similar to those created by the formulas. So the proposed method was considered to be validated to create various motion patterns with the control variable $s$ changed in the

formulas.

**Evaluation of muscle forces.** This study evaluated various motion patterns of the lifting operations created by the method described in the preceding section considering the muscle forces of the upper and lower limbs. This study used the musculoskeletal model to estimate muscle forces of the upper and lower limbs described in chapter 4. 2. The musculoskeletal model includes 6 representative muscles of the upper limb and 6 representative muscles of the lower limb in sagittal plane. The following muscles are included: deltoid anterior (Da), deltoid posterior (Dp), brachialis (Br), lateral head of triceps brachii (Tla), long head of biceps (Blo) and long head of triceps brachii (Tlo) on the upper limb and gluteus maximus (GMAX), iliopsoas (IL), biceps femoris and short head (BFSH), vastus lateralis (VAS), semimembranosus (SM), rectus femoris (RF) on the lower limb. Furthermore the musculoskeletal model can consider the roles of antagonistic muscles and biarticular muscles. The maximum output force distribution derived from the maximum force of each muscle is necessary to be clarified preliminarily to estimate the muscle forces during motions with the musculoskeletal model. Then, this study applied the method of measuring the maximum output force distribution suggested by Oshima *et al.* [5]. The results of the maximum output force distributions of the upper and lower limbs are shown in Fig. 4.13 that is the same as the participant 2 in Fig 4.5. Using these results and the musculoskeletal model, muscle forces can be estimated during various motion patterns of the lifting operations created by the method described in the preceding section.

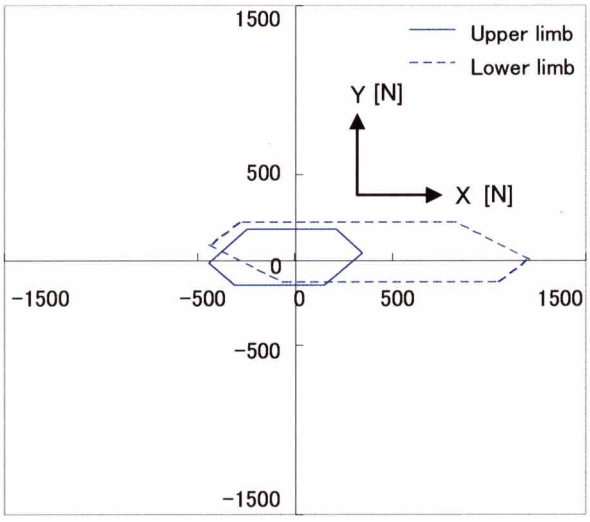


**Fig. 4.13** Measured output force distribution on the distal extremities of upper and lower limb

### 4.3.2 Results and discussion of lifting operations in computer simulation

This study evaluated various motion patterns of the lifting operations created by the proposed method based on the standard motion in the experiment. In this study, 5 motion patterns were created with the control variable *s*, which determines the motion pattern, changed to 0, 0.25, 0.5, 0.75 and 1. The motion pictures of each created motion are shown in Fig. 4.14. The net forces and the net moments of the joints were calculated on each created motion using the human rigid segment model described in chapter 2. The condition of the lifting operations was that the mass of the object was 10 kg. The results of the net moments of each created motion calculated with the human rigid segment model are shown in Fig. 4.15. Then, the net moments of the knee joint (flexion as a positive direction), the hip joint (extension as a positive direction), the shoulder joint (flexion as a positive direction) and the elbow joint (flexion as a positive direction) that have a great effect on the lifting operations are shown in the Figures. The results of the normalized muscle forces of each created motion of the upper and lower limbs estimated by the musculoskeletal model are shown in Fig. 4.16.

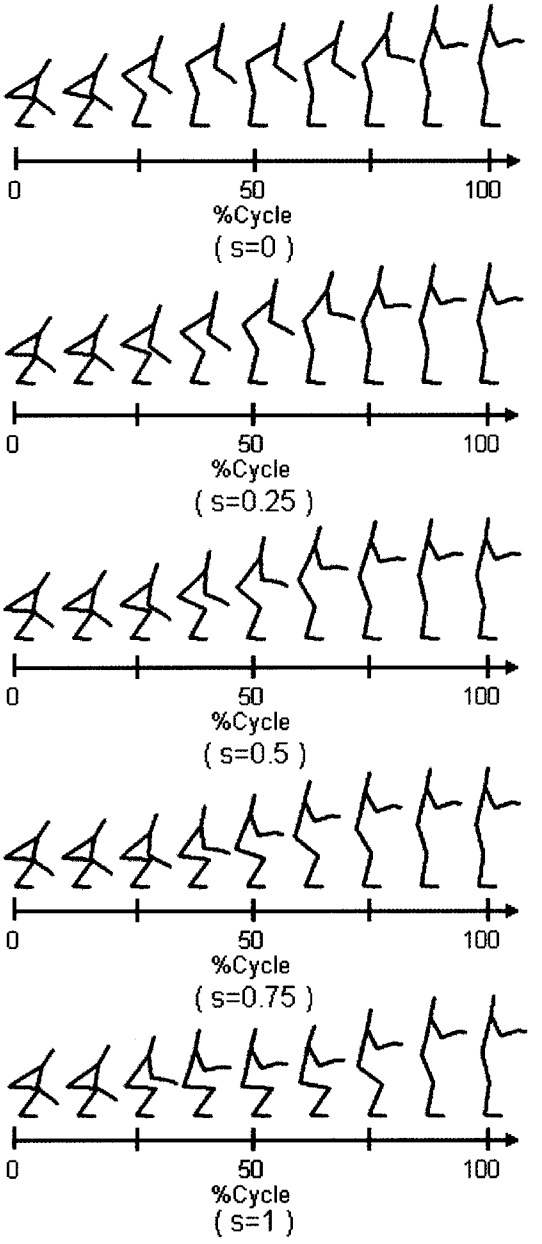


**Fig. 4.14** Motion patterns of lifting operations created with the control variable

Then the muscle forces were normalized by their maximums.

The results of the net moments of the knee joint showed that the net moments worked for the flexion of the knee joint on the motion with the control variable $s < 0.5$, where human gets off his hip before lifting up the object, and the net moments worked for the extension of the knee joint on the motion with the control variable $s \geq 0.5$, where human gets off his hip after

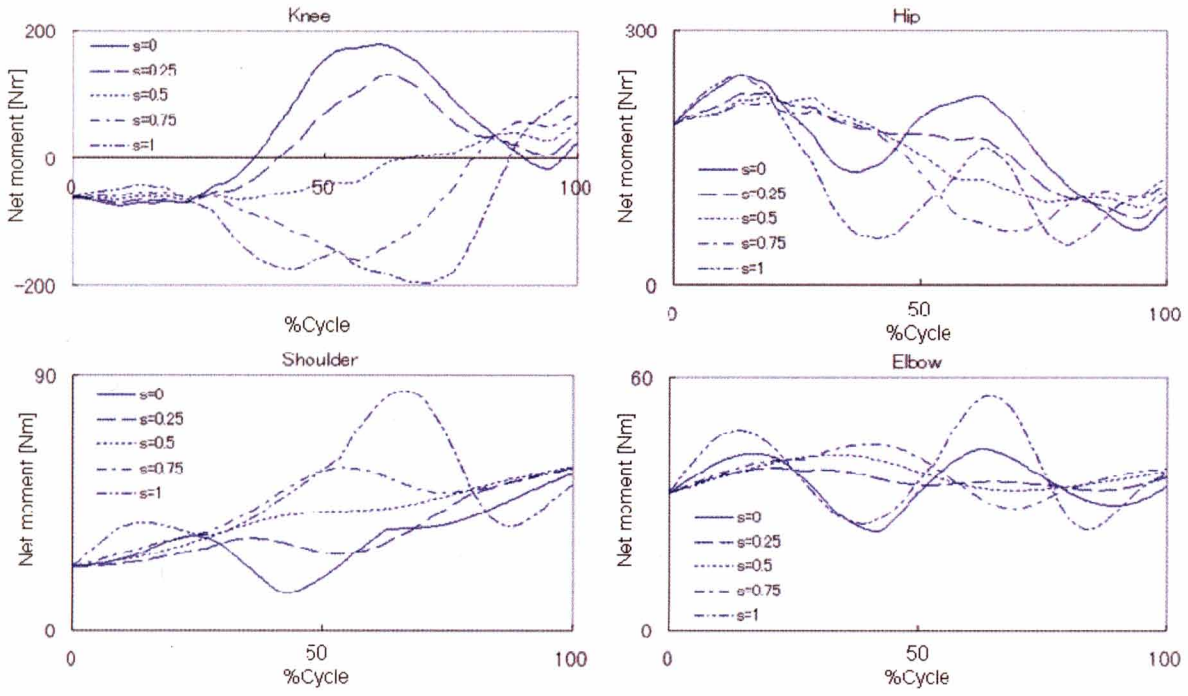


**Fig. 4.15** Net moments of the knee, hip, shoulder and elbow joints

lifting up the object.

The reason that the net moments of the knee joint worked for the flexion of the joint while the knee was extended is considered that the net moment working for the flexion of the joint made the body to be supported because the body gravity position was located in front of the knee joint. The reason that the net moments of the knee joint worked for the extension of the joint is considered that the net moment working for the extension of the joint made the knee joint to be extended because the body gravity position was located posterior to the knee joint.

The results of the net moments of the hip joint showed that the net moments were smaller as the control variable *s* was larger, where the motion pattern was changed to the motion that human gets off his hip after lifting up the object. The reason of this is considered that the horizontal length between the hip joint and the body gravity position was longer as the motion pattern was changed to the motion that human gets off his hip forward. However, the net

a.

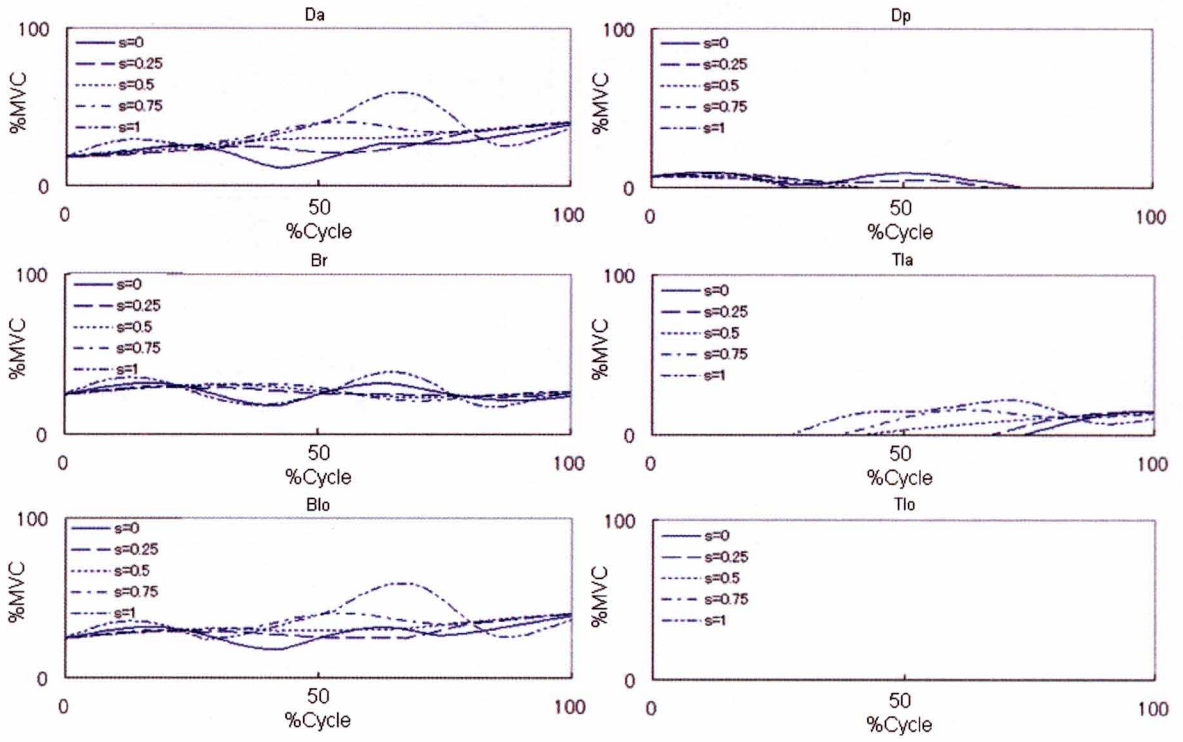


b.

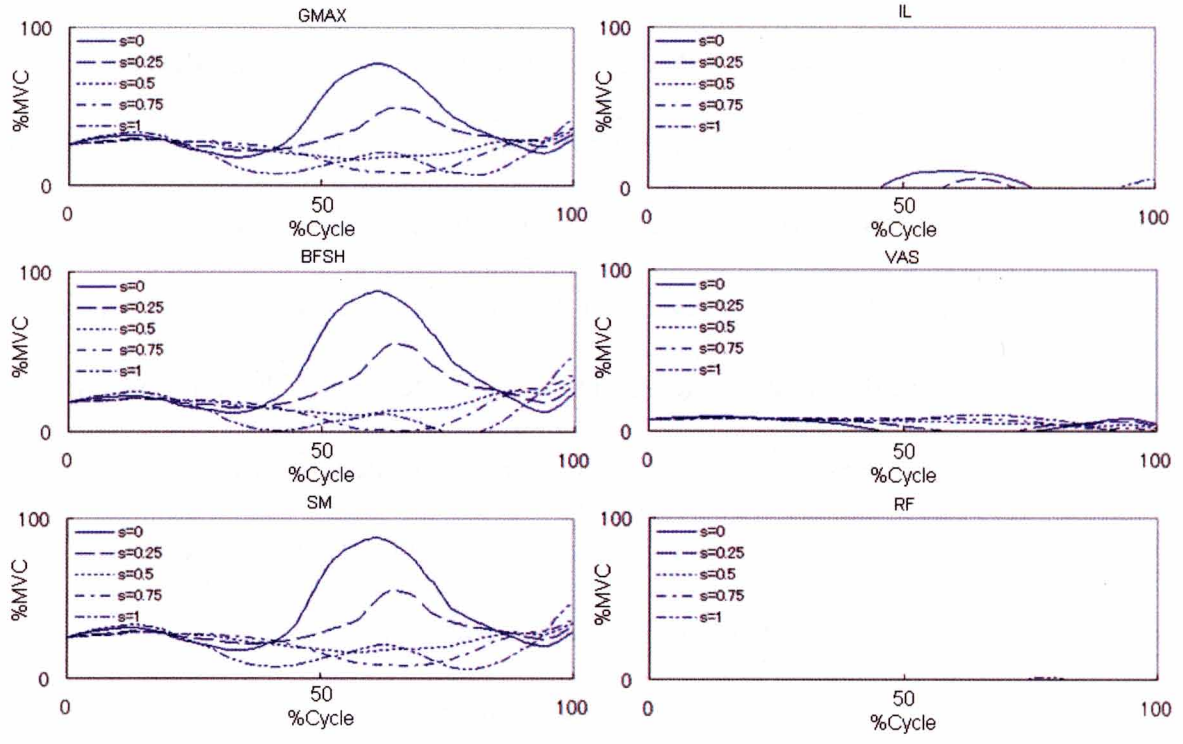


**Fig. 4.16** Estimated %MVC of each muscle (a = Upper limb, b = Lower limb)

moment of the hip joint on the motion with the control variable $s = 1$ was large after $\%Cycle = 50$. The reason of this is considered that the angle accelerations of the joints of the lower body were large as human gets off his hip at twice the speed of the standard motion.

The results of the net moments of the shoulder joint showed that the net moments were larger as the control variable $s$ was larger. The reason of this is considered that the horizontal length between the shoulder joint and the object was longer as human lifts the object forward, and that the external forces on the distal extremity derived from the object were larger with the acceleration of the object larger as human gets off his hip faster with the control variable $s$ larger such as 0.75 and 1.

The results of the net moments of the elbow joint showed that the net moments were not greatly different among the created motions. But the net moments were a little large on the motions with the control variable $s = 0$, 0.75 and 1. The reason of this is considered that the external forces on the distal extremity derived from the object were larger with the acceleration of the object larger as the motions were changed to the pattern A that human gets off his hip forward extremely or the pattern B that human lifts up the object forward extremely.

The results of the muscle forces of the upper limb showed that muscles Da, Br and Blo were activated greatly. The results of the muscle forces of the lower limb showed that muscles GMAX, BFSH and SM were activated greatly.

The muscle forces of muscle Br, which works for the flexion of the elbow joint, were not greatly different among the created motions. The muscle forces of muscle Da, which works for the flexion of the shoulder joint, and muscle Blo, which works for the flexion of the shoulder and elbow joints simultaneously, were larger as the control variable $s$ was larger,

where the motion pattern was changed to the motion that human lifts up the object forward. The reason of this is considered that the horizontal length between the shoulder joint and the object was longer as human lifts the object forward, and that the external forces on the distal extremity derived from the object were larger with the acceleration of the object larger as human gets off his hip faster with the control variable $s$ larger such as 0.75 and 1. Muscle Dp, which works for the extension of the shoulder joint, or muscle Tla, which works for the extension of the elbow joint, were also activated. These muscles were considered to work in opposition to the prime movers or agonists of the joints. These muscles are considered to have no effect on the evaluation of various lifting operations because of their slight activations.

The muscle forces of muscle VAS, which works for the extension of the knee joint, were small on each created motion. The results that muscle RF, which is biarticular muscle and works for the extension of the knee joint, was not activated showed that only muscle VAS were used for the extension of the knee joint on each created motion. Though muscle VAS was not activated greatly, muscle VAS is considered to contribute to the extension of the knee joint mainly because the maximum muscle force of muscle VAS was large. However, muscle VAS is considered not to have a great effect on the evaluation of various lifting operations because the muscle forces of muscle VAS were not greatly different among the created motions.

The muscle forces of muscle GMAX, which works for the extension of the hip, and muscle SM, which is biarticular muscle and works for the extension of the hip, were larger as the control variable $s$ was smaller, where the motion patterns were changed to the motion that human gets off his hip forward. Especially, muscles GMAX and SM were activated greatly on the motions with the control variable $s$ = 0 and 0.25. The results of this showed that the

motion that human gets off his hip forward was a back-straining work. The back-straining has been clarified to cause disorders on back such as a hernia of intervertebral disk and a spondylolysis in the lifting operations. Thus, muscles GMAX and SM are very important to evaluate various lifting operations.

Muscle BFSH, which works for the flexion of the knee joint, were also activated greatly. This muscle was considered to work in opposition to the prime movers or agonists of the joint. Muscle BFSH can be considered to have no effect on the evaluation of various lifting operations though muscle BFSH was activated greatly because muscle BFSH is a very small muscle.

The averages of normalized muscle force of muscles Da and Blo on the upper limb and muscles GMAX and SM on the lower limb, which have great effects on the lifting operations, are shown in Fig. 4.17 to discuss the relationship among the muscles on various created lifting operations. The results showed that the muscles on the upper limb were more activated, but

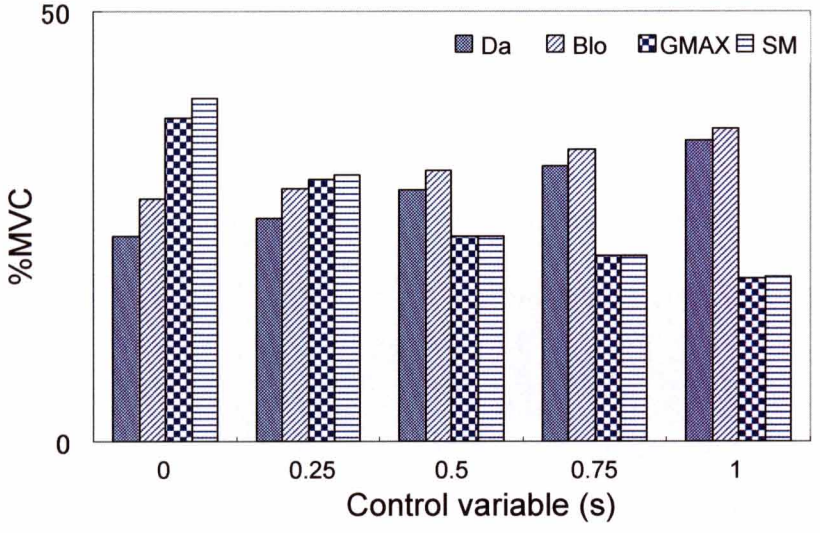


**Fig. 4.17** Average of normalized muscle force of each muscle on the various lifting operations

the muscles on the lower limb were less activated as the motion patterns were changed to the motion that human lifts up the object forward from the motion that human gets off his hip forward. Thus, the strain of the upper limb was more, but that of the lower limb was less on the motion that human lifts up the object forward. However, the results that muscles GMAX and SM, which work for the hip joint, were activated greatly as the maximum normalized muscle forces were over 80% during motion that human gets off his hip forward are considered that the motion that human lifts up the object forward is better to reduce the possibility of working injuries during the lifting operations. Thus, the proposed method to create various motions in computer simulation and evaluate the motions considering the role of muscles can provide ergonomically safe working motions. Furthermore, the proposed method can also provide the environments where humans can work efficiently and safely.

In this section, various motion patterns in lifting operations were created in computer simulation based on the experimental lifting operations and evaluated considering the muscle forces of the upper and lower limbs estimated with the musculoskeletal model that considers the roles of antagonistic muscles and biarticular muscles. The results of this study showed that the proposed method to create various motions in computer simulation and evaluate the motions considering the role of muscles can provide ergonomically safe working motions. Furthermore, the proposed method provides simulated environments where human motions can be tested safely for work efficiency.

## 4.4 Conclusion

Previously, computer human models that can evaluate for the products designs, the improvement of working environments and the efficiency of rehabilitation procedures have

been developed. However, they are not unfortunately enough to evaluate the workload of muscles because they have used the human rigid segment model or the musculoskeletal model that can not consider the roles of antagonistic muscles and biarticular muscles. Furthermore, the evaluation of various motion patterns for human considering the muscle forces has not been investigated sufficiently. Then, this study investigated a musculoskeletal model of the upper and lower limbs including the roles of antagonistic muscles and biarticular muscles. This study also proposed the method to estimate muscle forces during the lifting operations as an example of a working motion. Furthermore, this study proposed the method to create various motions in computer simulation and evaluate the motions considering the roles of muscles.

The lifting operations were conducted to estimate muscle forces of upper and lower limbs with the proposed method. Surface electromyograms (EMGs) of deltoid anterior (Da), deltoid posterior (Dp), brachialis (Br), lateral head of triceps brachii (Tla), long head of biceps (Blo) and long head of triceps brachii (Tlo) were measured to compare with the estimated muscle forces. The results showed that the proposed method was considered to successfully estimate the muscle activation patterns during the lifting operations. Various motion patterns in lifting operations were created in computer simulation based on the experimental lifting operations and evaluated considering the muscle forces of the upper and lower limbs. The results of this study showed that the proposed method was considered to successfully create various motions in computer simulation and evaluate the motions considering the roles of muscles. Thus, the proposed method provides simulated environments where human motions can be tested safely for work efficiency.

**References**

[1] SIEMENS, Tecnomatix, Jack and Process Simulate Human, <http: //www.plm.automation.siemens.com/en_in/products/tecnomatix/assembly_planning/jack/index.shtml>.

[2] HUMAN SOLUTIONS, RAMSIS COMMUNITY, <http://www.human-solutions.com/automotive/ramsis_community/index_en.php>.

[3]AnyBodyTech, Anybody Modeling System. Software package <http://www.anybodytech.com/>.

[4] Oshima T., Fujikawa T., Kumamoto M. : Functional Evaluation of Effective Muscle Strength Based on a Muscle Coordinate System Consisted of Biarticular and Monoarticular Muscles - Contractile Forces and Output Forces of Human Limbs, Journal of the Japan Society of Precision Engineering, 65(12), 1772-1777, 1999.

[5] Oshima T., Fujikawa T., Kumamoto M. : Functional Evaluation of Effective Muscular Strength Based on a Muscle Coordinate System Consisted of Bi-articular and Mono-articular Muscles – Simplified Measurement Technique of Output Force Distribution-, Journal of the Japan Society of Precision Engineering, 67(6), 943, 2001.

[6] Winter D. A., Sidwall H. G., Hobson D. A. : Measurement and reduction of noise in kinematics of locomotion, Journal of Biomechanics, 7, 157–159, 1974.

[7] Pezzack J. C., Winter D. A., Norman R. W. : An assessment of derivative determining techniques for motion analysis, Journal of Biomechanics, 10, 377–382, 1977.

[8] Robertson D. G. E., Dowling J. J. : Design and responses of Butterworth and critically damped digital filters, Journal of Electromyography and Kinesiology, 13, 569-573, 2003.

[9] Delp S., Loan P., Hoy M., Zajac F. E., Fisher S., Rosen J. : An interactive graphics-based

model of the lower extremity to study orthopaedic surgical procedures, IEEE Trans. on Biomedical Engineering, 37(8), 757-767, 1990.

[10] Passerello C. E., Huston R. L. : Human Attitude Control, Journal of Biomechanics, 4(1), 95-102, 1971.

# 5. Muscular fatigue model to evaluate muscle fatigue progress under several muscular force patterns

## 5.1 Introduction

For several decades, factory automation or unmanned factory productivity has been progressed to realize much higher productivity in manufacturing. However, human centered manufacturing system is getting attention to realize much more flexibility for manufacturing of wide product variety and volume. Previously, computer human models that duplicate the properties and the functions of human have been developed. Various researches [1, 2] for the evaluation of human properties have been investigated to improve the computer human models. This study have also investigated the human rigid segment model to estimate the net forces and the net moments of the joints during motions described in chapter 2 and the musculoskeletal model to estimate the muscle forces during motions described in chapter 3. Estimation of muscle fatigue progress is also important to evaluate the operability and the workability. Especially, the muscle fatigue can not be neglected to evaluate the operations that give great physical workload or need long hours. However, the previous computer human models have not considered the muscle fatigue practically. So the previous models are considered to be limited to apply to the short-hours motion that can neglect the muscle fatigue [3]. A few researches to model a mechanism of muscle fatigue have been investigated [4, 5]. But unfortunately they have only been applied to the muscle fatigue progress under the condition of maximum voluntary contraction.

Then, this study investigated a mechanism of muscle fatigue and proposed a muscular fatigue model to evaluate the muscle fatigue progress under several muscular force patterns.

Then, the endurance times for keeping constant forces of participants were estimated considering their physical characteristics. The iteration numbers for keeping constant forces with interval were also estimated. To validate the effectiveness of the proposed method, experimental verifications were conducted.

## 5.2 Muscular fatigue model

### 5.2.1 Muscular fatigue model suggested by Liu [4]

Liu *et al.* [4] suggested the muscular fatigue model including the states of activity, fatigue and recovery of a muscle. This model as shown in Fig. 5.1 includes three groups of muscular motor units: the motor unit of standby state represented by $M_{uc}$, that of activity state represented by $M_A$ and that of fatigue state represented by $M_F$. The parameter that effects on the strength to change the motor unit of standby state to that of activity state is represented by $B$. The parameter that effects on the strength to change the motor unit of activity state to that of fatigue state is represented by $F$. The parameter that effects on the strength to change the

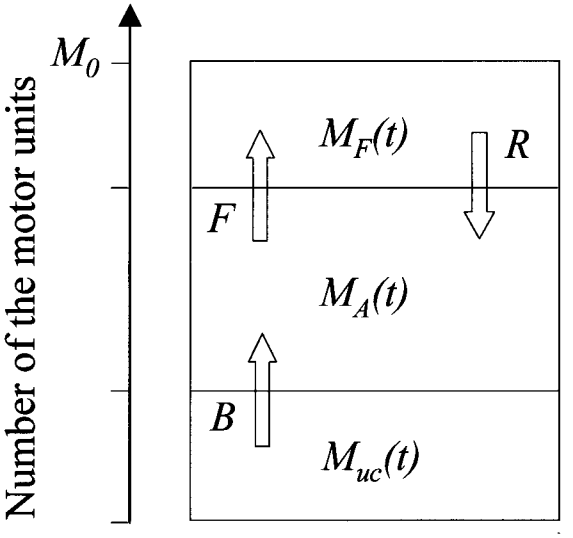


**Fig. 5.1** Dynamic relationship among three groups of muscular motor units

motor unit of fatigue state to that of activity state is represented by $R$. Then, this model defined the variation of each muscle state based on the physiological mechanism. The variation of each motor unit is described as follows.

$$\frac{dM_A(t)}{dt} = B \cdot M_{uc}(t) - F \cdot M_A(t) + R \cdot M_F(t) \tag{5.1}$$

$$\frac{dM_F(t)}{dt} = F \cdot M_A(t) - R \cdot M_F(t) \tag{5.2}$$

$$M_{uc}(t) = M_0 - M_A(t) - M_F(t) \tag{5.3}$$

The number of each motor unit is assumed as follows at the initial state ($t$ = 0).

$$\begin{aligned} M_{uc}(0) &= M_0 \\ M_A(0) &= 0 \\ M_F(0) &= 0 \end{aligned} \tag{5.4}$$

Then, if the parameters of the brain effort ($B$), the fatigue factor ($F$) and the recovery factor ($R$) are assumed to be constant, the following equations are obtained from the equations (5.1) and (5.2).

$$\frac{d^2M_A}{dt^2} + (B+F+R)\frac{dM_A}{dt} + B(F+R)M_A - BRM_0 = 0 \tag{5.5}$$

$$\frac{d^2M_F}{dt^2} + (B+F+R)\frac{dM_F}{dt} + B(F+R)M_F - BFM_0 = 0 \tag{5.6}$$

Then, the following equations [4] are obtained from the equations (5.3), (5.5) and (5.6).

$$\frac{M_A(t)}{M_0} = \frac{R}{F+R} + \frac{FB}{(F+R)(B-F-R)}e^{-(F+R)t} - \frac{B-R}{B-F-R}e^{-Bt} \tag{5.7}$$

$$\frac{M_F(t)}{M_0} = \frac{F}{F+R} + \frac{FB}{(F+R)(B-F-R)}e^{-(F+R)t} + \frac{F}{B-F-R}e^{-Bt} \tag{5.8}$$

$$\frac{M_{uc}(t)}{M_0} = 1 - \frac{M_A(t)}{M_0} - \frac{M_F(t)}{M_0} = e^{-Bt} \tag{5.9}$$

Fig. 5.2 shows the variation of each motor unit under the condition of maximum voluntary

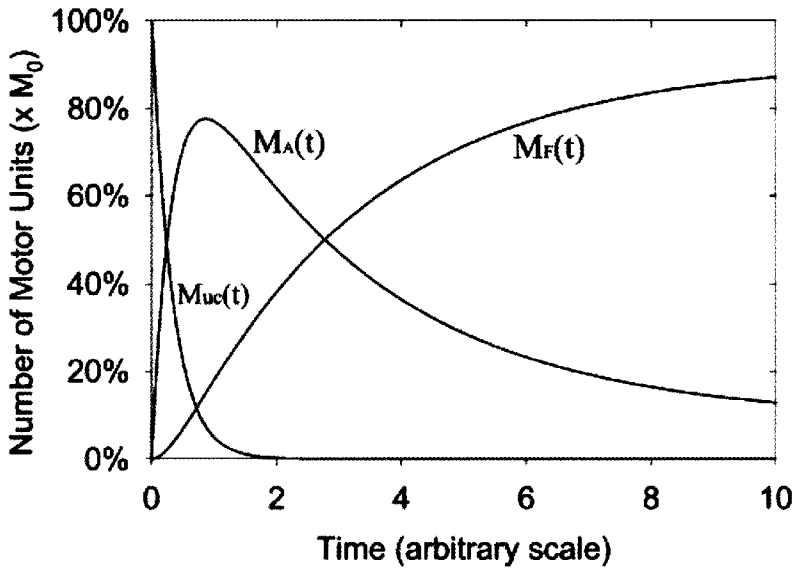


**Fig. 5.2** Variation of each motor unit in the muscular fatigue model suggested by Liu *et al.* [4]

contraction. However, the fatigue model suggested by Liu *et al.* [4] can be applied only to the condition of maximum voluntary contraction. The model cannot evaluate the muscle fatigue progress under several muscular force patterns.

### 5.2.2 Muscle fatigue progress under the condition for keeping constant output force

This study proposed the method to evaluate the muscle fatigue progress under the condition for keeping constant output force and estimate the endurance time for keeping constant forces with the help of the fatigue model suggested by Liu *et al.* [4]. This study proposed the variation of each motor unit with the unit $M_A$ arbitrarily constant though the model suggested by Liu *et al.* [4] can be applied only under the condition of maximum voluntary contraction. Fig. 5.3 shows the variation of each motor unit under the condition for keeping arbitrarily constant output force.

Phase *a* is the phase before output force, where every motor unit is standby state. Phase *b* is

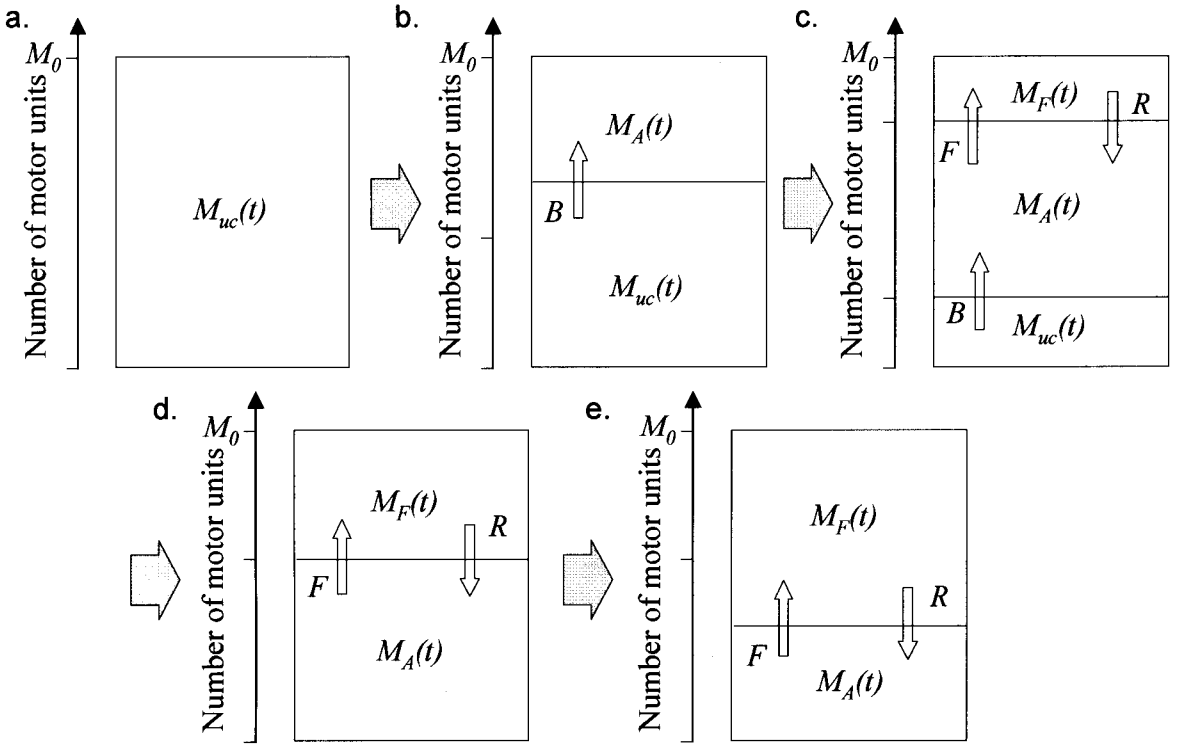


**Fig. 5.3** Muscle fatigue progress under the condition for keeping constant output force

the phase just after beginning constant output force, where the motor unit of standby state is changed to that of activity state gradually. Subsequently, the phase is changed to phase *c*, where the motor unit of standby state is changed to that of activity state and that of activity state is gradually changed to that of fatigue state, under the condition for keeping constant output force. Phase *d* is the phase where every motor unit of standby state has been changed to that of activity state, where the constant output force can not be kept. Then the phase is changed to the phase *e*, where the motor unit of activity state is balanced with that of fatigue state. This study can evaluate the variation of each motor unit under the condition for keeping arbitrarily constant output force by considering each phase separately. The percentage of constant output force is assumed to be $X$ %. Then, the variation of each motor unit between the phase *a* and the phase *b* is described by the formula (5.1) to formula (5.3). That between

the phase *b* and the phase *d* is described as follows.

$$M_A(t) = M_0 \times X / 100 \tag{5.10}$$

$$\frac{dM_F(t)}{dt} = F \cdot M_A(t) - R \cdot M_F(t) \tag{5.11}$$

$$\frac{dM_{uc}(t)}{dt} = -B \cdot M_{uc}(t) \tag{5.12}$$

Thus, the variation of each motor unit under the condition for keeping arbitrarily constant output force can be evaluated by defining the variation of each unit so that the output force can be changed arbitrarily. The phase between the phase *d* and the phase *e* is the same as the condition of maximum voluntary condition without the unit $M_{uc}$ in the model suggested by Liu *et al.* [4]. Then, the variation of each motor unit between the phase *d* and the phase *e* is described as follows.

$$\frac{dM_A(t)}{dt} = -F \cdot M_A(t) + R \cdot M_A(t) \tag{5.13}$$

$$\frac{dM_F(t)}{dt} = F \cdot M_A(t) - R \cdot M_F(t) \tag{5.14}$$

$$M_{uc}(t) = 0 \tag{5.15}$$

The number of each motor unit for each instant of time can be calculated with the formula described as follows. $\Delta t$ is the scale of timestep.

$$M_i(t+1) = M_i(t) + \frac{dM_i(t)}{dt} \cdot \Delta t \qquad (i = A, F, uc) \tag{5.16}$$

### 5.2.3 Muscle fatigue progress under the condition for keeping constant output force with interval

This study also proposed the method to evaluate the muscle fatigue and recovery progress

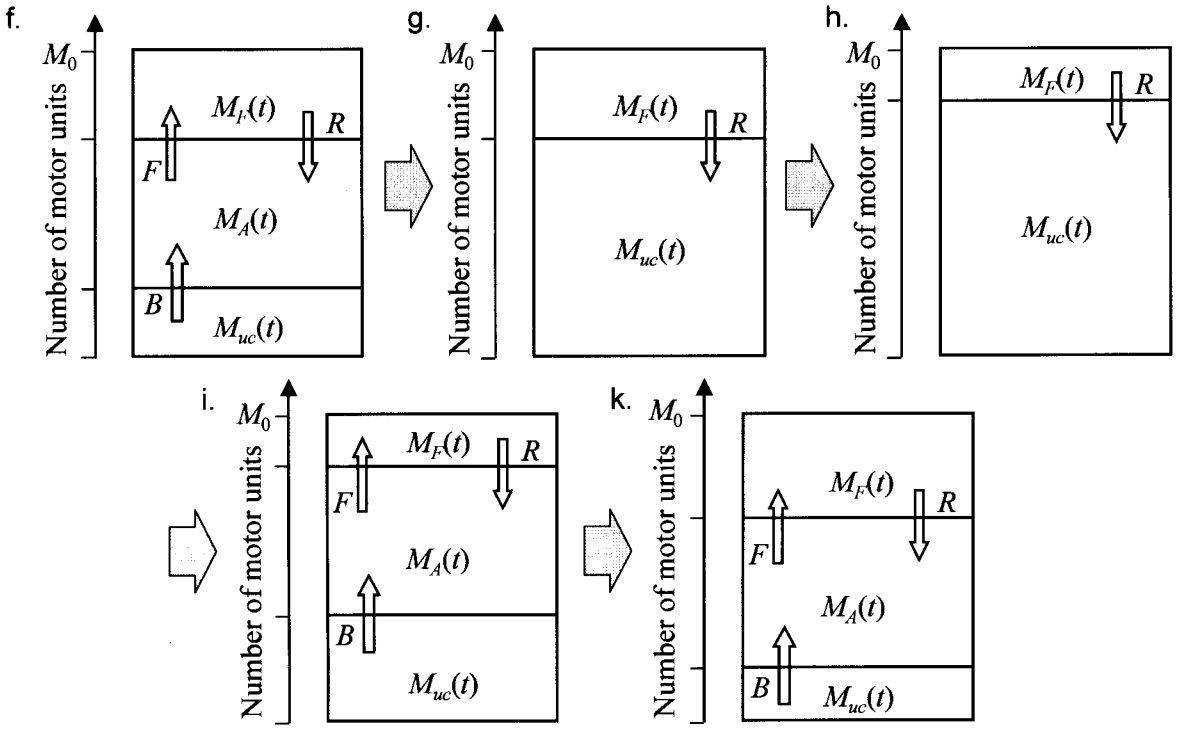


**Fig. 5.4** Muscle fatigue and recovery progress under the condition for keeping constant output force with interval

and estimate the iteration numbers for keeping constant forces with interval. Fig. 5.4 shows the variation of each motor unit under the condition for keeping constant output force with interval. Phase *f* is the phase where the motor unit of standby state is changed to that of activity state and that of activity state is gradually changed to that of fatigue state after constant output force same as the phase *c* in Fig. 5.3. Phase *g* is the phase just after stopping output force, where every motor unit of activity state in phase *f* is change to that of standby state with interval. Phase *h* is the phase where the motor unit of fatigue state is changed to that of standby state gradually with interval. Subsequently, after beginning constant output force again, the phase is changed to the phase *i*, that is the same as the phase *f*, and changed to the phase *k*, where the motor unit of standby state is decreasing and that of fatigue state is

increasing, for keeping constant output force. Then, the phase is changed to the phase $g$ with interval again. After that, the variation of the motor unit is the same with alternating between output force and interval. The variation of each motor unit between the phase $i$ and the phase $k$ is described by the formula (5.10) to formula (5.12) because this phase is the same as the condition for keeping arbitrarily constant output force. The variation of each motor unit during recovery between the phase $g$ and the phase $h$ is described as follows.

$$M_A(t) = 0 \tag{5.17}$$

$$\frac{dM_F(t)}{dt} = -R \cdot M_F(t) \tag{5.18}$$

$$\frac{dM_{uc}(t)}{dt} = R \cdot M_{uc}(t) \tag{5.19}$$

Thus, the endurance times for keeping arbitrarily constant forces and the iteration numbers for keeping arbitrarily constant forces with interval of participants can be estimated with the proposed muscular fatigue model described above when their physical characteristic parameters such as the maximum output force ($M_0$), the strength of muscle activity ($B$), the strength of muscle fatigue ($F$) and the strength of muscle recovery (R) are determined.

## 5.3 Experimental method

Five participants (height: 172.0±6.6 cm, mass: 60.0±4.9 kg), after informed consent, participated in this study to validate the proposed method.

First, the participants kept maximum output forces to one direction until the output forces were stagnated due to their muscle fatigue in order to determine their physical characteristic parameters, $M_0$, $B$, $F$ and $R$. Then, the parameters were determined with the sum of squares of differences between the measured output forces and the theoretical variation of the unit $M_A$ defined

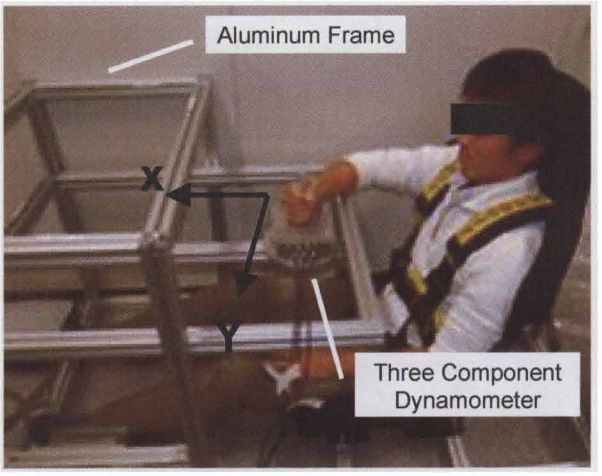


**Fig. 5.5** Measuring equipment of the output forces at the distal extremity

in the muscular fatigue model of Liu *et al.* [4] as the equation (5.7) minimized. The aluminum frame with a hand grip on a three component dynamometer (KYOWA Corp. LSM-B-SAI) shown in Fig. 5.5 was used to measure the output forces.

Subsequently, the endurance times for keeping constant forces were estimated with the determined physical characteristic parameters and the proposed method described in the preceding section. Then, the endurance times were estimated under the condition that the output forces are 50% of the maximum output forces. Furthermore, the participants kept 50% of the maximum output forces until they could not keep the constant output forces watching the monitor displaying their output force simultaneously to compare between the estimated times and the measured ones. The measuring equipment as shown in Fig. 5.5 was used to measure the endurance times.

Finally, the iteration numbers for keeping constant forces with interval were estimated with the proposed method described in the preceding section. The participants alternated between keeping 50% of the maximum output forces for 20 seconds and interval for 10 seconds until they could not keep the output forces to compare between the estimated numbers and the


**Fig. 5.6** Measuring equipment of iteration numbers for keeping constant force with interval

measured ones. The aluminum frame with a hand grip on a driving table of linear motor (GMC Hillstone Corp. S250D-420st) shown in Fig. 5.6 was used to measure the iteration numbers. The participants kept the hand grip alternating between burdening and interval without moving until the linear motor was turned off after the hand grip moved to 30 mm with their muscle fatigue.

### 5.4 Results and discussion

First, the results of the measured output forces and the theoretical curve of the muscular fatigue model of Liu *et al.* [4] in the experiment to keep maximum output forces until the output forces were stagnated are shown in Fig. 5.7. The physical characteristic parameters determined in the experiment are shown in Table 5.1.

The parameter $M_0$ depends on the maximum output force of the participant. So this parameter was different among the participants. The parameter $B$, which depends on the velocity to reach the maximum output force, was assumed to be same among the participants because the velocity to reach the maximum output force is considered not to be great different

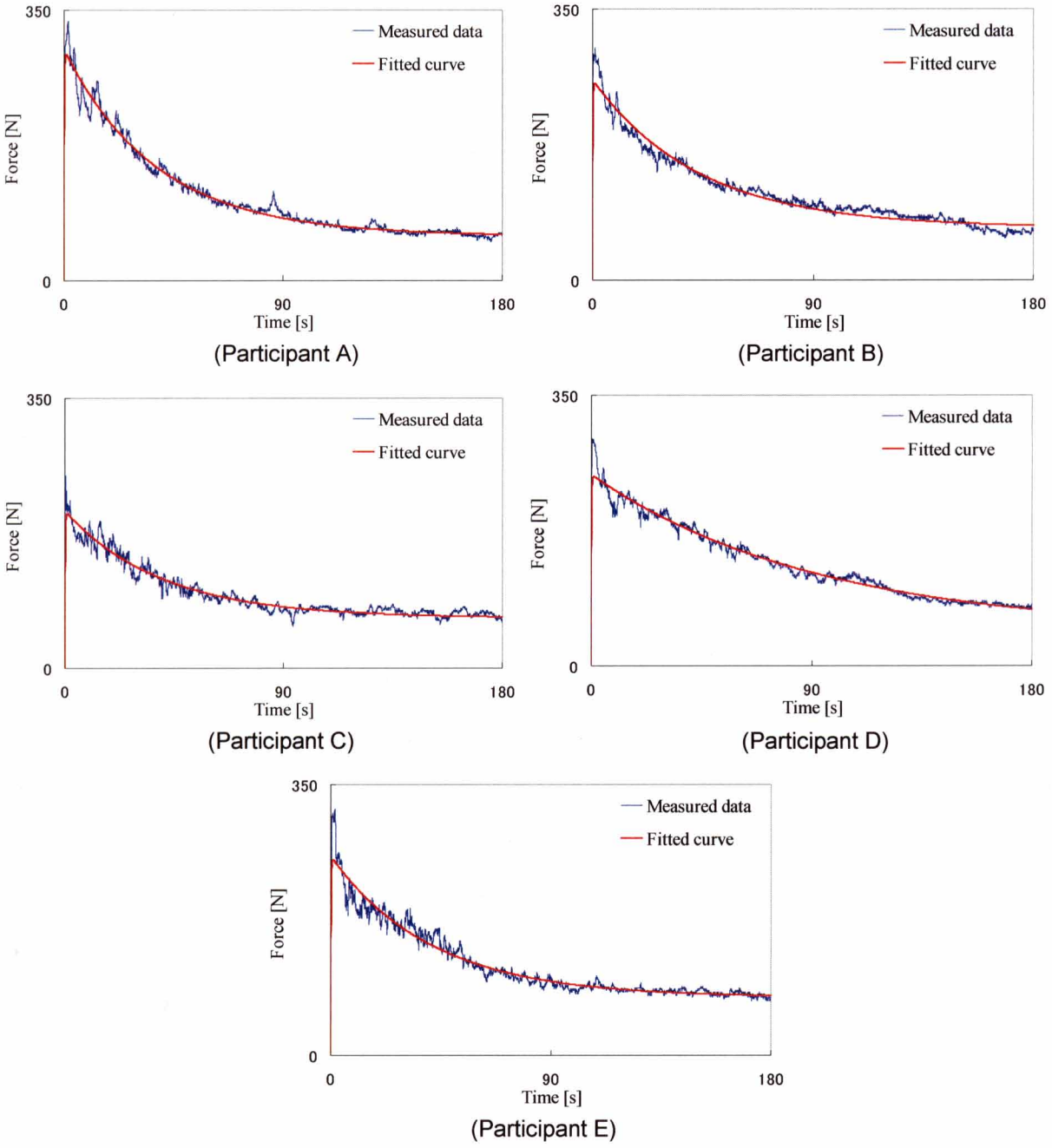


**Fig. 5.7** Comparison of the measured output forces and the theoretical curve

**Table 5.1** Determined physical parameters in the muscular fatigue model

| | $M_0$ | B | F | R |
|---|---|---|---|---|
| Participant A | 336 | 5 | 0.021 | 0.005 |
| Participant B | 300 | 5 | 0.017 | 0.006 |
| Participant C | 249 | 5 | 0.017 | 0.008 |
| Participant D | 294 | 5 | 0.009 | 0.002 |
| Participant E | 319 | 5 | 0.017 | 0.007 |

among the participants. The parameter $F$, which depends on the strength of muscle fatigue, determines the degree of depression of the output force in the maximum voluntary contraction. The parameter $R$, which depends on the strength of muscle recovery, determines the output force stagnated with muscle fatigue. These parameters of each participant were determined from the measured output forces as shown in Fig. 5.7.

Subsequently, the variations of the measured output forces in the experiment to keep 50% of the maximum output forces until the participants could not keep the output force and those of the motor units estimated in the muscular fatigue model are shown in Fig. 5.8. The results of the measured endurance times and the estimated ones are shown in Table 5.2. The results of the endurance times of participants A, B and D showed that the measured endurance times are almost the same as the estimated ones. Those of participants C and E showed that the differences between the measured times and the estimated ones were relatively large.

Finally, the variations of the motor units estimated in the muscular fatigue model under the condition of alternating between keeping 50% of the maximum output forces for 20 seconds and interval for 10 seconds are shown in Fig. 5.9. The results of the measured iteration numbers and the estimated ones are shown in Table 5.3. The results of the iteration numbers of participants A, C and D showed that the measured iteration numbers are almost the same as the estimated ones. Those of participants B and E showed that there were the differences between the measured iteration numbers and the estimated ones.

The reasons of the differences between the measured endurance times and the estimated ones and those between the measured iteration numbers and the estimated ones are considered to be the precision of the experiment to determine the physical characteristic parameters in the muscular fatigue model. The endurance times estimated in the muscular fatigue model depend

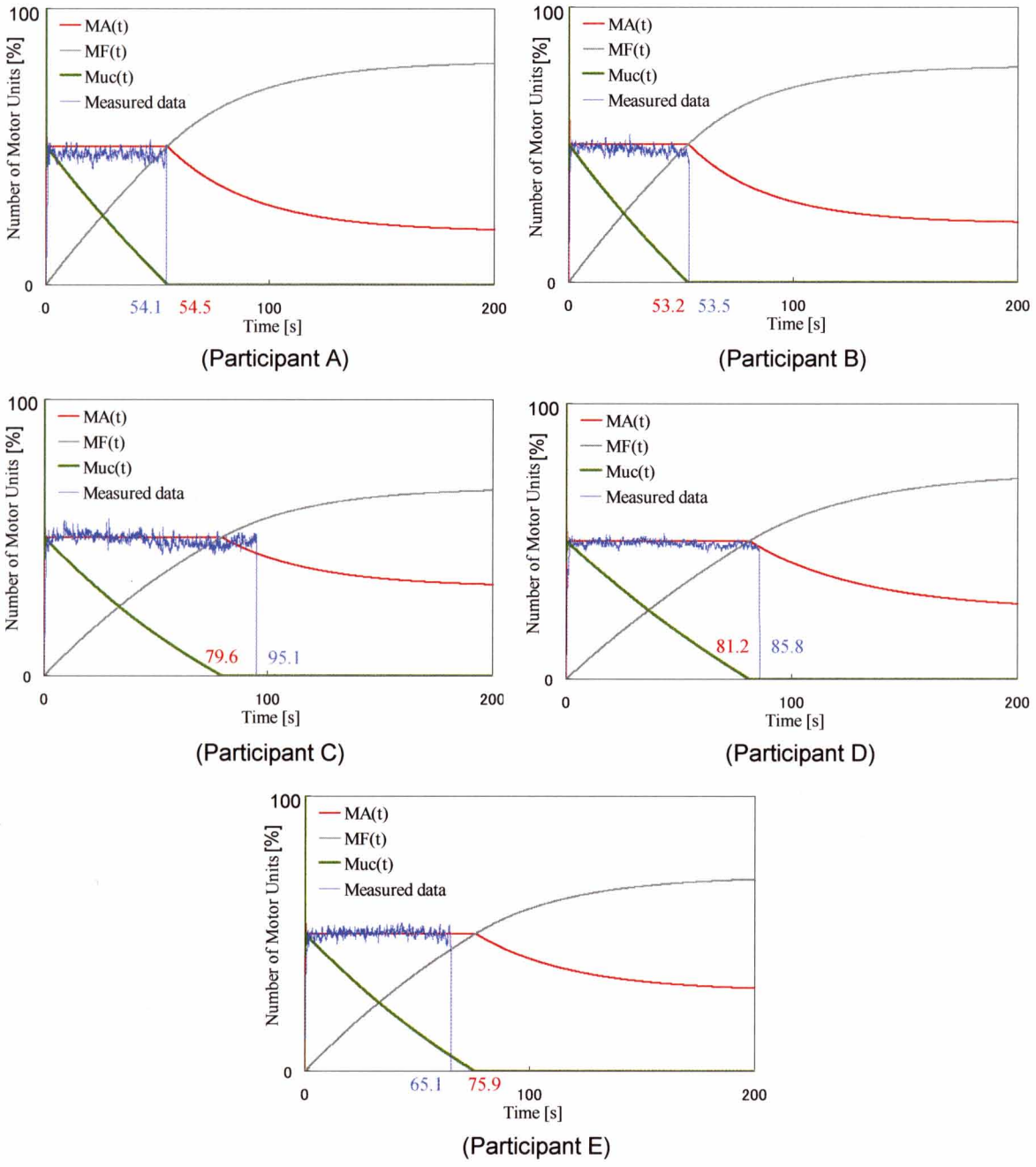


**Fig. 5.8** Variations of the measured output force and the motor units under the condition for keeping constant output force

**Table 5.2** Comparison of the measured endurance times and the estimated ones

| | Measured time [s] | Estimated time [s] | Differences [%] |
|---|---|---|---|
| Participant A | 54.1 | 54.5 | 0.7 |
| Participant B | 53.5 | 53.2 | 0.6 |
| Participant C | 95.1 | 79.6 | 19.5 |
| Participant D | 85.8 | 81.2 | 5.7 |
| Participant E | 65.1 | 75.9 | 14.2 |

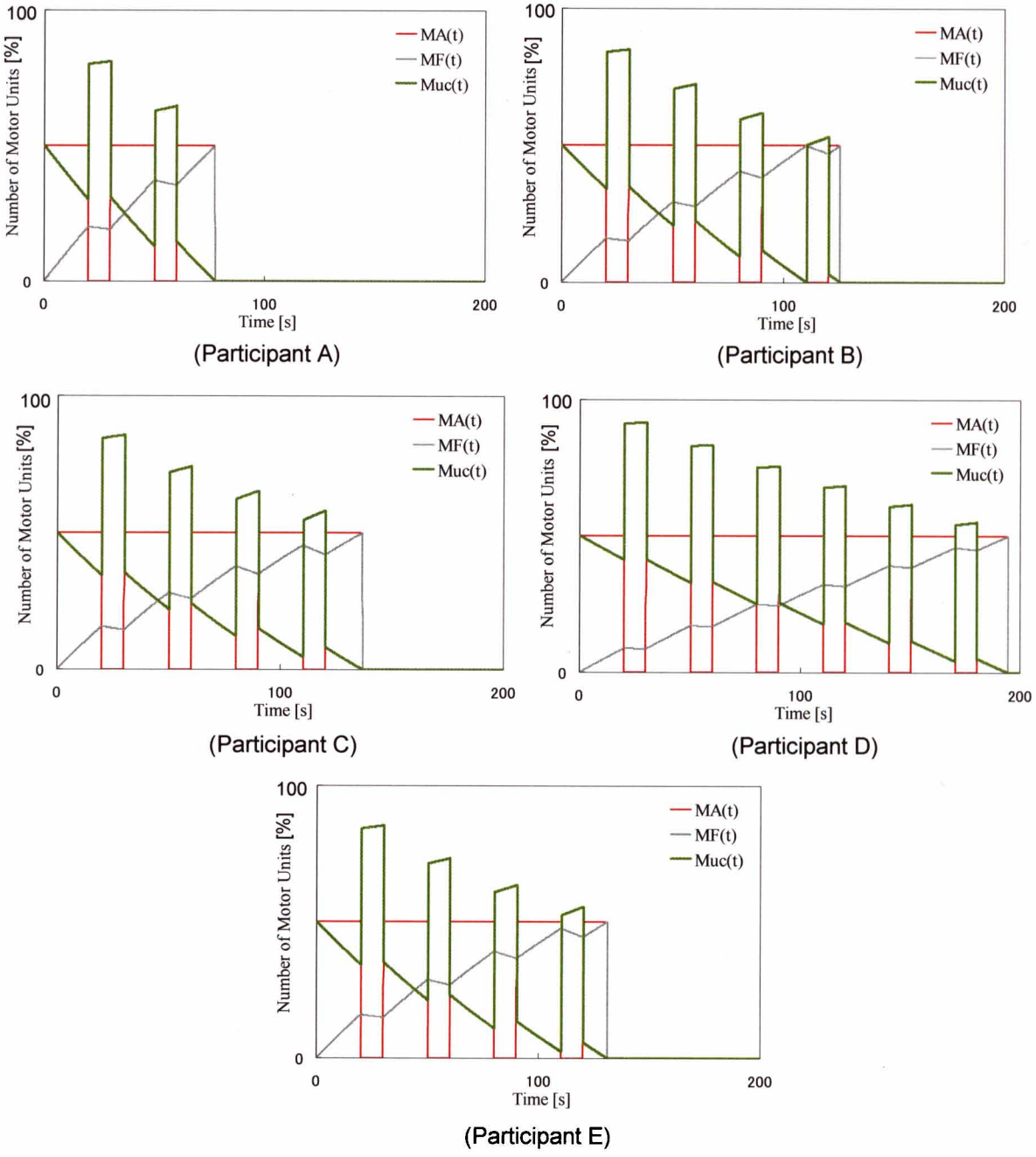


**Fig. 5.9** Variations of the motor units under the condition for keeping constant output force with interval

**Table 5.3** Comparison of the measured iteration numbers and the estimated ones

| | Measured iteration number | Estimated iteration number |
|---|---|---|
| Participant A | 2 | 2 |
| Participant B | 3 | 4 |
| Participant C | 4 | 4 |
| Participant D | 6 | 6 |
| Participant E | 6 | 4 |

largely on the parameter $F$ of the strength of muscle fatigue. The iteration numbers estimated in the muscular fatigue model depend largely on the parameters $F$ of the strength of muscle fatigue and $R$ of the strength of muscle recovery. Therefore, the estimated endurance times and iteration numbers are different from the measured ones without the physical characteristic parameters determined precisely. The reasons that the physical characteristic parameters were not determined precisely is considered that the physical and mental conditions of the participants were not always constant and made effects on the parameters.

However, the results that the differences between the measured endurance times and the estimated ones and those between the measured iteration numbers and the estimated ones were not so large showed that the proposed method was considered to successfully to evaluate muscle fatigue progress under several muscular force patterns.

## 5.5 Conclusion

This study investigated a mechanism of muscle fatigue and proposed a muscular fatigue model to evaluate muscle fatigue progress under several muscular force patterns. Then, the endurance times for keeping constant forces of participants were estimated considering their physical characteristics. The iteration numbers for keeping constant forces with interval were also estimated. To validate the effectiveness of the proposed method, experimental verifications were conducted. The results of this study showed that the proposed method was considered to successfully to evaluate muscle fatigue progress under several muscular force patterns. However, more validations are considered to be necessary to ensure the proposed method effectively and accurately because this study validated only the condition for keeping 50% of the maximum output force in the estimation of the endurance time for keeping

constant forces or the condition for keeping 50% of the maximum output forces for 20 seconds and interval for 10 seconds in the estimation of the iteration numbers for keeping constant forces with interval. These validations will enable the proposed model of muscle fatigue progress to provide the simulation that does not put human subjects at risk.

**References**

[1] Mochimaru M. : Dhaiba, The Digital Human Software to Represent Human Functions and Individual Variations, Journal of the Society of Instrument and Control Engineers 45(12), 999-1004, 2006.

[2] Matui T., Kanade T : Viewing a Human as a System in the Digital Human Technolgy, Journal of the Society of Instrument and Control Engineers, 45(12), 993-998, 2006.

[3] Hayamizu N., Tanaka E., Yamamoto S. : Formulation of a Mathematical Model of Muscular Fatigue and Recovery, Transactions of the Japan Society of Mechanical Engineers. A, 72(713), 100-105, 2006.

[4] Jing Z. Liu, Robert W. Brown, Guang H. Yue : A dynamical model of muscle activation, fatigue, and recovery, Biophys Journal, 82(5), 2344-2359, 2002.

[5] Hawkins D. A., Hull M. L. : Muscle force as affected by fatigue : mathematical model and experimental verification, Journal of Biomechanics, 26, 1117-1128, 1993.

# 6. Conclusion

This thesis proposed and validated methods to evaluate the walking cycle (a closed-loop motion), to estimate muscle forces during motion, and to assess muscle fatigue progress under several muscular force patterns. These methods improve computer human models and enable more realistic evaluations.

Chapter 2 reports on a study that investigated a whole-body human rigid segment model to calculate the net forces and the net moments from the captured images obtained with motion capture system. Furthermore, this study proposed a way to estimate net forces at all joints as well as the ground reaction forces throughout a walking cycle using only with motion capture data and body segment parameters. Several walking trials were conducted to validate the proposed method. The results of this study showed that the correlations between the estimated ground reaction forces and force platforms were very strong. Furthermore, the root-mean-squared differences between the estimated ground reaction forces and the measured ones were relatively small. Therefore the proposed method was considered to successfully estimate the net forces at the joints as well as the ground reaction forces throughout a walking cycle.

Chapter 3 outlines a study that investigated a musculoskeletal model of lower limb that considers the roles of antagonistic muscles and biarticular muscles. In addition, this study proposed a method to estimate muscle forces and muscle activation levels during motion using the musculoskeletal model. Vertical jumping was used as a representative 2-dimensional motion to validate the proposed method. A jogging motion was a representative 3-dimensional motion for further validation of the proposed method. Surface electromyograms (EMGs) of

tibialis anterior (TA), gastrocnemius (GAS), soleus (SOL), rectus femoris (RF), vastus lateralis (VAS), semimembranosus (SM), biceps femoris and short head (BFSH) and gluteus maximus (GMAX) were measured to compare with the estimated muscle activation levels. The results of this study showed that the patterns of the muscle activation levels by the proposed method were similar to those of the EMGs. Therefore, the proposed method was considered to successfully estimate the patterns of muscle activation during dynamic motions.

Chapter 4 presents a study that investigated a musculoskeletal model of the upper and lower limbs that includes the roles of antagonistic muscles and biarticular muscles. This study also proposed a method to estimate muscle forces during a lifting maneuver, which served as a representative motion. This study proposed a method to create various motions with a computer simulation to evaluate the motion considering the roles of muscles. The lifting operations were conducted to estimate muscle forces of upper and lower limbs with the proposed method. Surface electromyograms (EMGs) of deltoid anterior (Da), deltoid posterior (Dp), brachialis (Br), lateral head of triceps brachii (Tla), long head of biceps (Blo) and long head of triceps brachii (Tlo) were measured to compare with the estimated muscle forces. The results showed that the proposed method was considered to successfully estimate the muscle activation patterns during the lifting operations. Various motion patterns in lifting operation were created by a computer simulation based on the experimental lifting operations and evaluated considering the muscle forces of the upper and lower limbs. The results of this study showed that the proposed method was considered to successfully create various motions in computer simulation and evaluate the motions considering the roles of muscles. Thus, the proposed method provides simulated environments where human motions can be tested safely for work efficiency.

Chapter 5 investigated a mechanism of muscle fatigue and proposed a muscular fatigue model to evaluate muscle fatigue progress under several muscular force patterns. Then the endurance times for keeping constant forces of participants were estimated considering their physical characteristics. The iteration numbers for keeping constant forces with interval of the participants were also estimated. To validate the effectiveness of the proposed method, experimental verifications were conducted. The results of this study showed that the proposed method was considered to successfully to evaluate muscle fatigue progress under several muscular force patterns. Furthermore, the proposed model of muscle fatigue progress can provide safely simulation that does not put human subjects at risk.

Actually the musculoskeletal model that considers the roles of the antagonistic muscles and biarticular muscles, which this study used, have been in discussion about its effectiveness. It is pointed that this musculoskeletal model cannot consider the role of internal muscle forces because the model is based on the output forces. It is also pointed that this model can evaluate only the representative muscles included in the model. Thus, the model is difficult to be extended to evaluate muscles other than the representative muscles included in the model. However, this model is physiologically based on the relationship between the output forces and the muscle activation levels. Thus, this model can consider precisely the physiological muscle properties such as the roles of the antagonistic muscles and biarticular muscles. Furthermore, this model does not need much time to estimate muscle forces because it is simply defined the relationship between the distribution of muscles and the output force. The advantage of this model may contribute to realize the evaluation of human motion in real-time without depending the performance of computer. Then, antagonistic muscles are the muscles that act in opposition to the prime movers or agonists of a movement. The role of these

muscles enable human to realize the control function responding flexibly to disturbance. The role of these muscles also contributes to control accurately the direction of the output force. Biarticular muscles are the muscles that work simultaneously on two joints. Actually, the joint can be activated by monoarticular muscles without biarticular muscles. However, if only monoarticular muscles activate the joint, the defects of the muscles may be mortal. Then biarticular muscles, which look redundancy, can realize robust stability by constructing the control system coordinating with other muscles. Thus, the roles of the antagonistic muscles and biarticular muscles enable human to perform various motions including bipedal walking stably.

Another musculoskeletal model to estimate muscle forces physically and mathematically has been usually used. This model can estimate muscle forces with an optimization method on the condition that the net moments calculated by inverse dynamics are equal to those worked by muscles attaching the joints. This model can consider the role of the internal muscle forces. This model can also be easily extended to evaluate any muscles attaching the joints. The advantage of this model enables the model to apply any joints. However, this model needs much time to estimate muscle forces because the process of this includes repeated computation such as linear programming and sequential quadratic programming. The calculation time is increased as the number of muscles in the model is increased and the model is complicated. This disadvantage is considered to prevent the model from realizing the evaluation of human motion in real-time. Furthermore, this model unfortunately usually does not consider the role of the antagonistic muscles and biarticular muscles because the model estimate muscle forces optimally with the sum of the muscle forces or the sum of the muscle consumption energy minimized.

As mentioned above, there are two representative methods to estimate muscle forces during motions, one is based on the physical and mathematical model and the other is based on the physiological model. This study focused on the physiological model and evaluated muscles considering the roles of muscles, which human originally has, such as antagonistic muscles and biarticular muscles.

This thesis needs some future works to improve computer human models and to realize more realistic human evaluations. The proposed musculoskeletal model does not include muscles working on the trunk such as rectus abdominis muscles and muscles of the back. Actually, these muscles can be evaluated with the optimization method based on the physical and mathematical model. However, the roles of the antagonistic muscles and biarticular muscles cannot be negligible for these muscles. Then, it is necessary to suggest the model to evaluate these muscles considering these roles. The proposed musculoskeletal model does not also include muscles working for the abduction, adduction and internal and external rotation. The musculoskeletal model including the roles of these muscles can evaluate various ergonomic situations. Furthermore, the proposed muscular fatigue model can evaluate muscle fatigue progress as long as the muscular force pattern is constant or uncomplicated. The evaluation of muscle fatigue progress under the muscular force patterns which is changing dynamically is necessary to evaluate more ergonomic, dynamic and continuous motions. These functions can contribute to realize the following various ergonomic motions. They can evaluate not only the degree of the accumulated muscle fatigue of each muscle during single operation but also estimate the number of times that workers can keep the operation sequentially and repeatedly. Furthermore, they can estimate the optimal interval between the operations so that workers can keep the operation repeatedly.

In addition, the computer human model as this study proposed, which can evaluate net forces, net moments, muscle forces and muscle fatigue with only the motion, can also evaluate the motions created in the computer. The results of this are considered to contribute to provide athletes with motions that they can give the best performance and unprecedented technical advices by feedback of the muscle forces in a moment in the area of sports engineering, to provide workers with the optimal motions and environments that they can work safely, efficiently and comfortably in the area of manufacturing and to improve the efficiency of rehabilitation by giving the precise rehabilitation procedures considering the degree of muscle weakness different from one person to another. Thus, the computer human model can conduct innovative evaluation by adding the functions lacking in the developing computer human model and evaluating various motions in computer.

## Acknowledgement

I would like to express my deep and sincere gratitude to my supervisor, Professor Keiichi Shirase, Graduate School of Engineering, Kobe University. His wide knowledge and logical way of thinking have been of great value for me. His understanding, encouraging and personal guidance have provided a good basis for the present thesis.

I owe my most sincere gratitude to Professor D. Gordon E. Robertson, School of Human Kinetics, University of Ottawa, who gave me the opportunity to work with them at the University of Ottawa and gave me untiring help during my difficult moments. His detailed and constructive comments have been very helpful throughout this work.

I warmly thank Professor Tsuneo Kawano, School of Faculty of Science & Technology, Setsunan University, for his valuable advice and friendly help. His extensive discussions around my work and interesting exploration in operations have been very helpful for this study.

My warmly thanks are due to Professor Masato Maeda, Graduate School of Human Development and Environment, Kobe University, who gave me his valuable advice and helped me with experiments of my thesis. His king support and guidance have been of great value in this study.

My sincere thanks are due to the official referees, Professor Yasuyoshi Yokokoji, Graduate

School of Engineering, Kobe University and Professor Zhi Wei Luo, Graduate School of System Informaics, Kobe University, for their detailed review, constructive criticism and excellent advice during the presentation of this thesis.

During this work, I have collaborated with many colleagues for whom I have great regard, and I wish to extend my warmest thanks to all those who have helped me with my work in the Computer Integrated Manufacturing System Laboratory at the Kobe University in Japan and the School of Human Kinetics, University of Ottawa in Canada.

My special gratitude is due to my parents for their loving support. Without their encouragement and understanding it would have been impossible for me to finish this work.

Department of Mechanical Engineering,

Graduate School of Engineering, Kobe University

Isamu Nishida